

DESIGN AND DEVELOPMENT OF NOVEL
POLYPROPYLENE BASED ALUMINIUM-AIR BATTERY
SYSTEM

TAN WENG CHEONG

DOCTOR OF PHILOSOPHY (ENGINEERING)

LEE KONG CHIAN FACULTY OF ENGINEERING AND
SCIENCE
UNIVERSITI TUNKU ABDUL RAHMAN
OCTOBER 2023

**DESIGN AND DEVELOPMENT OF NOVEL POLYPROPYLENE
BASED ALUMINIUM-AIR BATTERY SYSTEM**

By

TAN WENG CHEONG

A thesis submitted to the Department of Mechanical and Material Engineering,
Lee Kong Chian Faculty of Engineering and Science,
Universiti Tunku Abdul Rahman,
in partial fulfillment of the requirements for the degree of
Doctor of Philosophy (Engineering)
October 2023

ABSTRACT

DESIGN AND DEVELOPMENT OF NOVEL POLYPROPYLENE BASED ALUMINIUM-AIR BATTERY SYSTEM

TAN WENG CHEONG

The global energy demand is increasing rapidly due to the rapid development and adoption of new technologies in every sector. Therefore, there is a need to introduce a clean energy source that does not harm the environment. Metal-air batteries have gained significant attention as promising storage system for the post lithium-ion era. These batteries generate electricity through oxidation and reduction reactions within the anode and cathode. Among various types of metal-air batteries, the aluminium-air battery is particularly attractive due to its high energy density and environmental friendliness. In this study, a novel polypropylene-based aluminium-air battery is developed. Polypropylene pads are utilized to absorb the electrolyte, isolate the anode and cathode, and reduce the hydrogen generation in the parasitic reaction. Two different types of electrolyte systems namely single electrolyte system and dual electrolyte system are analysed. The performance of the aluminum-air battery will be investigated using various electrochemical techniques, such as discharge tests, polarization tests, electrochemical impedance spectroscopy, and Tafel analysis. Next, surface morphology characterization of the aluminum anode and polypropylene will be performed using SEM and XRD. The single electrolyte system aluminium-air battery is constructed with an aluminium foil anode, a carbon fiber cloth air-cathode, and a polypropylene separator. The effects of electrolyte concentration

on the aluminium-air battery are investigated and analyzed using various discharge currents. The study reveals a negative correlation between battery capacity and electrolyte concentration. At discharge current of 30 mA, the aluminium-air battery achieves a specific capacity of 375 mAh.g^{-1} when 1M potassium hydroxide is used as the electrolyte. In the dual electrolyte system, potassium hydroxide is used as the anolyte and sulfuric acid is used as the catholyte. A parametric study is conducted to investigate the effect of electrolyte concentration and polypropylene separator thickness on battery performance. The results demonstrated that the dual-electrolyte system can increase the open circuit voltage to 2.2 V compared to the single electrolyte system when using 5M anolyte, while maintaining a specific discharge capacity of about $1390.92 \text{ mAh.g}^{-1}$. Furthermore, the maximum peak power density significantly increases from 100 mW.cm^{-2} to 350 mW cm^{-2} for the dual electrolyte system. Tafel analysis has shown that the concentration of KOH electrolyte used in the aluminum-air battery affects the corrosion rate of the aluminum anode. Specifically, a higher concentration of electrolyte increases the corrosion rate. On the other hand, the polypropylene pad has demonstrated superior performance in limiting the corrosion rate of the aluminum-air battery, reducing it by up to 89.1% when compared to the case without a polypropylene separator.

ACKNOWLEDGMENT

My research project would not be completed without the help and supports of many individuals. First of all, I would like to show my greatest appreciation to my main project supervisor, Ir. Ts Dr. Bernard Saw Lip Huat who gives me invaluable advice, guidance and enormous patience throughout my research period. His encouragement, and mentorship have helped me overcome numerous challenges, and his positive attitude has always kept me motivated to achieve my best. I am truly grateful for the mentorship and guidance. My appreciation also goes to my project co-supervisor, Ir. Ts Dr. Yew Ming Chian and Dr. Kuo Pei-Yu who gives me guidance and support throughout my research period. My appreciation also goes to Fundamental Research Grant Scheme (Grant No. FRGS/1/2018/TK07/UTAR/02/4) from Ministry of Higher Education Malaysia and University Malaya RU grant (Grant No. ST024-2019), UTAR Research Fund (IPSR/RMC/UTARRF/2022-C2/T05) and Research Environment Links Grant No. MIGHT/CEO/NUOF/1-2022 (2) from the British Council and Malaysia Industry-Government Group for High Technology, as part of the British Council's Going Global Partnerships programme. The Programme builds stronger, more inclusive, internationally connected higher education and TVET systems.

Besides that, I would also like to extend my gratitude towards Department of Mechanical and Material Engineering (DMME) and Department of Laboratory Management and Safety Administration (DLMSA) under Lee Kong Chian Faculty of Engineering and Science (LKCFES). Both DMME and DLMSA have provided me the facilities and resources to perform laboratory

works.

In addition, special thanks to my parents and my friends for giving great mental support for my study. Besides that, many thanks go to my course mates, who are willing to contribute their knowledge and ideas in helping me to accomplish my research project.

APPROVAL SHEET

This dissertation entitled “**DESIGN AND DEVELOPMENT OF NOVEL POLYPROPYLENE BASED ALUMINIUM-AIR BATTERY SYSTEM**” was prepared by TAN WENG CHEONG and submitted as partial fulfillment of the requirements for the degree of Doctor of Philosophy (Engineering) at Universiti Tunku Abdul Rahman.

Approved by:

saw

(Ir. Ts. Dr. Bernard Saw Lip Huat)
Date: 23/10/2023
Associate Professor/Supervisor
Department of Mechanical and Material Engineering
Lee Kong Chian Faculty of Engineering Science
Universiti Tunku Abdul Rahman



(Ir. Ts. Dr. Yew Ming Chian)
Date:.....23/10/2023.....
Associate Professor/Co-supervisor
Department of Chemical Engineering
Lee Kong Chian Faculty of Engineering Science
Universiti Tunku Abdul Rahman



(Dr. Kuo Pei-Yu)
Date: 25/10/2023
Associate Professor/Co-supervisor
Department of Forestry and Natural Resources,
National I-Lan University

LEE KONG CHIAN FACULTY OF ENGINEERING AND SCIENCE
UNIVERSITI TUNKU ABDUL RAHMAN

Date: 23 October 2023

SUBMISSION OF DISSERTATION

It is hereby certified that Tan Weng Cheong (ID No: 20UED06339) has completed this dissertation entitled “Design and development of Novel Polypropylene Based Aluminium-air Battery System” under the supervision of Ir. Ts. Dr. Bernard Saw Lip Huat (Supervisor) from the Department of Mechanical and Material Engineering, Lee Kong Chian Faculty of Engineering and Science, Ir. Ts. Dr. Yew Ming Chian (Co-Supervisor) from the Department of Mechanical and Material Engineering, Lee Kong Chian Faculty of Engineering and Science and Dr. Kuo Pei-Yu from the Department of Forestry and Natural Resources, National I-Lan University.

I understand that University will upload softcopy of my dissertation in pdf format into UTAR Institutional Repository, which may be made accessible to UTAR community and public.

Yours truly,

Weng Cheong

(Tan Weng Cheong)

DECLARATION

I hereby declare that the dissertation is based on my original work except for quotations and citations which have been duly acknowledged. I also declare that it has not been previously or concurrently submitted for any other degree at UTAR or other institutions.

Name Tan Weng Cheong

Date 23 October 2023

TABLE OF CONTENTS

	Page
ABSTRACT	ii
ACKNOWLEDGEMENTS	iv
APPROVAL SHEET	vi
SUBMISSION OF DISSERTATION	vii
DECLARATION	viii
LIST OF TABLES	xi
LIST OF FIGURES	xii
LIST OF ABBREVIATIONS	xv
CHAPTER	
1.0 INTRODUCTION	1
1.1 Research Background	1
1.2 Importance of Study	4
1.3 Problem Statement	6
1.4 Research Gap	8
1.5 Novelty	9
1.6 Aim and Objectives	9
1.7 Arrangement of thesis	10
2.0 LITERATURE REVIEW	11
2.1 Introduction	11
2.2 Metal-air Battery	13
2.3 Aluminium-Air Battery	14
2.4 Aluminium anode	16
2.5 Electrolyte	18
2.6 Dual electrolyte system	22
2.7 Separator	27
2.8 Cathode	30
2.9 Summaries	36
3.0 METHODOLOGY	38
3.1 Design of the Aluminium-air Battery	38
3.1.1 Structure of a Single Electrolyte System	38
3.1.2 Structure of a Dual Electrolyte System	40
3.2 Experiment Analysis	41
3.2.1 Polarization Test	42
3.2.2 Discharge Test	43
3.2.3 Tafel Test	44
3.2.4 Corrosion Analysis	46
3.2.5 Electrochemical Impedance Spectroscopy (EIS)	47
3.2.6 Surface Characterization	48
3.2.7 Wettability Characterization of Polypropylene Pad	49
3.3 Summary	50

4.0	RESULTS AND DISCUSSION	51
4.1	Introduction	51
4.2	Single Electrolyte System Aluminium-air Battery	51
4.2.1	Battery Performance with Aluminium Foil as Anode	52
4.2.2	Specific discharge capacity of aluminium-air battery	56
4.2.3	Performance of Polypropylene Against a Paper-Based Separator	58
4.2.4	Comparison of Aluminium Foil and Aluminium Alloy 6061 as Anode	62
4.2.5	Performance of Aluminium Alloy 6061 as Anode in Aluminium-air battery	59
4.3	Dual Electrolyte System Aluminium-air Battery	71
4.3.1	Effects of the Separator Thickness	72
4.3.2	Effects of Polypropylene Pad Thickness	74
4.3.3	Effects of Anolyte Concentration	77
4.3.4	Effects of Catholyte Concentration	82
4.3.5	Comparison Between Single and Dual Electrolyte System	90
4.3.6	EIS Analysis	95
4.4	Tafel Plot	99
4.5	Corrosion rate	102
4.6	Surface Characterization	106
5.0	CONCLUSIONS AND FUTURE WORKS	114
5.1	Conclusions	114
5.2	Recommendation and Future Work	116
6.0	REFERENCE	120
7.0	LIST OF PUBLICATIONS	133

LIST OF TABLES

Table		Page
2.1	Electrical properties of various type of metal-air battery.	16
3.1	Equations related to the electrical components.	48
4.1	Parameter of the electrical components in the equivalent circuit model for aluminium foil and aluminium alloy 6061 anode.	66
4.2	Parameter of the electrical components in the equivalent circuit model for different concentration of electrolyte.	71
4.3	Parameter of the electrical components in the equivalent circuit model for different catholyte concentration.	98
4.4	Parameter of the electrical components in the equivalent circuit model for different anolyte concentration.	98
4.5	Tafel plot data for aluminium alloy 6061 anode and aluminium foil.	101
4.6	Corrosion rate of the aluminium alloy 6061 anode and aluminium foil anode in 1 hour.	105

LIST OF FIGURES

Figures		Page
2.1	Structure of an Aluminum-air Battery	14
2.2	A dual electrolyte microfluidic aluminum-air battery	24
2.3	(a) Schematic diagram of a tri-electrolyte aluminum-air battery, (b) real trielectrolyte aluminum-air battery, (c) schematic diagram of single electrolyte aluminum-air battery, (d) real single electrolyte aluminum-air battery. (Wang et al., 2020).	27
2.4	Paper based aluminum-air battery (a) working principle, (b) cell composition.	29
2.5	Structure of an air cathode	32
3.1	(a) Schematic diagram of single electrolyte aluminium-air battery, (b) prototype of single electrolyte aluminium-air battery.	39
3.2	(a) Schematic diagram of dual electrolyte aluminium-air battery, (b) prototype of dual electrolyte aluminium-air battery.	41
3.3	Contact angle of the different concentration of KOH on the polypropylene (A) 1M KOH, (B) 2M KOH, and (C) 3M KOH.	50
4.1	Discharge performance of Al-air battery with 1M KOH electrolyte.	53
4.2	Discharge performance of Al-air battery with different KOH concentration with discharge current of 20 mA	55
4.3	Specific discharge capacity of the polypropylene-based aluminium-air battery under various concentrations and magnitude of discharge currents	57
4.4	Discharge performance of polypropylene and kimwipes separator	59
4.5	SEM image of 300X magnification of (a) polypropylene pad before discharging, (b)	61

	polypropylene pad after discharging for 1 h, (c) kimwipes before discharging and (d) kim wipes after discharging for 1 h.	
4.6	(a) Polarization curve and (b) discharge curve comparing the performance of aluminium foil and aluminium alloy 6061 as anode in aluminium-air battery.	63
4.7	(a) Nyquist plot comparing aluminium foil and aluminium alloy 6061 anode ; (b) Equivalent circuit model derived from the EIS analysis	65
4.8	(a) Polarization curve, (b) discharge curve, (c) discharge curve of various discharge currents, and (d) Nyquist plot comparing the effect of concentration of KOH electrolyte	70
4.9	Discharge curve of different thickness of separator in the dual electrolyte aluminium-air battery.	73
4.10	(a) Polarization curve and (b) discharge curve of the thin vs thick polypropylene pad in the dual electrolyte aluminium-air battery	77
4.11	Polarization characteristics of the aluminium-air battery (a) Voltage vs current density, and (b) Power density vs current density and the discharge curve for various current densities (c) 10 mA, (d) 30 mA and (e) 50 mA using different concentrations of anolyte.	82
4.12	Polarization characteristics of the aluminium-air battery (a) Voltage vs current density, and (b) Power density vs current density and the discharge curve at 30 mA for (c) 1M KOH and (d) 5M KOH in comparing the effects of catholyte concentration.	85
4.13	Discharge curve for (a) 3M of KOH, (b) 5M of KOH and (c) 8M of KOH in comparing the effects of catholyte concentration using discharge current of 100 mA.	90
4.14	Polarization characteristics of the aluminium-air battery (a) Voltage vs current density, (b) Power density vs current density and (c) discharge curve at discharge current of 30 mA for single electrolyte and dual electrolyte system.	94
4.15	Nyquist plot comparing (a) effects of concentration	98

	of catholyte and (b) effects of concentration of anolyte.	
4.16	Tafel plot comparing the effects of KOH concentration (a) aluminium alloy 6061, (b) aluminium foil.	101
4.17	SEM images of 1000x magnification and macroscopic view of (a) pristine aluminium anode and after discharging using (b) 1M of KOH, (c) 3M of KOH, (d) 5M of KOH.	109
4.18	SEM image at 500x for Al alloy 6061 discharge for 1 hour for under 5M KOH electrolyte (a) without polypropylene, (b) with polypropylene.	109
4.19	Energy-dispersive X-ray spectroscopy (EDX) spectra for (a) Al foil without discharge, (b) Al foil discharge for 1 hour in 3M KOH without polypropylene, (c) Al alloy 6061 without discharge, (d) Al alloy 6061 discharge for 1 hour in 3M KOH without polypropylene.	112
4.20	XRD results of the aluminium anode after discharge test.	113

LIST OF ABBREVIATIONS

A	Expose area, cm^2
Ag	Silver
AgCl	Silver chloride
Al	Aluminium
$\text{Al}(\text{OH})_3$	Aluminium hydroxide
A_w	Warburg coefficient
C	Capacitance
C_{dl}	Double layer capacitance
$C_{S,O}$	Surface concentration of oxidized form
$C_{S,R}$	Surface concentration of reduced form
D	Diffusion coefficient
EV	Electrical vehicle
e^-	Electron
E_{corr}	Corrosion voltage, V
EDX	Energy Dispersive X-ray
EIS	Electrochemical Impedance Spectroscopy
F	Faraday constant, 96850 C/mol
H^+	Hydrogen ion
H_2	Hydrogen gas
H_2O	Water
H_2SO_4	Sulphuric acid
I	Current, A
I_{corr}	Corrosion current density, A/cm^2
Im	Imaginary part

j	Imaginary symbol
KOH	Potassium hydroxide
M	Metal anode
m	Mass, g
M	Molarity
m_{al}	aluminium atomic mass, g
n	Oxidation number
NaCl	Sodium chloride
NaOH	Sodium hydroxide
O ₂	Oxygen
OCV	Open circuit voltage
OH ⁻	Hydroxide ion
ORR	Oxygen reduction reaction
P	Power, W
Q	Specific capacity, mAh/g
R	Resistance, Ω
R	Universal gas constant
R _{ct}	Charge transfer resistance
Re	Real part
R _p	Polarization resistance, Ω
R _s	Solution resistance
SEM	Scanning electron microscope
t	Time, h
T	Absolute Temperature

V	Voltage, V
XRD	X-Ray Diffraction
Z	Impedance
β_a	Tafel slopes at the anode, V. dec-1
β_c	Tafel slopes at the cathode, V. dec-1
ω	Angular frequency
E	Potential difference
Greek Symbols	
Δ	change

CHAPTER 1

INTRODUCTION

1.1 Research Background

Rapid growth of the economy in the world has led to an increase in energy demand in daily lives and industries. It is projected that world energy consumption will grow by 50% between 2018 and 2050 particularly, in the Asia region (Kahan, 2019). On the other hand, global energy-related CO₂ emissions will grow by 0.6% per year from 2018 to 2050 (Kahan, 2019). As a result, human-induced climate change is also increasing steadily. Hence, renewable energy sources are being explored to minimize the burning of fossil fuel and environmental pollution. One of the alternative solutions is using the electrochemical energy storage system to replace the conventional internal combustion engine to generate electricity for the vehicle. There are several advantages associated with the electrochemical energy storage system on fuel cell powered vehicles, such as reduced harmful emission, less noise pollution and reduced dependence on fossil fuels (Clark et al., 2018).

The primary energy source of the Electrical Vehicles (EVs) is the electrochemical energy storage system such as lead-acid batteries, Li-ion batteries, NiCd, NiMH, and others. Among the various batteries used in EVs, Li-ion batteries, with their high energy density (250-300 Wh.kg⁻¹) are a popular

choice nowadays (Wang et al., 2022). Additionally, Li-ion batteries have a longer cycle life and depth of discharge compared to other types of energy storage systems (Abdin et al., 2019). However, Li-ion batteries are very sensitive to the operating temperature and prone to thermal runaway (Tan et al., 2011). On the other hand, EVs equipped with rechargeable batteries will require the construction of new charging facilities. Fast charging of electric vehicles during peak hours will certainly increase the electric load on the existing electricity networks which is not cater for such application. Moreover, the disposal of used Li-ion batteries is also an unresolved issue. Hence, research on the energy storage system has been conducted to find an alternative solution to replace Li-ion batteries, and one of the potential solutions is using a metal-air battery.

Metal-air batteries, offering high energy density, are anticipated as promising clean energy solutions for the post-Li-ion battery era (Li et al., 2017). The operating principle of the metal-air batteries is very simple; the electrochemical reaction occurs when the battery consumes oxygen from the air at the cathode and forms hydroxide ions. At the anode, the metal is oxidized to metal oxide to generate the electricity. Various types of metal electrodes are being used in a metal-air battery, such as zinc, aluminium, magnesium, iron, lithium (Xiang et al., 2020) and sodium (Jiang et al., 2018). Among the various types of metal, aluminium is considered an attractive candidate due to its unique characteristics, such as high specific energy, high conversion rate, low operating cost, and environmental friendliness, making it one of the best prospect as anode material in metal-air batteries (Liu et al., 2017). Moreover, aluminium is widely

available in the world, and it is easy to handle, transport, and recycle through industrial treatment. The recycling process of aluminium is very mature in current technology. Aluminium-air batteries have the highest theoretical voltage and power density among various types of batteries, recorded at 2.7 V and 8100 Wh.kg⁻¹, respectively (Schwarz, 2014; Nestoridi et al., 2008).

In this study, a new type of polypropylene-based aluminium-air battery was developed. Experimental work was performed to investigate the performance of the aluminium-air battery. Compared to the conventional aqueous aluminium-air battery system which, required a complicated electrolyte circulating system, this design enables the compact design of the aluminium-air battery and reduces the self-corrosion of aluminium. Besides that, due to the simplicity of the design, polypropylene-based aluminium-air battery offers the advantages of being cheap, portable, and lightweight, which is ideal for miniature application.

1.2 Importance of Study

Industrial revolution 4.0 has pushed the agenda to promote green technology as a future trend. This is aimed at providing a sustainable environment for future generations by reducing dependency on fossil fuels for energy generation while also providing affordable energy source for human beings. Electrochemical batteries have gained a lot of attention nowadays due to their reliability, small size and cost effectiveness. Hence, it is widely used in transportation industry and in portable appliances.

However, most of the batteries used nowadays have their own weaknesses. The lead-acid battery is well-known for its mature, robust and well-understood chemistry, resulting in producing more bursts of power and necessity for smooth internal engine combustion. With these advantages, lead-acid batteries have become widely used in vehicles worldwide and as backup power supplies. However, the usage of lead-batteries raises concerns about specific environmental issues due to the significant emission of heavy metals and acidic gases, which are harmful to humans, animals, plants, and soil. On the other hand, lithium-ion batteries also pollute the environment as there is no proper disposal method for used lithium-ion batteries. They are also susceptible to thermal runaway, which may cause the battery degradation and failure. Moreover, the development of lithium-ion batteries has reached its peak, and there is a need to introduce a new type of battery in the future.

Metal-air batteries may serve as an alternative energy source. Among other metals, aluminium has gained attention due to its unique advantages, such

as immense specific energy and conversion rate, low management cost, and abundant raw material supply (Liu et al., 2017). Metal-air batteries showed promising prospect in becoming the next energy storage technology due to their high energy density of 8100 Wh.kg^{-1} and theoretical potential of 2.7 V. Furthermore, aluminium is one of the most abundant metal resources and second largest metal market in the world. Additionally, aluminium is easy to transport and recycle through industrial retreatment added to the potential advantages to be implemented as the next-generation alternative source of energy storage.

1.3 Problem Statement

The development of aluminium-air batteries is still in the infant stage, with many discoveries yet to be investigated. The performance of aluminium-air batteries depends on several factors, such as the type and concentration of electrolyte, types of separator, types of aluminium anode, and types of air cathode. The electrical performance of the aluminium-air battery changes due to the different components used within the battery's cell. There is no universal agreement on the relationship between each factors mentioned above. Hence, investigation is needed to determine the relationship that affects the performance of the aluminium-air battery.

The performance of the aluminium-air battery is often limited by the types of electrolyte used. Although alkaline electrolyte works well in producing high electrical performance, it also causes corrosion to the aluminium anode, which reduces the specific capacity of the battery. On the other hand, acidic and neutral electrolytes does not generate good electrical performance, but they can help reduce the corrosion on the aluminium anode. A study is required to find a solution that can reduce the corrosion rate while still producing high electrical performance in the aluminium-air battery.

Most aluminium-air batteries have an aqueous system to circulate the electrolyte. However, this circulation system requires special design such as pumps and tubing to circulate the electrolyte to the aluminium-air battery, which increase the complexity of the aluminium-air battery design and may cause

leakage. In this study, a simple aluminium-air battery is proposed by implementing a new separator to eliminate the circulation system, thereby removing the complexity of the battery design and cost. This is ideal for miniature applications as the size and mass are greatly reduce while providing portability for various application.

1.4 Research Gap

Most of the design involving aluminium-air batteries that are currently under investigation is an aqueous based system. This system is notorious for its high corrosion rate on the aluminium anode once it comes into contact with the alkaline electrolyte. As for now, there is no prevention method for these corrosion issues. Most of the proposed solutions aim to slow down the corrosion rate, such as alloying the aluminium anode or using corrosion inhibitor in the electrolyte of the aluminium-air battery.

This study aims to solve this problem by taking an alternative approach. A polypropylene pad will be used as the separator to separate the anode and cathode. It can help to control the supply of the electrolyte to the aluminium anode. Thus, reducing the direct contact of the aluminium anode with the electrolyte and consequently, reduce the corrosion of the aluminium-air battery.

1.5 Novelty

The novelty of this study lies in the type of separator employed in the aluminium-air battery. Polypropylene fiber was tested as a separator in the study. The effects of electrolyte concentration, types of electrolytes and discharge current on the performance of the polypropylene separator of the aluminium air battery are investigated for single and dual electrolyte system. The corrosion of the aluminium anode is also investigated.

1.6 Aim and Objectives

The aim of this study is to develop a simple and small aluminium-air battery. Based on this aim, several objectives are outline below:

- 1) To construct a polypropylene-based aluminium-air battery.
- 2) To evaluate the electrical performance of the polypropylene-based aluminium-air batteries experimentally.
- 3) To conduct a parametric study on the performance of polypropylene-based aluminium-air batteries.
- 4) To investigate the corrosion capabilities of polypropylene-based aluminium-air battery

1.7 Arrangement of thesis

The thesis is arranged in the following manner: Chapter 1 presents the research background, importance of the study, problem statements, novelty, research gap and objectives of the study. Chapter 2 focuses on the literature review of this study. Chapter 3 explains the design of the aluminium-air battery and the experimental setup for this study. Chapter 4 discusses the results based on the experiments conducted on the aluminium-air battery. The findings included single electrolyte system and dual electrolyte system and corrosion characteristics of the aluminium-air battery. Lastly, Chapter 5 concludes the findings of this study.

CHAPTER 2

LITERATURE REVIEW

2.1 Introduction

Global pollution is becoming more severe nowadays due to the rapid development of technology, which requires high energy usage. Burning of fossil fuels remains the primary energy extraction method available in the market. Increasing consumption of fossil fuels, such as coal, petroleum, and natural gas, has led to severe environmental issue due to the emission of dangerous gases such as carbon dioxide. Dependency on fossil fuel does not ensure sustainability for future generation, as the reservoir for fossil fuel is limited and will eventually be depleted in the near future. Hence, a paradigm shift is necessary to reduce reliance on fossil fuels and replace them with clean energy harvesting system.

Renewable energy is widely promoted globally as an alternative energy sources. It offers attractiveness in terms of low pollution impact, economic development, and energy supply diversification. However, the application of renewable energy is still limited due to its poor efficiency and high investment cost. Most renewable energy sources, such as wind energy, tidal energy and solar energy are rely heavily on nature factors for energy harvesting and exhibit low reliability. Energy output is highly dependent on time, location, and weather, causing fluctuations in power generation throughout the day. Although

renewable energy provides clean energy with minimal environmental impact, it still suffers from inconsistency in power output, limiting its application. Incorporating an energy storage system into renewable energy systems can help solve the consistency problem, as unused and excess energy can be stored in batteries and used to power the grid during periods of low renewable energy output.

In the transportation sector, electric vehicles (EVs) have gained attention due to their ability to reduce greenhouse gas emissions by eliminating fossil fuels in power generation. Battery is the most popular alternative to replace the internal combustion engine of the vehicle (Chen et al., 2019). Some of the most common batteries used in EVs include lithium-ion batteries, nickel-cadmium batteries, nickel-metal hydride batteries, and lead-acid batteries. Among these options, the lithium-ion battery is the most popular due to its high energy capacity and longer cycle life. However, it also presents environmental issues, as there is currently no proper solution for recycling used lithium-ion batteries. The recycling rate of lithium-ion batteries is very low due to high costs and immature technology. Lithium batteries are often contaminated with metals such as nickel, cobalt, and manganese, which are harmful and can contaminate the soil if the batteries are disposed of in landfills. The significant increase in the usage of lithium-ion batteries has raised major environmental concerns due to the pollution they caused. The extraction of lithium from the earth's crust harms the soil and contaminates the surrounding air. Moreover, lithium-ion batteries are also prone to thermal runaway due to their narrow range of operating temperature (Tan et al., 2011). Currently, the performance of lithium-

ion batteries is limited by existing technology, and their energy density is nearly at its peak. It is predicted that the energy density of the battery can only be increased by 30% in the future, limiting the travel distance to 500 km (Van, 2014). Therefore, it is crucial to explore new types of batteries as substitutes for lithium-ion batteries to extend the travel distance of EVs.

2.2 Metal-air Battery

A metal-air battery is a new type of energy system in which the anode is made of a specific metal, with an air cathode separated by an electrolyte. The energy is extracted from the metal anode through its oxidation, while oxygen is reduced at the air cathode. The electrolyte facilitates the movement of ions, enabling the completion of the redox reaction. Various metals, such as lithium, aluminium, sodium, potassium, and zinc, are available as options for the metal anodes in metal-air batteries. Metal-air batteries are considered promising candidates for replacing lithium-ion batteries, as studies have shown that their energy density is about three to ten times higher than that of lithium-ion batteries (Zhou et al., 2020).

Metal-air batteries exhibit different behaviors depending on the type of metal anode used. However, they share the same fundamental principle: the consumption of the metal anode through oxidation and the reduction of oxygen at the cathode in the presence of an electrolyte, which facilitates ion movement. This redox reaction generates electrons and produces electricity. The electrochemical reactions are illustrated as in Eq 2.1 and Eq 2.2.

Anode (oxidation):



Cathode (reduction):



Where M – metal anode

n – oxidation number

2.3 Aluminium-Air Battery

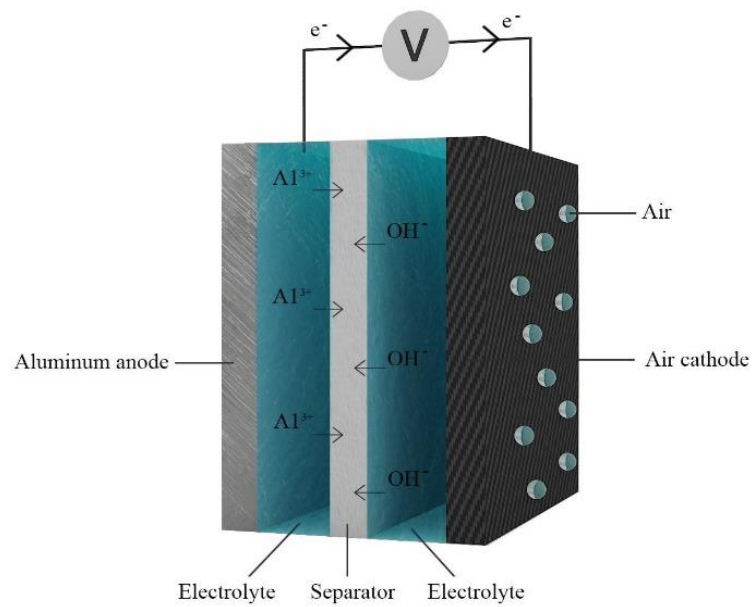


Figure 2.1: Structure of an Aluminum-air Battery

Among the various types of metal-air batteries, aluminium-air batteries show vast potential as future energy storage systems. Aluminium-air batteries

possess a high energy density of 8.1 kWh.kg^{-1} and a high theoretical potential of 2.7 V . This is due to aluminium being low cost, readily available, and having good electrical properties. Moreover, the recycling process for used aluminium is mature, further encouraging the application of aluminium as a metal anode. Besides that, the aluminum-air battery has show good performance in high temperature. It is observed that at high temperature up to 100°C actually facilitate the electrochemical reaction and the aluminum-air battery can generate higher OCV (Hu et al., 2019). As for low temperature below 0°C , the aluminium-air battery benefits from slow corrosion and hence, releasing lower amount of hydrogen at a drawback of reduced power output (Zuo et al., 2019). Although the structure of an aluminium-air battery is simple as illustrated in Figure 2.1, the design becomes complicated due to the different components that affect its performance in various ways. Extensive studies have been conducted to develop aluminium-air batteries, yet there is no universal solution for a design that incorporates all the components of an aluminium-air battery. Table 2.1 summarizes a comparison of the electrical properties of various types of metal-air batteries. When comparing the theoretical performance of the aluminum-air battery with other types of metal-air batteries, the aluminum-air battery ranks second in terms of energy density. Although the lithium-air battery shows the highest energy density, it is not suitable for development due to pollution issues caused by lithium. Meanwhile, aluminum exhibits high recyclability, and the recycling process is mature and affordable. Hence, the aluminum-air battery becomes a better choice compared to the lithium-air battery. On the other hand, the voltage offered by the aluminum-air battery is about 60%-70% of that of the sodium-air battery, but it has a much higher energy

density, making it a better selection over the sodium-air battery. Among all the various types of metal-air batteries, the aluminum-air battery can provide optimum energy density and cell voltage while offering sustainability as an additional benefit.

Table 2.1: Electrical properties of various type of metal-air battery (Liu et al., 2017)

Type of battery	Cell Voltage, V	Energy density, Wh kg ⁻¹
Li/air	2.4	13000
Al/air	1.2-1.6	8100
Na/air	2.3	1600
Mg/air	1.2-1.4	6800
Zn/air	1.0-1.2	1300

2.4 Aluminium anode

The main energy source for the aluminium-air battery comes from the aluminium anode. The aluminium anode will be consumed in the electrochemical reaction and generate electricity by releasing electrons. During this electrochemical process, the mass of the aluminium will gradually reduce and used up eventually. To recharge the aluminium-air battery, a physical change of the aluminium anode is required. Hence, it is a type of primary battery that cannot be recharged by reversing the electrochemical reaction. Pure aluminium anode is not an ideal candidate as the anode for the aluminium-air battery. This is because when pure aluminium is used as the anode, the aluminium anode can suffer severe corrosion by forming Al₂O₃ and Al(OH)₃ layers on the anode surface when reacting with water (Doche et al., 1999). This

reduces the aluminium utilization efficiency as the oxide layer impedes the reaction, and hydrogen gas is generated as a parasitic reaction. Therefore, there is a need to reduce the corrosion rate of the pure aluminium anode.

Alloying pure aluminium is an effective method to reduce corrosion (Macdonald et al., 1988). The presence of zinc in aluminium alloy can help improve the life cycle of the aluminium-air battery as zinc can reduce the hydrogen evolution (Pino et al., 2015). The presence of indium can control the generation of hydrogen and cause a positive shift in anode potential (Sun et al., 2015). Furthermore, aluminium with tin as an additive can improve the aluminium dissolution rate in an aqueous solution while hindering corrosion (Sun et al., 2015). A study has concluded that the aluminium-air battery's voltage range and component dissolution are not affected by using aluminium alloy with high purity grade (MacDonald et al., 1988; Tuck et al., 1987). Cho et al. (2015) analyzed and compared the aluminium anode with 99.5% purity and 99.99% purity. It has been shown that the discharge voltage is an important factor that affects the corrosion rate of the aluminium alloy.

Studies were also conducted to compare the performance of industrial aluminium alloys as the anode in aluminium-air battery. Aluminium alloy 1070 was used as an anode, and it was found that the presence of calcium (Ca) is an effective corrosion inhibitor (Xu et al., 2019). It can help to reduce the corrosion rate while improving the discharge voltage, which in turn improves the anode efficiency. A performance analysis between aluminium alloys 1085, 2024, and 7475 as anodes was performed by Pino et al. (2014, 2015). The results showed

that aluminium alloy 7475 performed the best and recorded a specific capacity of 426 mAh.g^{-1} which is higher than using aluminium alloy 2024 with specific capacity of 242 mAh.g^{-1} . The improvement is due to the addition of copper, Cu which worked well in reducing the corrosion. The performance of various aluminium grades: 1050, 2011, 3003, 4031, 5052, 6061, 7050, 8011 as anodes were investigated (Fan et al., 2016). The results revealed that aluminium alloy 8011 performed the best with an energy density of 2243 kWh.kg^{-1} .

Generally, it is certain that the performance of pure aluminium is weak in the aluminium-air battery. It is subjected to a high corrosion rate while also providing a low output voltage, which reduces the anodic efficiency. Using aluminium alloy as the anode in the aluminium-air battery is necessary. Additives such as Zn, In, Ga, Mg, and Tin have shown positive effects in reducing the corrosion rate, which can aid in enhancing the anodic utilization efficiency of the aluminium anode. However, an improper selection of the aluminium alloy as the anode may cause the battery's performance to drop. Hence, it requires some knowledge on the selection of an aluminium alloy so that the performance of the aluminium-air battery can be improved.

2.5 Electrolyte

In an electrochemical reaction, the electrolyte is an important component that facilitates the movement of ions between the anode and the cathode. In an aqueous aluminium-air battery, the electrolyte can be alkaline, acid, or neutral.

Among the three different types of electrolytes, alkaline has been proven to perform the best in power generation. Wang et al. (2013) conducted a comparison of three different types of electrolytes in an aluminium-air battery. The electrolytes used were sulfuric acid (acid electrolyte), potassium hydroxide (alkaline electrolyte), and potassium nitride (neutral electrolyte). The comparison indicated that the potassium hydroxide electrolyte had the highest reaction rate of aluminium compared to potassium nitride and sulfuric acid. For instance, the maximum energy density achieved by the potassium hydroxide electrolyte was 72.57 Wh.kg^{-1} as opposed to 9.45 mWh.kg^{-1} in sulfuric acid electrolyte. The open-circuit voltage of the aluminium battery tends to reduce as the pH value decreases (Ma et al., 2013). Since alkaline electrolytes perform better than acidic and neutral electrolytes, most studies focus on optimizing the alkaline electrolyte in an aluminium-air battery. The most popular alkaline electrolytes are potassium hydroxide (KOH) and sodium hydroxide (NaOH). A gradual increase in the concentration of KOH electrolyte ranging from 0.2M to 4M was performed in aluminium-air batteries (Pino et al., 2014). The battery capacity tends to increase due to the increasing amount of OH^- ions in a higher concentration of KOH solution. However, high OH^- ion concentration also induces a higher corrosion rate. Hence, there is a compromise between electrical performance and hydrogen generation rate in the system. Numerical work supports the observation from Wang et al. (2015). The simulation was conducted using FLUENT, and it concluded that the amount of OH^- ions affects the corrosion rate and current density of the aluminium-air battery. To achieve a high current density, the concentration of the electrolyte should be high. This is attributed to the increase of concentration of OH^- ions. Nevertheless, the

corrosion rate is also faster due to the high concentration of electrolyte used. However, if the concentration of the electrolyte is too high, it can actually reduce the corrosion rate of the aluminium anode in the KOH electrolyte (Wu et al., 2020). A 16M of potassium acetate-potassium hydroxide (HCPA-KOH) aluminium-air battery was proposed. It can reduce the hydrogen generation rate from $0.738 \text{ ml}\cdot\text{min}^{-1}\text{cm}^{-2}$ in a pure KOH electrolyte to $0.127 \text{ ml}\cdot\text{min}^{-1}\cdot\text{cm}^{-2}$. In response to the reduction in the corrosion rate, the specific capacity is improved to $2324 \text{ mAh}\cdot\text{g}^{-1}$ instead of $745 \text{ mAh}\cdot\text{g}^{-1}$ in a pure KOH electrolyte. This suggests that severe mass loss is observed in pure KOH electrolyte. Instead of contributing to power generation, the mass loss is wasted in corrosion.

Another way of suppressing corrosion is to limit the contact between the KOH electrolyte and the aluminium anode. Tan et al. (2021) demonstrated the use of a polypropylene-based aluminium-air battery to reduce corrosion. In the design, a polypropylene pad is used as a medium to absorb KOH electrolyte. The polypropylene pad serves not only as an electrolyte but also as a separator to separate the anode and cathode. Since the supply of KOH electrolyte to the aluminium anode is limited, the corrosion becomes less severe. By increasing the concentration of KOH, the electrical performance also improves.

Sodium hydroxide (NaOH) is another popular electrolyte that is widely investigated. The voltage output behaves linearly with increasing the concentration of NaOH (Ilyukhina et al., 2017). However, this can also increase the hydrogen generation rate due to promoting corrosion in the aluminium anode (Wang et al., 2013). In a 5M NaOH electrolyte aluminium-air battery, the

battery achieved the highest performance of 44.9 mW.cm^{-2} compared to the performance achieved for 1M to 4M NaOH electrolyte. Nevertheless, it showed the poorest anodic efficiency due to a higher corrosion rate. The differences between KOH and NaOH electrolytes in the aluminium-air battery were analyzed by Fan et al. (2015). A pure aluminium anode was used, and the concentration of both electrolytes was fixed at 4M. Under the discharge current at 10 mA. cm^{-2} on the aluminium-air battery, KOH electrolyte provided a specific capacity of 2479 mAh.g^{-1} , as opposed to 2308 mAh.g^{-1} in the NaOH solution. In terms of anodic efficiency, the KOH electrolyte achieved an additional 20% compared to the NaOH electrolyte and recorded an anodic efficiency of 85.3%. These results show that the KOH electrolyte is the best candidate for the aluminium-air battery electrolyte.

Most of the studies focusing on using alkaline electrolyte always suffer from corrosion of the aluminium anode. To reduce this effect, it is suggested to use a neutral or acidic electrolyte. However, using a neutral electrolyte shows very poor performance. A combination of using sodium chloride (NaCl) with pure aluminium shows no performance as there is no aluminium dissolution (Fan et al., 2015). A comparative study comparing the performance of an aluminium-air battery using NaCl and NaOH was conducted using aluminium alloy doped with Mg and Sn (Ma et al., 2014). The aluminium-air battery recorded an operating voltage of 0.43 V for NaCl electrolyte, whereas it was 1.22 V for NaOH electrolyte, suggesting that although NaCl was good in reducing corrosion, the electrical performance was also significantly affected. The idea of using an acidic electrolyte such as hydrochloric acid (HCl) and

sulphuric acid (H_2SO_4) was proposed to reduce the dendrite formation along the surface of the aluminium anode (Li et al. 2016). Rota et al. (2017) investigated the performance of an aluminium-air battery in alkaline and acid media. The open-circuit voltage (OCV) is generally 30% lower for acid electrolyte compared to alkaline electrolyte. The result matches the conclusion drawn by the study from Di Palma et al. (2021), in which the OCV reduces with decreasing pH value. Although acidic electrolyte generates a lower OCV and operating voltage, it can actually increase the anodic efficiency due to a lower corrosion rate.

In short, the aluminum-air battery exhibits a declining performance trend when ranked by the type of electrolyte used, with the alkaline electrolyte showing the best performance, followed by the acid electrolyte, and finally the neutral electrolyte. Although alkaline electrolyte shows the highest OCV and discharge voltage, it is usually associated with a high corrosion rate, which reduces the anodic efficiency. Extensive work is still required to ensure high performance while also limiting the corrosion rate, which, in turn, increases the anodic efficiency.

2.6 Dual electrolyte system

The idea of using a dual electrolyte system in an aluminium-air battery is proposed to further improve the performance of the battery. Using sulphuric acid has shown enhancement in the oxidation reduction reaction (ORR) at the

cathode (Wang et al., 2016). Since the aluminium-air battery requires good ORR to perform better, it is suggested to use an acidic medium along the cathode side of the battery. In this system, two different types of electrolytes are used in the anode and cathode with a separator in between to prevent crossover of the electrolyte.

Studies have revealed positive performance of the aluminium-air battery using a dual electrolyte system. Chen et al. (2015) combined a dual electrolyte system with alkaline and acid electrolytes in an aluminium-air battery as shown in Figure 2.2. The anolyte was a KOH solution, while the catholyte was sulfuric acid (H_2SO_4). This configuration further enhanced the power density by almost 100% compared to a single electrolyte system, reaching a peak of $176 \text{ mW}\cdot\text{cm}^{-2}$. In another work done by Wen et al. (2020), the alkaline-acid electrolyte combination also improved the open-circuit voltage. There was about a 30% improvement in the open-circuit voltage compared to traditional aluminium-air batteries.

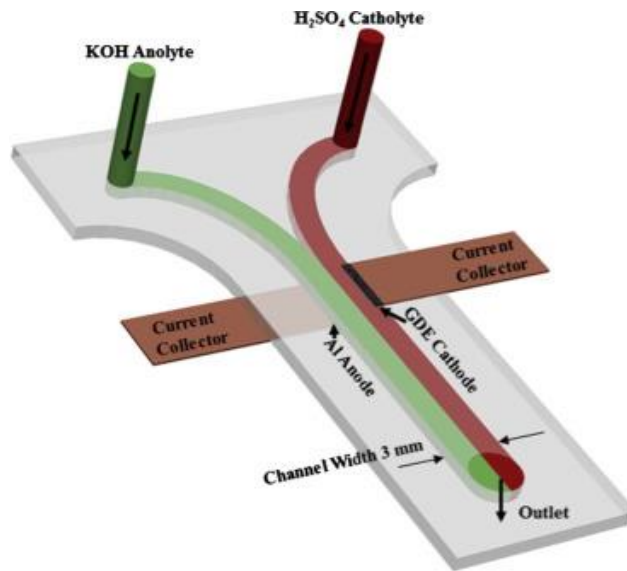


Figure. 2.2: A dual electrolyte microfluidic aluminum-air battery (Chen et al., 2017). Copyright 2017 Elsevier

Tan et al. (2022) proposed a polypropylene-based separator for a dual electrolyte system aluminium-air battery and concluded that the dual electrolyte system performed 30% better in terms of OCV. In the study, KOH was used as the anolyte while H_2SO_4 was used as the catholyte. The peak power density of the aluminium-air battery was improved greatly from $100 \text{ mW}\cdot\text{cm}^{-2}$ for a single electrolyte system to about $350 \text{ mW}\cdot\text{cm}^{-2}$ for a dual electrolyte system. Moreover, a dual electrolyte system was also made possible by adding methanol to the anolyte (Wang et al., 2014). The KOH anolyte was mixed with methanol, while the catholyte used was a KOH solution. The presence of methanol was able to improve the coulomb efficiency up to 74% due to the lower corrosion rate at the anode side. In comparison, the coulomb efficiency of the single electrolyte system was about 2.4% at $30 \text{ mA}\cdot\text{cm}^{-2}$. Teabnamang et al. (2020) conducted a similar study to investigate the effect of the water content in the mixture of methanol/KOH in the anolyte of an aluminium-air battery. A higher

water content corresponded to a higher maximum power output in the system and induced the anode to corrode at a higher rate. The power density improved from 4.78 mW.cm^{-2} to 19.60 mW.cm^{-2} when the water content increased from 0% to 20% in the methanol/KOH mixture. Additionally, the open-circuit voltage showed a slight improvement from 1.45 V to 1.50 V. This improvement was due to a lower internal resistance in high water content. The effects of reducing the corrosion rate are more significant than those of reducing the battery's internal resistance (Chen et al., 2016; Chen et al., 2017). A specific capacity of 2507 mAh.g^{-1} and a Coulomb efficiency of 84.1% were noted at 0% water content, which is higher than the methanol/KOH electrolyte with water content. Although the electrical performance is improved due to the addition of methanol, it is not widely applied due to its toxicity.

Ethylene glycol/ethanol was also proven to be an effective solution for the anolyte, as indicated by the work of Phusittananan et al. (2020). A polymer gel electrolyte was used as the cathode. This combination of electrolytes enabled an improvement from 1.25 mW.cm^{-2} to 3.75 mW.cm^{-2} compared to the case when using 3 M KOH only. This is because the ethylene glycol/ethanol anolyte can reduce the polarization resistance as a result of lower charge transfer resistance. However, the performance is considered lower compared to adding methanol to the electrolyte. Nevertheless, it provides a greener approach as methanol is harmful and toxic to the environment.

Combining two different types of gel electrolyte as both the anolyte and catholyte is also made possible by Wang et al. (2022). This is considered a solid-state battery, thus free from leaking issues. The discharge performance is 0.5 V

higher than that of a single-gel electrolyte aluminium-air battery.

Zhao et al. (2020) investigated the performance of a dual electrolyte aluminium-air battery through numerical simulation and compared it with experimental data. NaCl was used as the anolyte, while NaOH was used as the catholyte. It was revealed that the power density of the aluminium-air battery was affected by the thickness of the electrolyte. A thin thickness is essential to improve the power density and, hence, improve the discharge capacity.

The studies revealed that a dual electrolyte system has shown superior performance compared to the single electrolyte system due to the enhancement along the cathode side. The ORR is improved by using an acidic electrolyte. However, the performance of the dual electrolyte system is affected by the type of separator used to separate the anolyte and catholyte, which remains a challenge in designing a dual electrolyte aluminium-air battery. Tri-electrolyte aluminium-air battery is also made possible in recent studies (Wang et al., 2020). A third electrolyte, namely the bridging electrolyte, is introduced and sandwiched between the anolyte and catholyte as indicated in Figure 2.3. The three electrolytes used in this study are methanol/NaOH (anolyte), NaCl (bridging electrolyte), and HCl (catholyte). This design generates an OCV of 2.2 V while effectively reducing the self-corrosion along the aluminium anode. This can serve as a direction for future studies as the literature on trielectrolyte systems is still limited. However, the separator used to separate the electrolytes remains a critical problem that affects the life cycle of the battery.

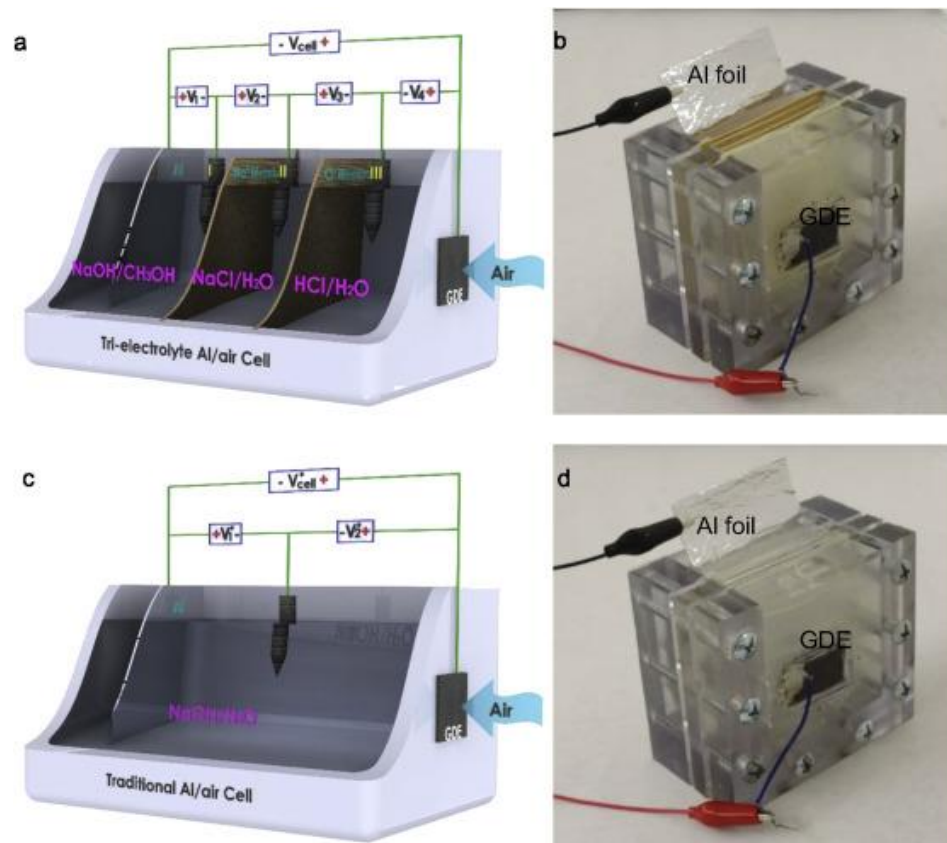


Figure 2.3: (a) Schematic diagram of a tri-electrolyte aluminum-air battery, (b) real trielectrolyte aluminum-air battery, (c) schematic diagram of single electrolyte aluminum-air battery, (d) real single electrolyte aluminum-air battery. (Wang et al., 2020). Copyright 2020 Elsevier

2.7 Separator

There are two main problems associated with aqueous aluminium-air batteries. Firstly, liquid electrolytes require proper sealing to prevent leakage. Secondly, liquid electrolytes require a separator to separate the anode and cathode and prevent short circuits. A proper selection of a separator is needed to solve both problems simultaneously.

These issues can be resolved by introducing solid electrolytes. Solid electrolytes can act as a separator, separating the anode and cathode, while also eliminating the leakage problem. One commonly used solid electrolyte is gel electrolyte. Several researchers have used gel electrolytes as corrosion inhibitors in aluminium-air batteries. Zhang et al. (2014) conducted a study on polyacrylic acid-based gel electrolytes. The gel electrolyte showed similar ionic conductivity (460 mS.cm^{-1}) to the aqueous electrolyte while effectively inhibiting corrosion at the anode. This electrolyte was able to produce a power density of 91.13 mW.cm^{-2} . Mohammad (2008) created a hydroponics gel from KOH electrolyte, which showed similar performance to the aqueous electrolyte, with the concentration of KOH positively correlated to the maximum power output. However, this also induced a higher corrosion rate.

A simpler and more cost-effective approach for solid electrolytes is using filter paper as in Figure 2.4. The electrolyte can be absorbed by filter paper through capillary action. Wang et al. (2019) used paper to absorb a small amount of KOH and NaCl electrolyte, which acted as a separator. In their study, paper was soaked with NaOH and NaCl electrolytes through capillary action. The soaked paper was then sandwiched between the anode and cathode of an aluminium-air battery. The power density recorded for KOH and NaCl electrolytes were 21 mW.cm^{-2} and 6.7 mW.cm^{-2} , respectively. This design is small, low cost, and simple, as it does not require an electrolyte circulation system to feed fresh electrolyte to the anode. A maximum voltage output of 13.2 V was achieved when the batteries were connected in series to form a battery

pack. Additionally, paper soaked with KOH electrolyte is also possible, with a power density of 28 mW.cm^{-2} , which is higher than NaOH electrolyte (Katsoufis et al., 2020). Hu et al. (2012) demonstrated that paper has low resistance (about $1 \Omega.\text{sq}^{-1}$) and possesses good electrical conductivity and mechanical flexibility when coated with a layer of carbon nanotubes (Hu et al., 2009). Avoundjian et al. (2017) designed a 9 cm^2 aluminium-air battery with paper as the separator, providing a total power of 3 mW. Shen et al. (2019) suggested a microfluidic aluminium-air battery using a paper separator, which achieved an energy density of 2900 Wh.kg^{-1} while maintaining a specific capacity of 2750 Ah.kg^{-1} . Most studies involving solid electrolytes in aluminium-air batteries show good performance and can be further developed for miniature applications.

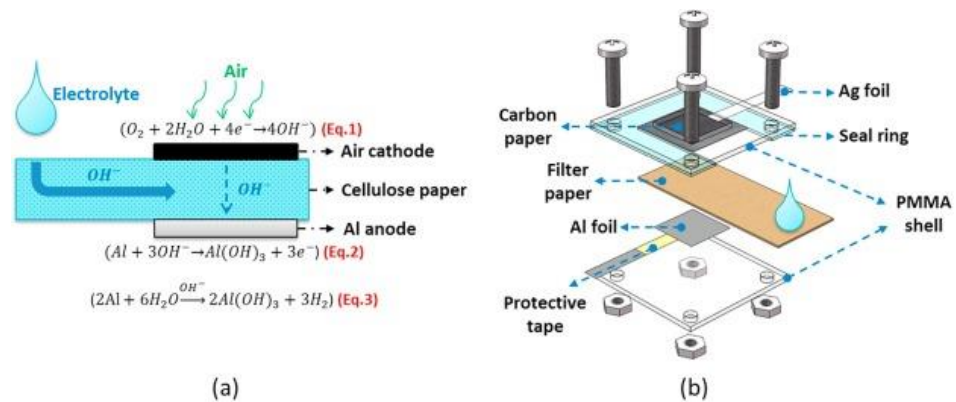


Figure 2.4: Paper based aluminum-air battery (a) working principle, (b) cell composition. (Wang et al., 2019). Copyright 2019 Elsevier

The selection of the battery separator is essential, as it will influence the battery's performance. The separator should have porous properties to allow the movement of ions, which is crucial for electrical performance. The separator's nanoporous structure can help retain more electrolytes, ensuring a uniform

deposition of the electrolyte (Song et al., 2019). Additionally, the separator should possess good thermal stability and mechanical strength (Moon et al., 2019). A cellulose-based separator is an ideal candidate as it satisfies both requirements (Pan et al., 2018; Pan et al., 2019). It offers advantages such as thermal stability, uniform pore size distribution, and wettability. A double-sided conductive separator with a porous and conductive layer in its structure was able to provide a stable and longer cycle life in an aluminium-air battery (Pan et al., 2019). However, the main drawback of using the separator is that it tends to swell and weaken when immersed in an electrolyte for an extended period. The weakening effect has been studied, and it has been discovered that the cellulose separator loses its Young's modulus over time. Furthermore, the expansion coefficient tends to increase when the cellulose separator is immersed in the electrolyte (Xie et al., 2019).

The selection of the separator is crucial as it plays an important role in separating the anode and cathode, facilitating the movement of ions, and supplying electrolyte to the battery. The structure should be made porous and should not degrade over time since the aluminium-air battery needs to function for an extended period.

2.8 Cathode

The air cathode plays a crucial role in an aluminium-air battery as it allows the diffusion of oxygen from the atmosphere to the anode. The oxygen

reduction reaction (ORR) along the cathode should be kept high to ensure fast electrochemical reactions in the aluminium-air battery, resulting in higher power generation. The structure of the air cathode is crucial as it faces four main challenges. Firstly, it should be designed to improve the ORR by incorporating electrocatalysts that increase the surface area and provide more binding sites for the ORR (Yang et al., 2002). Secondly, flooding is a critical issue along the air cathode, as water molecules tend to accumulate on the surface and block the diffusion of oxygen. The air cathode should exhibit hydrophobic properties to prevent water molecules from sticking to the surface and blocking the pores (Wu et al., 2003). Additionally, the alkaline electrolyte reacts with carbon dioxide in the atmosphere, leading to the precipitation of carbonate compounds. This results in a loss of electrical conductivity over time and a decrease in battery performance (Bidault et al., 2009). Lastly, the air cathode is prone to water evaporation due to its porosity, which can eventually lead to the drying out of the electrolyte (Wu et al., 2003). Therefore, the architecture of the air cathode is complex and requires careful design to ensure optimal performance in an aluminium-air battery. The structure of the air cathode is as shown in Figure 2.5.

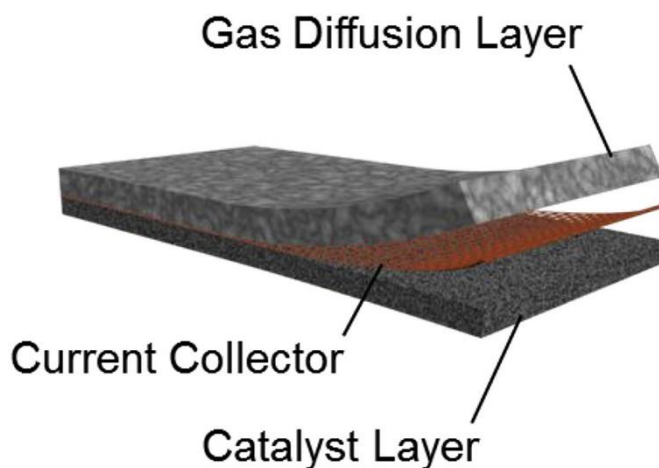


Figure 2.5: Structure of an air cathode (Liu et al. 2020). Copyright 2020 Elsevier

Activated carbon is widely used as a raw material for constructing the air cathode due to its benefits such as low cost, chemical stability, environmental friendliness, and good electrocatalytic activity. Liu et al. (2018) demonstrated an activated carbon-based cathode by incorporating $\text{Cu}_2\text{O-Cu}$ and found that it improved the cathode's performance due to enhanced catalytic activity. On the other hand, Zhang et al. (2018) modified activated carbon with $\text{Co}_3\text{O}_4/\text{NiCo}_2\text{O}_4$ resulting in a power density boost to 1810 mW m^{-2} , approximately 104 % higher than the traditionally used activated carbon air cathode. These findings demonstrate that activated carbon performs well as an air cathode material.

Various catalysts have been used to improve the ORR of air cathodes, including alloys, metals, and transition metal oxides (Cheng et al., 2012). Ren et al. (2019) concluded that modified activated carbon can alter the characteristics of the activated carbon and improve its performance compared to bare activated carbon. Lai et al. (2017) employed a Fe-N-C catalyst in an aluminium-air battery, which improved the ORR and achieved performance on par with Pt/C air cathodes. A high discharge current of 1.33 V was recorded at

a discharge current density of 50 mA cm^{-2} . Another catalyst that performs similarly to Pt/C air cathodes is Cu/N/C electrocatalyst (Wang et al., 2018). When applied in an aluminium-air battery, this catalyst outperformed a 5 wt% Pt/C air cathode.

Silver (Ag) doped MnO_2 is used as a catalyst in an aluminum-air battery, and the results showed significant improvement in catalytic activity compared to using MnO_2 alone (Sun et al., 2017). The specific surface area of the air cathode is increased by three times through the addition of Ag. Thus, providing more surface area for the electrochemical reaction. Moreover, the stability of using Ag- MnO_2/C is better than that of Pt/C, suggesting that an inexpensive catalyst can outperform the notoriously expensive Pt catalyst. Peak power density of 315 mW cm^{-2} was recorded in an electrochemical performance test of the aluminium-air battery. Similarly, Huo et al. (2017) achieved a peak power density of 318 mW cm^{-2} by using $\gamma\text{-MnO}_2$ as a catalyst. $\gamma\text{-MnO}_2$ was heat-treated at $300 \text{ }^\circ\text{C}$ with argon gas to improve oxygen vacancies in its structure, resulting in improved ORR. The power density improvement was approximately 80% compared to $\gamma\text{-MnO}_2$ without any heat treatment.

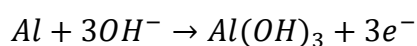
A combination of Co and Fe as catalyst in a carbon-based air cathode has shown a 20% improvement in power density compared to Pt/C (Jiang et al., 2021). This catalyst provides abundant interfaces along its structure and is well suited for both alkaline and neutral media. However, the improvement in power density is less significant in a neutral medium, with only a 9% improvement compared to 20% in an alkaline medium. Carbon nitride is a catalyst capable of

providing four-electron oxidation kinetics, greatly enhancing the ORR in the air cathode (Niu et al., 2018). When used in a rechargeable aluminium-air battery, the peak power density reached 89 mW cm^{-2} , higher than Pt/C+RuO₂/C with a peak power density of 79 mW cm^{-2} . This suggests that there are several cheaper options capable of outperforming Pt as a catalyst.

2.9 Electrochemical Mechanisms of Aluminium-air Battery

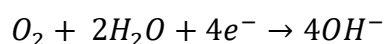
Redox reaction occur within the aluminium-air battery, leading to an exchange of ions between the anode and cathode and generating electricity in the process. The specific half-cell reactions depend on the type of battery being used. In a single electrolyte aluminium-air battery, the half-cell reactions are indicated below (Xie et al., 2019).

Oxidation reaction at the anode in an alkaline electrolyte:



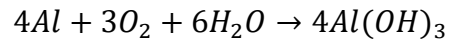
$$E = -2.55 \text{ V vs. Ag/AgCl.} \quad (2.3)$$

Reduction reaction at the cathode in an alkaline electrolyte:



$$E = 0.2 \text{ V vs. Ag/AgCl.} \quad (2.4)$$

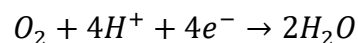
Overall redox reaction:



$$E = 2.75 V \quad (2.5)$$

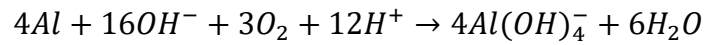
Based on the reaction, it is observed that the aluminium anode will eventually be converted into aluminium hydroxide through the oxidation reaction. Eventually, it is necessary to replace the aluminium anode over time to extend the lifespan of the aluminium-air battery. This concept is known as mechanical recharge since aluminium-air battery does not offer recharging capabilities by reversing the movement of ions. On the other hand, only oxygen and water are consumed at the cathode, and therefore, there is no concern with the oxygen supply as it is found abundantly around the atmosphere. However, it is noted that the battery required water molecules to breakdown the oxygen. The water can be obtained from the alkaline electrolyte. The output voltage and current of the aluminium-air battery widely depends on the ORR occurring at the cathode. It is essential to improve the ORR at the cathode for better performance. The dual electrolyte system in an aluminium-air battery can help to enhance the ORR rate through the introduction of acidic electrolyte at the cathode. The ORR is improved in such a way as shown in the Eq. below (Chen et al., 2017) .

Reduction reaction at the cathode in an acidic electrolyte:



$$E = 1.03 V \text{ vs. } Ag/AgCl. \quad (2.6)$$

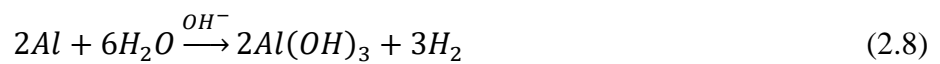
Overall redox reaction:



$$E = 3.58 V \quad (2.7)$$

The theoretical voltage shows an improvement of about 30 % as it can increase the OCV from 2.75 V to 3.58 V. This improvement has the potential to enhance the output current and power of the aluminium-air battery. However, there is an unavoidable phenomenon observed in both designs of the aluminium-air battery. The aluminium is known for its bad performance in alkaline solution. In such conditions, it tends to react with the water in the alkaline electrolyte in the presence of OH⁻ ions. This is known as corrosion and is indicated in Eq. 3.6 (Liu et al., 2017). As a result, the aluminium utilization rate will be reduced as not all aluminium anode is consumed in electricity generation. Hydrogen will be released as a byproduct due to the corrosion.

Corrosion reaction of the aluminium:



2.10 Summaries

In the aforementioned context, most aluminium-air batteries still face challenges in terms of low performance, corrosion issues, and leakage problems. The low performance is often attributed to the poor selection of the aluminium

anode and electrolyte. Corrosion issues can be mitigated by opting for acidic or brine electrolytes, albeit at the expense of compromised electrical performance. Conversely, the leakage problem can be addressed by using solid electrolytes, but this also leads to lower electrical performance. The proposed solutions only address the mentioned problems individually, lacking a universal solution that simultaneously reduces corrosion while improving performance. The relationship between corrosion rate and performance is intricately linked, as a higher corrosion rate of the aluminium anode can enhance the electrical performance of the aluminium-air battery due to faster aluminium dissolution during the electrochemical reaction

CHAPTER 3

METHODOLOGY

3.1 Design of the Aluminium-air Battery

This study focuses on the investigation of polypropylene-based separator for aluminium-air battery. The addition of polypropylene aims to reduce the corrosion of the aluminium anode by limiting the supply of electrolyte to the anode, thereby minimizing parasitic reactions. Polypropylene serves two purposes when placed between the anode and cathode. Firstly, it acts as a separator to prevent short circuits. Secondly, it provides a medium that facilitates the movement of ions between the anode and cathode.

3.1.1 Structure of a Single Electrolyte System

The design of the polypropylene-based aluminium-air battery is illustrated in Figure 3.1. The battery reaction area is about 5 cm x 5 cm. The battery consists of four components; two acrylic plates are used as casing to enclose the aluminium-air battery, an anode made of aluminium foil (100% Al and 0.01 mm thick), an air cathode made of carbon fiber cloth (0.167 mm), and a separator made of a polypropylene absorbent pad (Crisben, 100% Polypropylene, ~89% porosity, 200 gsm). Acrylic-based material is chosen as the enclosure of the battery due to its inert properties, which do not affect the

reaction of the aluminium-air battery. An air-breathing window of 5 cm x 5 cm is cut on the acrylic plate in the air cathode side to allow the diffusion of oxygen from the atmosphere to the air cathode. Potassium hydroxide (KOH) (ACS Reagent, System Chemicals) is used as the electrolyte in this study, with a concentration varied from 1 M to 3 M. The electrolyte is prepared by dissolving the KOH pellet into distilled water, and 1.5 ml of KOH solution is injected into the polypropylene separator. The polypropylene will absorb the KOH electrolyte gradually. The aluminium foil is also cut to the reaction area of 5 cm x 5 cm and inserted into the enclosure. The advantages of this type of battery are its low cost and simple fabrication process. Moreover, the parasitic reaction at the anode can be controlled by limiting the amount of electrolyte present in the battery, eliminating the need for a bulky electrolyte recirculation system.

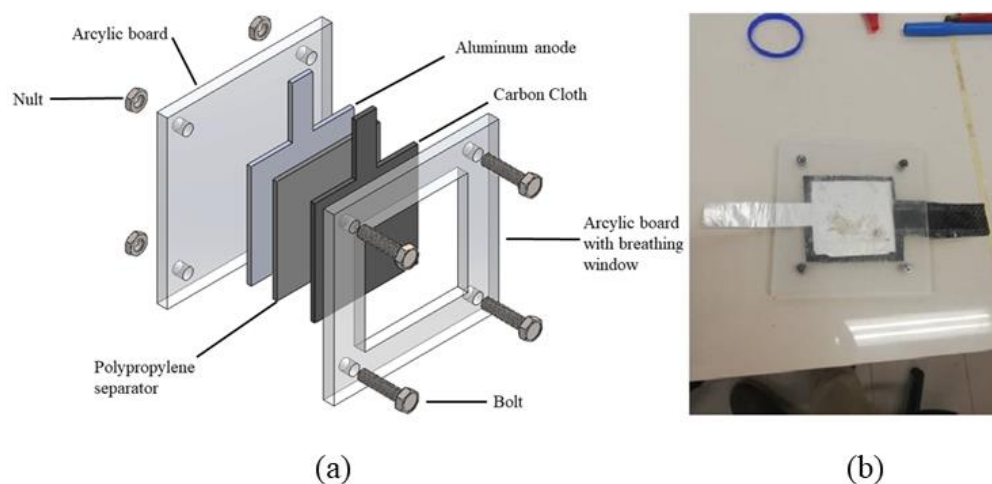


Figure 3.1: (a) Schematic diagram of single electrolyte aluminium-air battery, (b) Prototype of single electrolyte aluminium-air battery.

3.1.2 Structure of a Dual Electrolyte System

Figure 3.2 illustrates the design of the dual electrolyte polypropylene-based aluminium-air battery. A filter paper (Smith, Qualitative filter paper, medium speed with a pore size 8-10 μm) plays the role of a separator, isolating the anode from the cathode of the aluminium-air battery. Acrylic boards were used to construct the body of the battery to contain the electrodes and separator. The aluminium anode used in this study was a commercial-grade aluminium alloy 6061 with a thickness of 2 mm. A polypropylene absorbent pad from Crisben, with a thickness of 2 mm (100% Polypropylene, ~89% porosity, 200 gsm), was used as the absorbent for the alkaline electrolyte at the anode and acidic electrolyte at the cathode. Two breathing windows measuring 40 mm x 45 mm were cut on the acrylic board at the cathode side to supply oxygen to the battery. The cathode is made of a graphite plate, which provides a medium for the oxygen reduction reaction (ORR) and acts as a current collector for the battery. A rubber gasket is used as a sealant and houses the aluminium anode and graphite plate cathode in the battery. Lastly, bolts and nuts were used to secure the battery. The current design limits self-corrosion at the anode by controlling the amount of electrolyte absorbed by the polypropylene pad. This design eliminates the need for an electrolyte recirculation system.

Potassium hydroxide electrolytes with different molarities were used in the study. The electrolyte is prepared by dissolving a potassium hydroxide pellet (ACS Reagent, System Chemicals) in distilled water. A total of 4 ml of KOH electrolyte was absorbed by the polypropylene pad and used anolyte at the

anode side. On the other hand, sulfuric acid with different concentrations was prepared by diluting a concentrated sulfuric acid (ACS Reagent, Merck). A total of 2 ml of H_2SO_4 was absorbed by polypropylene pad and used as catholyte in the cathode. A layer of activated carbon (residue from burning coconut) and manganese oxide, MnO_2 (QP grade, HmbG Chemicals), is deposited on the graphite surface to act as an electrocatalyst. MnO_2 is an excellent catalyst to enhance the ORR reaction. The activated carbon and MnO_2 mass ratio are fixed at 1:1 (Choi et al., 2020).

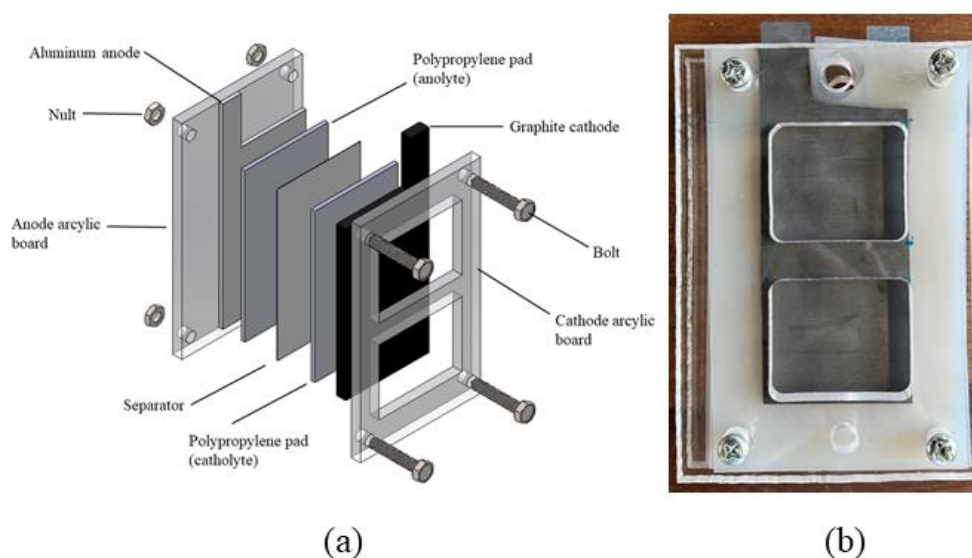


Figure 3.2: (a) Schematic diagram of dual electrolyte aluminium-air battery, (b) Prototype of dual electrolyte aluminium-air battery.

3.2 Experiment Analysis

In this study, experimental work was conducted to investigate the performance of the aluminium-air battery. An electrochemical workstation

(VersaSTAT 4, Ametek) was used to measure the battery's performance. Various electrochemical techniques were employed to analyze the electrical performance. All the electrochemical techniques can be analysed using the electrochemical workstation (VersaSTAT 4, Ametek). Besides that, different factors such as electrolyte system of the battery, concentration of electrolyte, types of aluminium anode, magnitude of discharge current, thickness of polypropylene separator, thickness of filter paper separator, and types of air cathode were also studied.

3.2.1 Polarization Test

A polarization test was performed on the aluminium-air battery to study the changes in the battery's voltage as a function of current drawn from the battery, or vice versa. This test helps to understand the internal resistance of the aluminium-air battery and the power that the battery can supplied at a specific current and voltage levels. It provides useful insights to optimize the performance of the battery. In this study, the polarization curve of the battery was obtained using a voltage sweep starting from the OCV of the battery to 0 V. A scan rate of $5 \text{ mV}\cdot\text{s}^{-1}$ was applied to the battery. To ensure the consistency of the result obtained, 1.5 ml of KOH solution is dropped on the polypropylene pad to activate the single electrolyte system aluminium-air battery. The polatization test was conducted 5 minutes after the battery was activated to ensure the stability of the aluminium-air battery. For the dual electrolyte system, 4 ml KOH and 2 ml of H_2SO_4 were absorbed by the polypropylene pad

respectively as the anolyte and catholyte, respectively. This test was repeated for different concentrations of KOH and H₂SO₄.

Since the voltage is swept from OCV to 0 V, current is drawn from the battery and the battery loses energy during the polarization test. The voltage is negatively correlated with the current. According to Ohm's law, as shown in Eq. 3.1, a negative value for the current is needed to account for the effect of reducing voltage as the current increases. As for the power achieved by the battery as a function of current, it is calculated using Eq. 3.2.

$$V = IR \quad (3.1)$$

$$P = VI \quad (3.2)$$

Where V – Voltage, V

I – Current, A

R – Resistance, Ω

P – Power, W

3.2.2 Discharge Test

A discharge test is performed to identify the discharge performance of the aluminium-air battery when a constant current is drawn from the battery. It provides useful information on the battery's lifetime and the operating voltage of the battery when discharged at a constant current. This test helps determine the suitability of the aluminium-air battery for a particular application. In this

study, various discharge currents ranging from 10 mA, 20 mA, 30 mA, 50 mA, to 100 mA were applied to both the single electrolyte system aluminium-air battery and the dual electrolyte system aluminium-air battery. The specific capacity of the battery can also be obtained from this study by examining the discharge duration of the battery. The specific capacity is calculated as shown in Eq. 3.3.

After the discharge test, the aluminium anode is removed. It is then rinsed with distilled water, followed by ultrasonic cleaning for 15 minutes to remove all impurities on the surface of the aluminium anode. The aluminium anode is subsequently measured using an analytical balance to determine its mass, which is then compared with the initial mass to calculate the mass loss.

$$Q = \frac{It}{\Delta m} \quad (3.3)$$

Where Q – specific capacity, mAh/g

t – time, h

Δm – change in anode mass, g

3.2.3 Tafel Test

The electrochemical performance of the battery is investigated using Tafel analysis to measure corrosion behavior. The test is conducted using three electrode configurations, with an Ag/AgCl electrode used as the reference

electrode. The working electrode is an aluminium alloy 6061 plate, and the counter electrode is a graphite plate. A swept rate of 5 mV in the range of -0.5 V (vs OCV) to 0 V (vs Ag/AgCl) (Teabnamang et al., 2020).

The polarization resistance, R_p , which explains the corrosion resistivity of the aluminum anode, can be calculated using the Butler-Volmer equation and Stern-Gear equations (Shinagawa et al., 2015; Abdel et al., 2019). The equations are shown below:

$$I = I_{corr} \left(e^{\frac{2.303(E-E_{corr})}{\beta_a}} - e^{\frac{2.303(E-E_{corr})}{\beta_c}} \right) \quad (3.4)$$

$$R_p = \frac{\beta_a |\beta_c|}{2.303 I_{corr} (\beta_a + |\beta_c|)} \quad (3.5)$$

Where, I – measured current density, A

I_{corr} – corrosion current density, A/cm²

E – voltage of the electrode, V

E_{corr} – voltage of the corrosion, V

β_a – Tafel slopes at the anode

β_c – Tafel slopes at the cathode

R_p – polarization resistance

All the data required to calculate the R_p can be obtained from the experimental data. The value of β_a is estimated by taking the gradient of the slope on the anode side, while the value of β_c is estimated by taking the gradient of the slope on the cathode side. I_{corr} refers to the current value at the intersection of the anode slope and the cathode slope, while E_{corr} represents the

voltage at I_{corr} . All of this data is important for calculating the R_p value, which predict the corrosion inhibition capabilities of the aluminium anode when used in an aluminium-air battery.

3.2.4 Corrosion Analysis

The corrosion rate of the aluminium anode in the battery is an important factor that be used to calculate the anode utilization efficiency of the aluminium anode in generating electricity. The corrosion rate can be calculated by using the Eq. 3.6.

$$\text{Corrosion rate (mg min}^{-1}\text{cm}^{-2}) = \frac{\Delta m}{At} \quad (3.6)$$

Where, A – expose area, cm^2

Δm – mass loss, mg

t – discharge time, min

On the other hand, the anode utilization efficiency of the aluminium is then calculated using the equation below.

$$Q_{\text{experiment}} = \frac{nF\Delta m}{9m_{al}} \quad (3.7)$$

$$Q_{\text{real}} = It \quad (3.8)$$

$$\eta = \frac{Q_{real}}{Q_{experiment}} \times 100 \% \quad (3.9)$$

Where, Q – specific capacity of the aluminium anode, mAh

n – number of electron

F – Faraday constant; $96850 C/mol$

Δm – changes in mass of the aluminium anode, g

m_{al} – aluminium atomic mass

I – discharge current, A

t – discharge time, s

η – anode utilization efficiency.

3.2.5 Electrochemical Impedance Spectroscopy (EIS)

Electrochemical impedance spectroscopy (EIS) is performed to estimate an equivalent circuit for the aluminum-air battery. A frequency range from 0.1 Hz to 100,000 Hz is swept through the battery with a swept amplitude of 10 mV (Wang et al., 2019). The curve fitting and analysis of the equivalent model are conducted using the EIS Spectrum Analyzer software by ABC Chemistry. This software assists in determining the values of each component used in the equivalent circuit. Based on the study, a Randall's cell combined with a Warburg impedance adequately models the aluminum-air battery and requires only four components: a solution resistor, a polarization resistor, a double-layer capacitor, and a Warburg impedance. The equations describing the behavior of each component are shown in Table 3.1 below (EIS Spectrum Analyzer, 2008;

PalmSens, 2023).

Table 3.1: Equations related to the electrical components

Component	Resistance	Impedance
Resistor	$V = IR$ (3.7)	$Z = R$ (3.10)
Capacitor	$I = C \frac{dV}{dt}$ (3.11)	$Z = \frac{1}{j\omega C}$ (3.12)
Warburg	$ReZ(\omega) = \frac{A_W}{\omega^{0.5}}$ (3.13)	$ImZ(\omega) = \frac{-A_W}{\omega^{0.5}}$ (3.14)

A_W is the Warburg coefficient which can be defined as in Eq. 3.15

$$A_W = \frac{RT}{An^2F^2\sqrt{2}} \left(\frac{1}{\sqrt{D_O}C_{S,O}} + \frac{1}{\sqrt{D_R}C_{S,R}} \right) \quad (3.15)$$

Where, R – universal gas constant

T – absolute temperature

A – electrode surface area

n – number of electrode

F – Faraday constant

D – diffusion coefficient of the electroactive species

$C_{S,O}$ – surface concentration of oxidized form

$C_{S,R}$ – surface concentration of reduced form

3.2.6 Surface Characterization

The surface of the aluminum anode was analyzed before and after the discharge test using a scanning electron microscope (Hitachi, S-3400N).

Subsequently, the powder on the surface of the aluminum anode after discharge was removed and analyzed using energy-dispersive X-Ray spectroscopy (EDX) to study the impurities present. X-Ray diffraction (XRD) (Shimadzu, XRD-6000) was also performed to identify any impurities on the aluminum anode.

3.2.7 Wettability Characterization of Polypropylene Pad

A wettability test was conducted to analyze the hydrophobic properties of the polypropylene separator. 1, 2, and 3 M KOH solutions were dropped on the surface of the polypropylene separator, and the contact angle was measured to assess the wettability performance. The contact angle measurements were performed using ImageJ, as shown in Figure 3.3, which depicts the contact angle of the polypropylene separator.

The results indicated that the contact angle tends to increase as the electrolyte concentration rises from 1 to 3 M. Specifically, the contact angles were 70.1° , 76.5° , and 97.6° for 1, 2, and 3 M concentrations, respectively. These findings suggest that the hydrophobic properties of the separator improve with increasing concentration. Notably, only the 3 M electrolyte achieved true hydrophobic potential, as the contact angle exceeded 90° (Doshi et al., 2018). This is because high concentration of KOH electrolyte is more viscous, hence, the flow of the KOH electrolyte is slower and sluggish. The hydrophobicity properties of the separator can limit the flow of water molecules from the cathode to the anode, thereby helping to prevent corrosion.

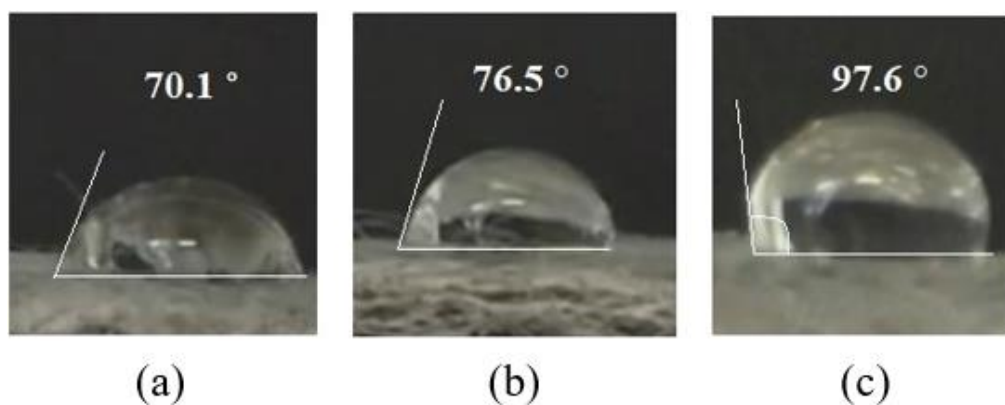


Figure 3.3: Contact angle of the different concentration of KOH on the polypropylene (a) 1 M KOH, (b) 2 M KOH, and (c) 3 M KOH.

3.3 Summaries

The aluminium-air battery served as a test rig for the experimental study. The study begin with a detailed analysis of a single electrolyte system aluminium-air battery. Subsequently, a novel dual electrolyte polypropylene-based aluminium-air battery will be introduced. Two different electrolytes were used for the anode side (anolyte) and cathode side (catholyte) respectively. The anolyte was alkaline-based electrolyte, while the catholyte was acidic-based electrolyte. This design aims to improve the oxygen reduction reaction (ORR), thereby enhancing the overall battery performance. Tafel analysis was conducted to analyse the corrosion behaviour of the aluminium anode in the aluminium-air battery. In addition, scanning electron microscopy (SEM) and X-Ray diffraction (XRD) analyses were performed to investigate any changes in the microstructure of the aluminium anode.

CHAPTER 4

RESULTS AND DISCUSSION

4.1 Introduction

This chapter will begin with a thorough analysis of the performance of the single electrolyte system aluminium-air battery, followed by the introduction of the dual electrolyte system to enhance its performance. Both designs utilized various electrochemical techniques. Initially, factors such as the type of aluminum anode, thickness of polypropylene, and thickness of filter paper were considered to identify the optimal combination for maximizing the battery's performance. Once identified, this combination was used to replicate the experiment, while varying other factors that may impact the battery performance. Next, the study was continued with a corrosion study and surface analysis of the aluminium anode, providing a complete understanding of the polypropylene-based aluminium-air battery.

4.2 Single Electrolyte System Aluminium-air Battery

This section discuss the performance of a single electrolyte system in an aluminium-air battery. The aluminium anode used are aluminium foil and aluminium alloy 6061. The electrolyte used in this study are KOH with concentrations of 1 M, 2 M and 3M. Firstly, the discharge performance of the

aluminium foil was investigated by using discharge current and different concentrations of KOH electrolyte. Next, the performance for these two anodes was compared by studying the polarization performance, discharge performance and perform EIS analysis. The study is then followed by a comprehensive analysis on the performance of the aluminium alloy 6061 in a single electrolyte system.

4.2.1 Battery Performance with Aluminium Foil as Anode

In this study, aluminium foil is used as the anode in the battery. Different discharge current and concentration of KOH electrolyte are applied to the battery to investigate the performance. The open circuit voltage of the battery was measured and the voltage tends to drop until 0 V to capture the battery capacity when discharge current is applied on it. The discharge currents used in this study were 10 mA, 20 mA, 30 mA, and 50 mA. Figure 4.1 shows the discharge performance of the Aluminium-air battery with 1M of KOH. It indicated that the battery discharge with 10 mA took a longer time to completely exhausted. It can last for about 1 hour and 36 minutes before the battery dried out. The discharge duration is inversely proportional to the discharge current. At discharge current of 50 mA, the battery can last for about 20 minutes only. During the discharging process, the aluminium and hydroxyl ions were consumed and lead to a reduction of battery voltage. When the remaining of the hydroxyl and aluminium ions are fully consumed and unable to fulfill the required discharging current, the battery voltage drop to 0 V. This phenomenon is more obvious when a high current was used to discharge the battery and lead

to a quicker drop in the battery voltage. Based on the result, aluminium-air battery with small current load will produce a higher voltage and the discharge period is also longer when benchmarking with high discharge current. The initial voltage achieved by 10 mA, 20 mA, 30 mA and 50 mA of discharge current is about 1.1 V, 1.0 V, 0.8 V, and 0.3 V, respectively. This is because the electrochemical reaction at the battery is positively correlated with the discharge current and more ions are involved in the reaction. Rapid consumption of ions available in the battery will cause a sudden drop in the battery voltage. Therefore, increasing the amount of electrolyte present in the battery or increasing the size of aluminium anode can further increase the capacity of the battery and prolong the discharging period. Besides, increasing the thickness of the polypropylene is directly proportional to increase the amount of electrolyte stored in the polypropylene separator or using a better electrocatalyst to enhance the oxygen reduction reaction will certainly help to improve the performance of the battery.

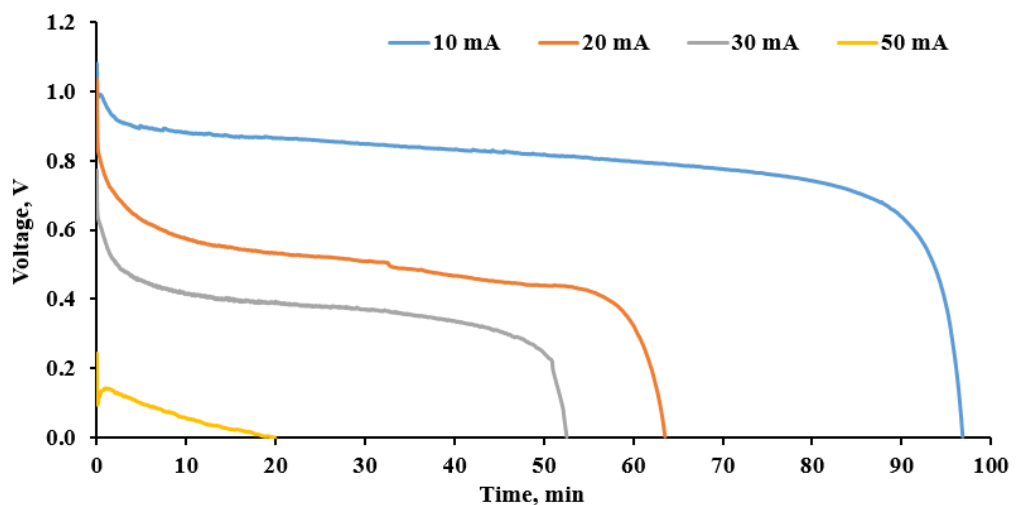


Figure 4.1: Discharge performance of Al-air battery with 1M KOH electrolyte.

The performance of the battery discharging characteristics is compared with different concentrations of electrolytes. In this study, the discharge current was fixed at 20 mA. Strong alkaline solution will certainly reduce the performance of the battery. As shown in Figure 4.2, as the concentration of the electrolyte increases, the capacity of the battery is also reduced. For high concentration of KOH, the battery takes a shorter time to discharge. The discharge time was about 28 minutes for 3M of electrolyte. On the other hand, the discharge time was improved to about 59 minutes and 64 minutes for 2M and 1M of electrolyte respectively. The concentration of electrolyte is negatively correlated with the discharge performance of the aluminium-air battery. This observation is coherent with the work by Mohammad (2008). The reduction of discharge time is due to the corrosion rate of the battery. As the concentration of the electrolyte increases, the concentration of OH^- ions increased as well. This will favor the formation of aluminium hydroxide, $\text{Al}(\text{OH})_3$ and hydrogen as by-product as shown in Eq 2.8. Most of the aluminium at the anode was consumed in the side reaction rather than used in the electrochemical reaction. As the discharging process continue, the aluminium was covered by the aluminium hydroxide during the electrochemical process and reduced the battery performance. Hence, using a high concentration of electrolyte will increase the frequency of replacing the aluminium anode.

Although high concentration shows a shorter discharge time, the voltage stabilizes at a higher value for high concentration of electrolyte. At 20 mA, the voltage stabilized at 0.8 V when 3M electrolyte was used in the study whereas it dropped to about 0.5 V when 1M of electrolyte was used. This is because

strong alkaline has better ionic conductivity and facilitates better ionic movement. Higher amount of OH^- ions is available in the electrolyte solution and react with the aluminium at the anode to produce electricity. It also helps to reduce the resistance of ion movement in the separator. Hence, there exists a compromise between the concentrations of electrolyte, discharge capacity and the operating voltage. However, increasing the concentration of the electrolyte does not affect the open-circuit voltage of the battery. As shown in Figure 4.2, the open-circuit voltage tends to remain the same at about 1.1 V for 1M, 2M and 3M of KOH whereas the effect of concentration of the electrolyte on open circuit voltage is insignificant.

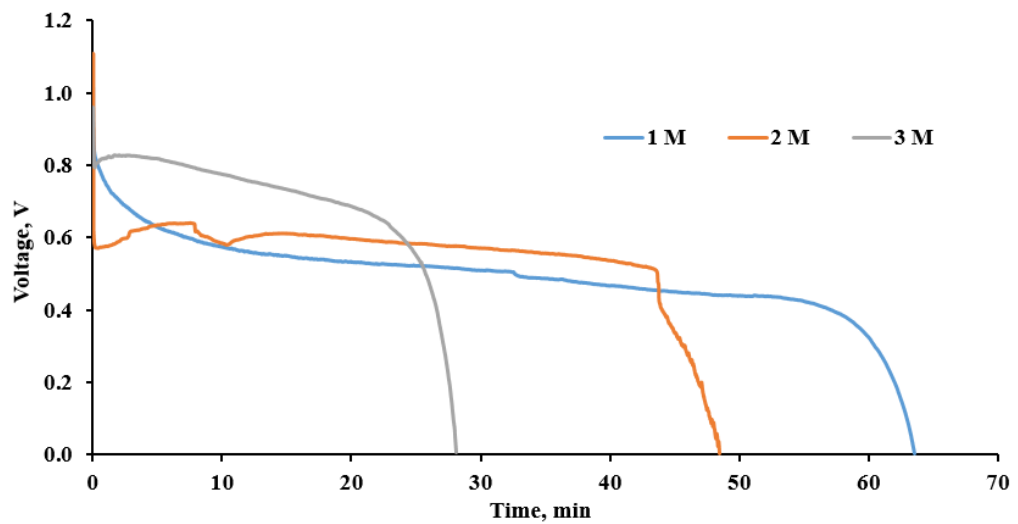


Figure 4.2: Discharge performance of Al-air battery with different KOH concentration with discharge current of 20 mA

4.2.2 Specific discharge capacity of aluminium-air battery

The aluminium-air battery is a primary battery and cannot be recharged. The lifecycle depends a lot on the amount of the aluminium anode used in the battery. The battery will stop operating when all the aluminium is consumed. To 'recharge' the battery, a mechanical aluminium swapping is necessary. When a fresh aluminium anode is added to the aluminium-air battery, the battery can function again. The specific discharge capacity provides an understanding of how long the aluminium-air battery can last and offers information on its performance.

Figure 4.3 showed the specific capacity of the aluminium-air battery for different concentrations and discharge current. As shown in the Figure 4.3, 1M of the electrolyte always showed the highest specific capacity for discharge current of 10 mA, 20 mA, 30 mA and 50 mA. Due to the low corrosion rate of 1M electrolyte, most of the aluminium was consumed in the electrochemical reaction rather than the parasitic loss in the side reaction. Hence, the specific capacity increased as the anode utilization improved. Specific discharge capacities of 228 mAh.g⁻¹ and 375 mAh.g⁻¹ were obtained for discharge current of 10 mA and 30 mA, respectively. However, this improvement is not observed at discharge current of 50 mA. The specific capacity for 1M electrolyte tends to reduce at 50 mA. This is due to the limitation of OH⁻ ions in the 1M electrolyte. There was insufficient OH⁻ supplied to the anode and hence, reducing the electrochemical reaction and leads to a drop in specific capacity.

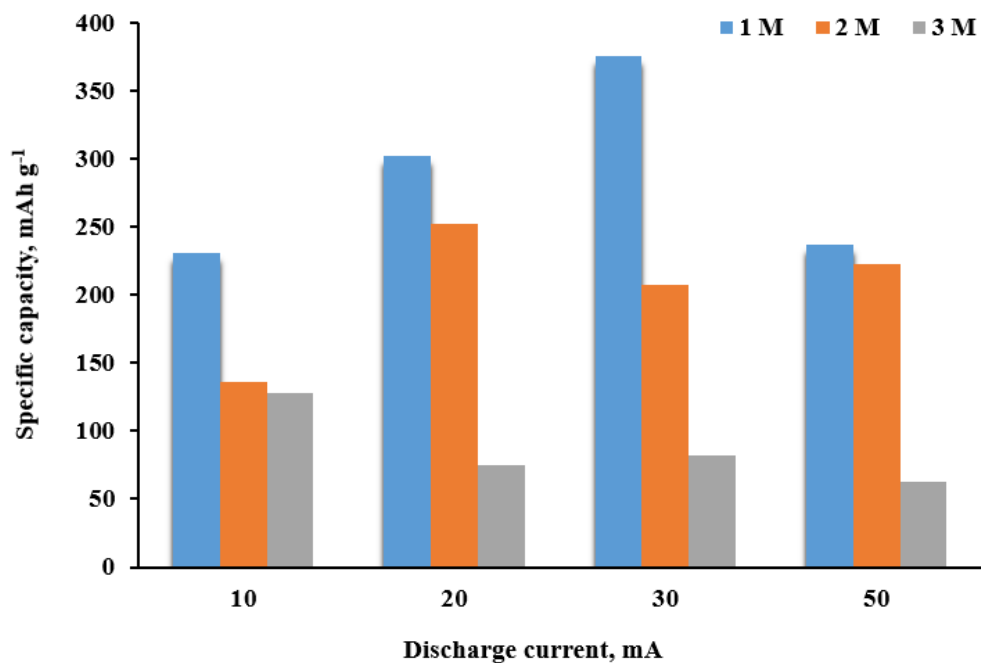


Figure 4.3: Specific discharge capacity of the polypropylene-based aluminium-air battery under various concentrations and magnitude of discharge currents.

In 2M and 3M electrolytes, the specific capacities were always lower than 1M. As the concentration increases, the corrosion rate increases which leads to poor anode utilization. Some of the aluminium was consumed by reacting with OH⁻ ions to form aluminium hydroxide, causing a reduction in anode utilization which lead to the specific capacities dropped. 3M electrolyte always showed the lowest specific capacity. This suggested that the effect of corrosion is very serious for the battery using 3M of electrolyte.

Among all the tests, the best performance was achieved by 1M electrolyte at discharge capacity of 30 mA in which a specific capacity of 375 mAh g⁻¹ was recorded. The performance is better than previous research on the aluminium based battery: 65 mAh.g⁻¹ (Elia et al., 2017) , 239 mAh.g⁻¹ (Yu et al., 2018), and 350 mAh.g⁻¹ (Wang et al., 2016).

4.2.3 Performance of Polypropylene Against a Paper-Based Separator

The study is continued by comparing the discharge performance of the polypropylene separator and paper-based separator-Kimwipes when both of them are used in aluminium-air battery. In this study, 1 M of KOH was used as the electrolyte. Kimwipes was cut into a square with 5 cm x 5 cm and used as the separator in the aluminium-air battery. From the results shown in Figure 4.4, it can be shown that higher performance is achieved by the polypropylene separator for all discharge currents as compared to paper-based separator. At discharge current of 10 mA, polypropylene separator maintained a discharge duration of about 97 minutes while paper-based separator is only able to maintain a discharge duration of about 33 minutes only. There is about triple improvement for polypropylene separator as compared to paper-based separator. Besides, a sharp drop of voltage is observed in paper-based aluminium-air battery. At 10 mA, the open circuit voltage drop from 1.18 V to about 0.82 V, and maintaining a constant discharge voltage at about 0.8 V. On the other hand, polypropylene-based separator shown a initial voltage drop from 1.1 V to 0.9 V and able to provide a constant discharge voltage of 0.9 V before a sudden drop in voltage due to electrolyte dried out. This suggested that the electrical performance of the polypropylene separator is better than the kimwipes. Paper-based separator does not produce a good stability in voltage output when the discharge current is increased to 20 mA and 30 mA. The voltage tends to fluctuate as shown in Figure 4.4. Besides that, the discharge duration tends to reduce as the discharge current increases. At 30 mA, the paper-based aluminium-air battery can only survive for 18 minutes. There is no obvious

constant discharge voltage plateau in the discharging curve. On the other hand, using polypropylene as separator can achieve discharge duration of 52 minutes while keeping a constant discharge voltage of about 0.4 V. The discharge duration was improved by 3 folds.

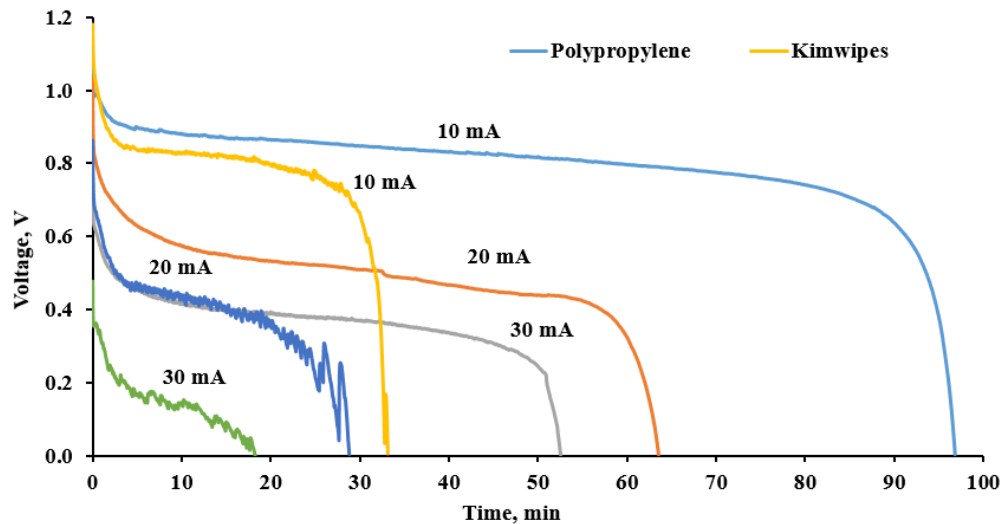


Figure 4.4: Discharge performance of polypropylene and kimwipes separator.

The performance of paper-based aluminium-air battery at discharge current of 20 mA is similar to the performance of polypropylene-based aluminium-air battery at discharge current of 30 mA. Both the battery showed a constant discharge voltage of 0.4 V. However, the paper-based aluminium-air battery lasted only 28 minutes and was much shorter than the polypropylene-based aluminium-air battery which was recorded at 52 minutes. The discharge performance indicates that polypropylene separator was able to provide a better battery performance at higher discharge current as compared to paper-based separator at lower discharge current.

Besides that, polypropylene separator did not suffer a severe sharp drop in voltage as compared to kimwipes for all discharge current. The sharp drop in the initial voltage of the kimwipes separator will produce a lower discharge voltage. The effects of fluctuation in voltage and large drop in initial voltage suggested that kimwipes does not provide a stable electrical performance. This maybe due to the higher internal resistance of the paper-based separator. Polypropylene separator can provide a stable discharge performance for a longer period of time. Although kimwipes possess a better chemical absorbent property than the polypropylene, it does not show a good performance when used as a separator in aluminium-air battery. This may be due to the physical microstructure of the Kimwipes. Kimwipes is a cellulose-based material while polypropylene is a fiber-based material. When cellulose-based material is used as a separator in the battery, it can cause swelling when immersed in the electrolyte. This will alter the material properties of the separator. Nevertheless, the geometry of the fiber-based polypropylene does not distort when it is immersed in the electrolyte. Hence, polypropylene separator will produce better battery performance. This observation is coherent with the work by Xie et al. (2019).

Figure 4.5 shows the SEM image of polypropylene pad and kimwipes before and after the discharge. It can be seen that after discharging, the surface of kimwipes is covered with spherical structure. This spherical structure is actually aluminium hydroxide. It will stick on it and filling the porosity of the kimwipes. The surface of the kimwipes is damaged after the discharge. Hence, it can no longer function as most of the porosity is filled with aluminium

hydroxide and need to be replaced in the aluminium-air battery so that the battery can be reused again. On the other hand, the surface of the polypropylene pad show almost no changes after discharging. The aluminium hydroxide is not able to stick on the surface and the structure is unaffected. This explains why the performance of polypropylene is better than kimwipes in terms of discharge time and output voltage. Since the damage on the structure of the polypropylene pad is minimal, it can be reused again, offering sustainability as a benefit over kimwipes.

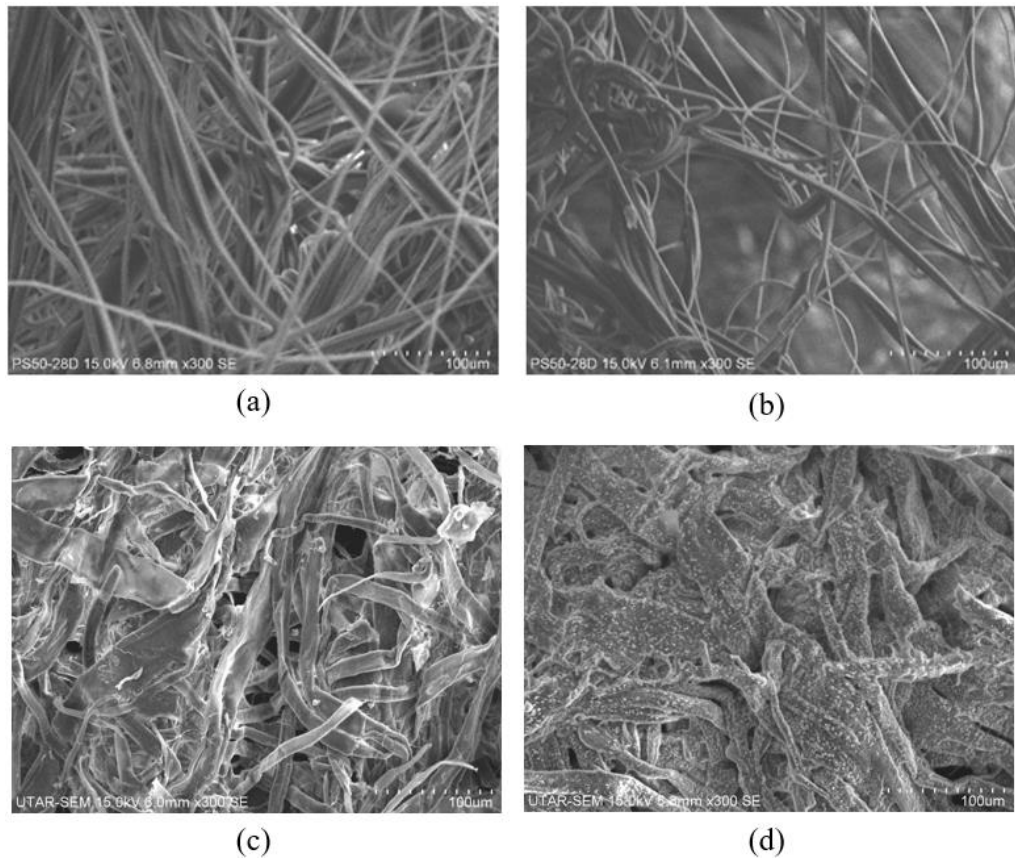


Figure 4.5: SEM image of 300X magnification of (a) polypropylene pad before discharging, (b) polypropylene pad after discharging for 1 h, (c) kimwipes before discharging and (d) kim wipes after discharging for 1 h.

4.2.4 Comparison of Aluminium Foil and Aluminium Alloy 6061 as Anode

A comparison of the polarization curve of aluminium foil and aluminium alloy 6061 is conducted to analyze the performance. In Figure 4.6, aluminium foil seems to perform better than aluminium alloy 6061 as the peak power achieved is about 7 mW as compared to 5 mW for aluminium alloy 6061. Aluminium foil is much thinner as compared to aluminium alloy 6061 which in turn shows much less electrical resistance. This shows that aluminium foil is more readily subjected to corrosion as it can react easily with the OH^- in the KOH electrolyte. Using aluminium foil in aluminium-air battery shows better performance in the discharge curve too when it is compared with aluminium alloy 6061. In the discharge curve, the output voltage is generally much higher than aluminium alloy 6061. Under a discharge current of 20 mA, the output voltage is about 0.8 V but it quickly drops to 0 V in about 28 minutes. This is significantly shorter than aluminium alloy 6061 which recorded a discharge duration of 130 minutes at an output voltage of 0.6 V. This comparison shows that aluminium foil although provides higher voltage when it is used as an anode but the short discharge duration has limited its application.

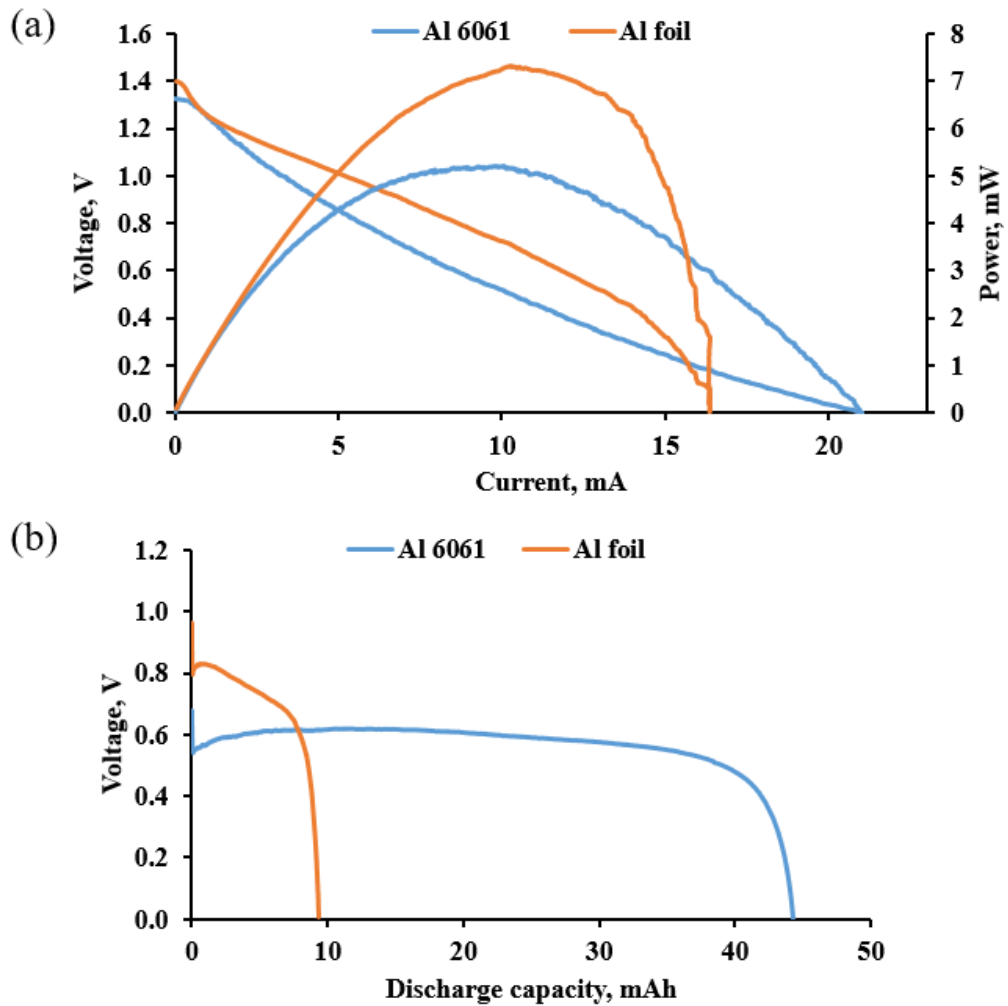


Figure 4.6: (a) Polarization curve and (b) discharge curve comparing the performance of aluminium foil and aluminium alloy 6061 as anode in aluminium-air battery.

Electrochemical impedance spectroscopy (EIS) is used to study the characteristics of the battery by applying different frequencies to the battery. A Nyquist plot with the curve fitting of the raw data comparing the performance of aluminium-air battery using aluminium foil and aluminium alloy 6061 as anode is plotted as shown in Figure 4.7 (a). Both curves show a similar pattern. By using electrical modeling on the Nyquist plot, it is found that the battery behaves similarly to a Randles cell in which the circuit is as shown in Figure

4.7 (b) (Instruments, 2017). All the circuit parameters are tabulated in Table 4.1. From the Nyquist plot, the semicircle is observed at the high frequency region followed by a 45° straight line at the low frequency region. The R_s value represents the solution resistance. Solution resistance is the sum of the resistance between the counter electrode and the working electrode in the battery. Changing the aluminium foil to aluminium alloy 6061 has increased the R_s value while maintaining the same concentration of electrolyte suggesting that the aluminium alloy 6061 has higher resistance as compared to aluminium foil. Since the resistance is higher, it is estimated that aluminium alloy 6061 will produce less power as compared to aluminium foil. The resistance is inversely proportional to the conductance. The conductance of the aluminum alloy is approximately $0.102 \Omega^{-1}$, which is roughly twice the conductance of aluminum alloy 6061, recorded at about $0.048 \Omega^{-1}$. Therefore, an increase in the R_s value actually indicates that aluminum alloy 6061 has poorer conductance compared to aluminum alloy and generates lower power.

The semicircle is indicated by the R_{ct} and C_{dl} which are associated with the charge transfer characteristics of the battery. The high value of R_{ct} and C_{dl} is observed when aluminium alloy 6061 is used as anode showing the aluminium dissolution of aluminium alloy 6061 is difficult as compared to aluminium foil. This is due to the passivation layer of the aluminium anode as a layer of aluminium oxide is formed owing to the nature of the aluminium behavior. Hence, it is more difficult to break down the aluminium oxide film and therefore, causing an increase in the charge transfer resistance (Koroleva et al., 1999). As for the low frequency region, a Warburg resistance is observed and it shows the

diffusion capabilities of the battery. The values recorded for both the aluminium foil and aluminium alloy 6061 are $11.86 \Omega/s^{1/2}$ and $12.56 \Omega/s^{1/2}$ respectively, which is quite similar. This is due to the fact that the diffusion of OH^- ions are not affected by the types of aluminium anode used.

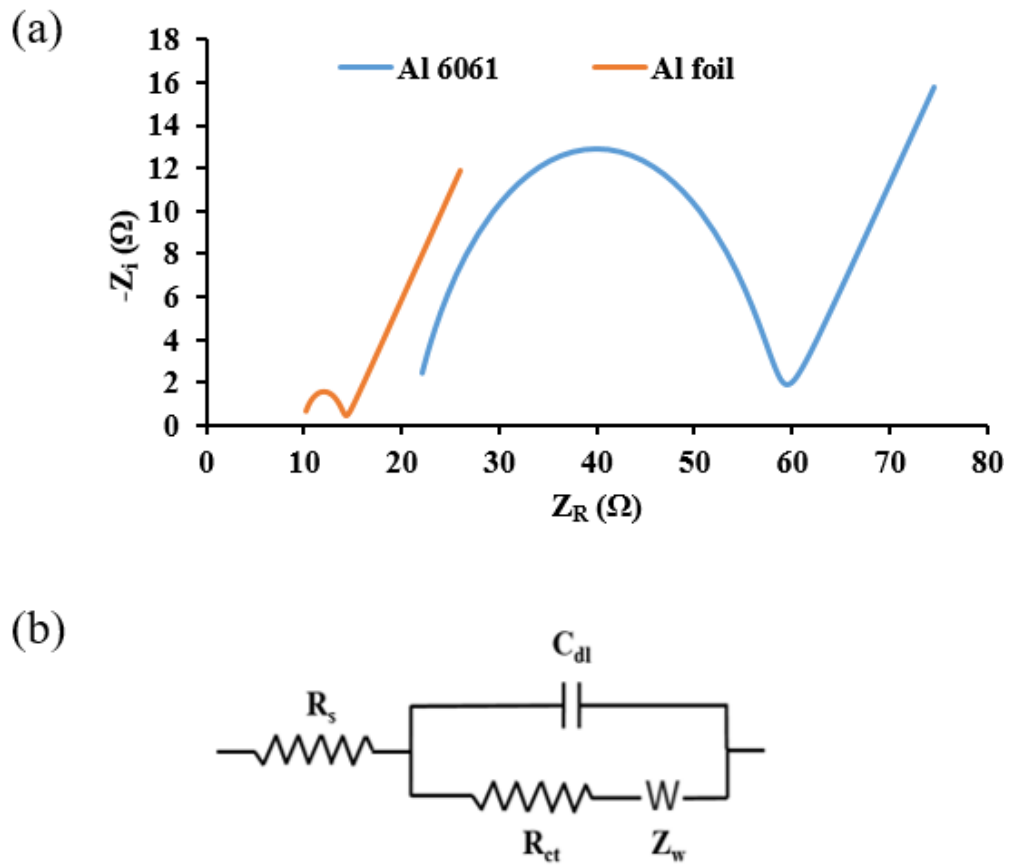


Figure 4.7: (a) Nyquist plot comparing aluminium foil and aluminium alloy 6061 anode ; (b) Equivalent circuit model derived from the EIS analysis.

Table 4.1: Parameter of the electrical components in the equivalent circuit model for aluminium foil and aluminium alloy 6061 anode.

Aluminium anode	R_s (Ω)	R_{ct} (Ω)	W ($\Omega/s^{1/2}$)	C_{dl} (μF)
Al foil	9.84	4.29	11.86	26.1
Al 6061	20.94	37.78	12.54	13.8

4.2.5 Performance of Aluminium Alloy 6061 as Anode in Aluminium-air Battery

This work focus on the application of aluminium alloy 6061 as the aluminium anode. The concentrations of the KOH electrolyte used in the single electrolyte system are 1M, 2M, and 3M. The polarization result is tabulated in Figure 4.8 (a). It is observed that increasing the concentration of the KOH electrolyte help to improve the performance of the aluminium-air battery. The maximum power achieved for 1M of KOH electrolyte is about 5 mW and it is improved to about 9 mW when 3M of KOH electrolyte is used. The improvement is about 80 % suggesting that high concentration of electrolyte can boost the power output. This is because higher amount of OH^- is present in high concentration of KOH electrolyte. Eq. 2.3 has shown that OH^- is important in the oxidation of aluminium anode. This can leads to more amount of aluminium anode being consumed and releasing more electrons for electricity production.

Moreover, the voltage is negatively correlated with the current. This is due to current is drawn from the aluminium-air battery. As more energy is extracted from the battery, the voltage of the battery start to drop in order to

supply the required current to the external circuit. However, the curve shows a linear relation suggesting that the output voltage and the output current is obeying ohm's law. In 1M of KOH electrolyte, the maximum current that the aluminium-air battery can support is about 21 mA. It is improved to 32 mA when 3M of KOH electrolyte is used. These observations agree well with the fact that a high concentration of electrolyte used can improve the battery performance (Wang et al. 2019).

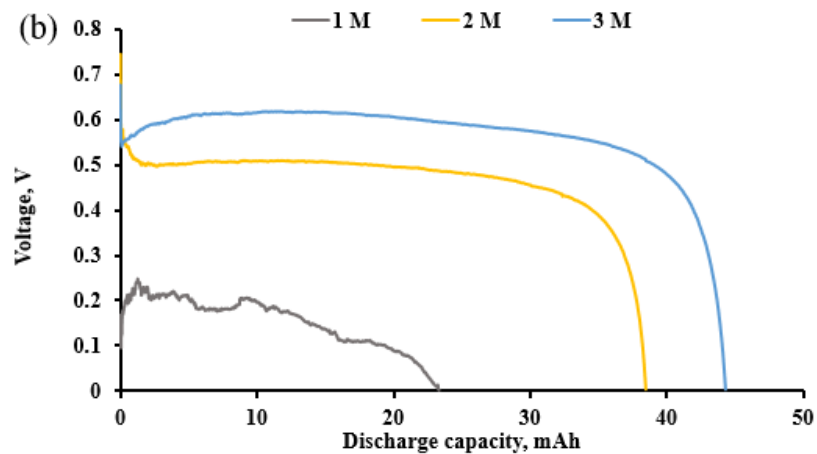
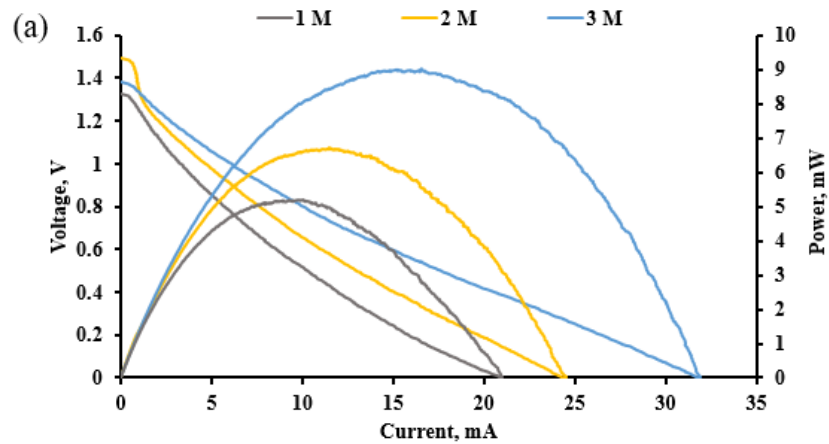
The discharge curve of aluminium alloy 6061 at a discharge current of 20 mA is as shown in Figure 4.8 (b). When 1M of KOH electrolyte is used, the performance seems rather weak and maintain at 0.2 V for a short amount of time. This is due to the low amount of OH^- ions available in low concentration of KOH electrolyte. The reaction is not fast enough to support the amount of current drawn from the workstation. The aluminium-air battery is struggle to supply enough electrons as a result of low rate of electrochemical reaction. The battery completely stops at about 70 minutes. Increasing the concentration of KOH electrolyte to 3M boosts the discharge capacity to about 44 mAh which is equivalent to a discharge time of 132 minutes. This improvement is attributed to high amount of OH^- ions as discussed previously. Since the amount of OH^- is sufficient, the voltage is able to maintain at about 0.6 V. On the other hand, the performance of a 2M of KOH electrolyte aluminium-air battery can sustain for 100 minutes at roughly 0.5 V. Both the discharge capacity and discharge time is improved by increasing the concentration of KOH electrolyte.

These results show contradiction with the result from Tan et al. (2021).

Previous work suggests that high concentration of KOH electrolyte will reduce the discharge capacity and discharge time while current work shows a positive correlation ship between discharge time, discharge capacity, and concentration of KOH electrolyte. The main reason behind this phenomenon is the types of aluminium anode used. The aluminium anode used in this study is aluminium alloy 6061 while previous work used only aluminium foil. The amount of aluminium presented in this study is far more than the aluminium foil. Thus, in this study, the battery will only stop functioning when the OH^- ions present in the polypropylene are fully consumed as the supply of aluminium is almost infinite. On the contrary, aluminium foil is thin and can be easily fully consumed by KOH electrolyte. When high concentration of KOH electrolyte is used, it will cause the aluminium foil to corrode even faster and cause the battery to stop functioning when it is fully consumed. Therefore, the limiting factor that determines the discharge capacity in this study is the amount of OH^- ions while the limiting factor that determines the discharge capacity in previous work is the amount of aluminium anode.

The discharge curve using various discharge currents on the aluminium-air battery is also performed. 3M of KOH electrolyte is used in the aluminium-air battery and the result is shown in Figure 4.8 (c). The output voltage tends to drop as the discharge current rises. At 10 mA, the aluminium-air battery is able to provide about 0.75 V and discharge for about 5 hours before the drop to 0 V which is equivalent to 48.7 mAh. On the contrary, the output voltage and the discharge duration drop to only about 0.3 to 0.2 V and 49 minutes respectively, when the discharge current used is 30 mA. The discharge capacity is only 24.7

mAh. Since the concentration and the volume of the KOH electrolyte are fixed, the same amount of OH^- ions are present for all cases. As the discharge current rise, a faster rate of electrochemical reaction is needed so to fulfill the energy demand. Hence, more OH^- is consumed and leads to faster depletion of OH^- ions and eventually shorter discharge time. On the other hand, the drop in output voltage is due to the internal resistance of the battery. As more current is drawn from the battery, some of the energy is consumed by the internal resistance of the battery and leading to lower output voltage of the aluminium-air battery. Reducing the internal resistance of the battery can help to minimize the voltage drop.



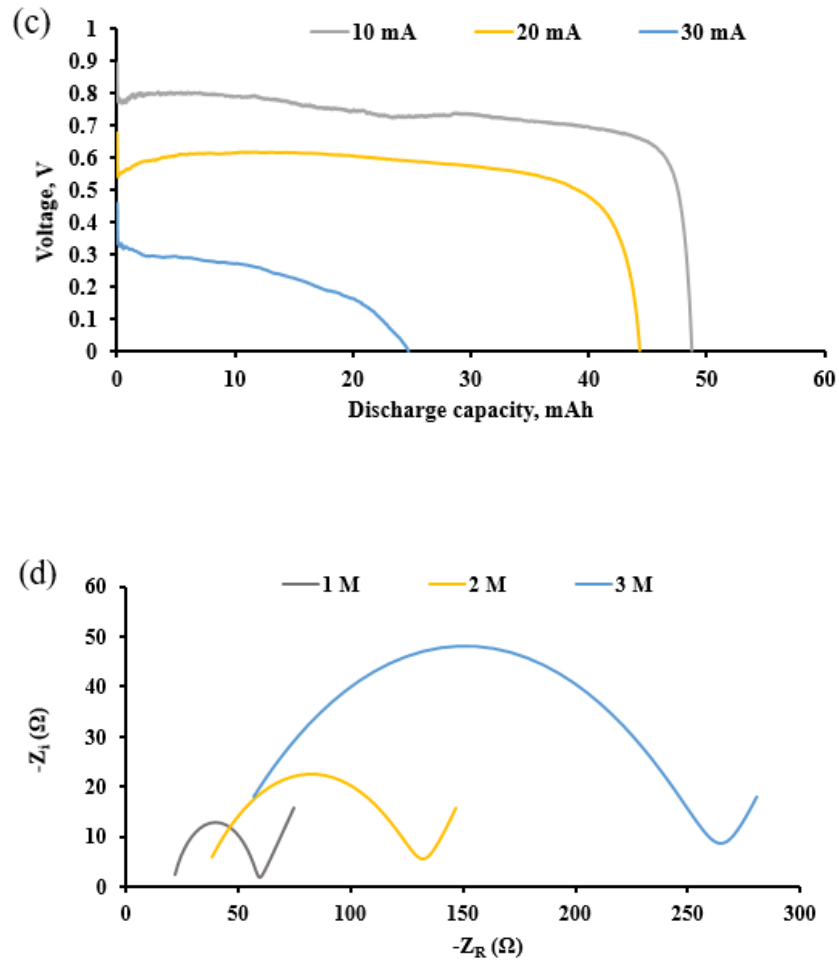


Figure 4.8: (a) Polarization curve, (b) discharge curve, (c) discharge curve of various discharge currents, and (d) Nyquist plot comparing the effect of concentration of KOH electrolyte.

Table 4.2 presents the comparative results of EIS conducted on different electrolyte concentrations. The value of R_s and R_{ct} is getting larger correspond to the raise of the concentration of the electrolyte from 1M to 3M. High concentration of the electrolyte has induced a higher charge transfer resistance. This occurs due to the migration of ions within the polypropylene pad becomes more difficult at elevated electrolyte concentrations. However, despite the

increase in resistance, the battery's performance is not adversely affected since high concentration of OH⁻ ions present at the polypropylene separator in the high concentration of KOH electrolyte. This increase in the rate of the oxidation reaction at the anode side has compensated for the effects of the charge transfer resistance.

Table 4.2: Parameter of the electrical components in the equivalent circuit model for different concentration of electrolyte.

Concentration	R _s (Ω)	R _{ct} (Ω)	W (Ω/s ^{1/2})	C _{dl} (μF)
1 M	20.94	37.78	12.54	13.8
2 M	32.46	99.88	12.14	8.2
3 M	36.07	229.26	13.35	3.8

4.3 Dual Electrolyte System Aluminium-air Battery

The performance of dual electrolyte system aluminium-air batteries are investigated in this study. The aluminium anode used is aluminium alloy 6061 due to the longer discharge time it can sustain in the aluminium-air battery. The anolyte used is KOH while the catholyte used is H₂SO₄. An optimization of the aluminium-air battery is conducted to determine the design with the best performance by proper investigating the thickness of the separator and thickness of the polypropylene. The experiment is then proceeded by investigating the effect of anolyte and catholyte on the performance of the dual electrolyte system aluminium air-battery. Lastly, a comparison between single electrolyte system and dual electrolyte system are compared and investigated.

4.3.1 Effects of the Separator Thickness

Several factors such as thickness of the separator, concentration of the anolyte and catholyte and thickness of the polypropylene pad can affect the aluminium-air battery performance. The role of the separator is to isolate the polypropylene pad at the anode and polypropylene pad at the cathode and reduce the mixing of anolyte and catholyte in the battery but allow the ions transfer to occur. Mixing of anolyte and catholyte is unfavorable as it can reduce the battery's performance. Individual thickness of the filter paper is 0.2 mm. Filter papers are stacked to increase the separator thickness in the aluminium-air battery. Stacking two layers, and three layers of filter papers will produce separator thickness of 0.4 mm, and 0.6 mm respectively. Although a thin separator will reduce the ionic resistance, it will also causing the anolyte and catholyte to mix with each other and affect the performance of the battery. The dual electrolyte battery will behave like a single electrolyte battery. Hence, there is a need to optimize the separator thickness to ensure the power output of the battery is always at its peak.

As shown in Figure. 4.9 of the battery's discharge curve using discharge current of 10 mA, the discharge duration for the 0.2 mm thick separator is about 30 mins. As time passes, infiltration of the electrolyte will occur and cause mixing of anolyte and catholyte. Increasing the thickness of the separator to 0.6 mm helps to prevent the mixing and slow down the movement of OH⁻ ions. Hence, the voltage is generally lower than using a 0.4 mm thick separator. Besides that, the

discharge duration is also shorter than that of the separator with 0.4 mm thickness. The best performance is achieved by using the thickness of 0.4 mm; it achieved an optimum setting for the ion transfer process and infiltration of the electrolytes. As a result, it can provide higher voltage and longer discharge duration. This observation is in good agreement with the study by Wang et al. (2019) on the aqueous dual electrolyte system. The thickness of the filter paper plays an important role in affecting the movement of OH^- ions. Since the 0.4 mm separator provides the best performance on the aluminium-air battery, the experiment will be conducted using two filter papers for the rest of the study.

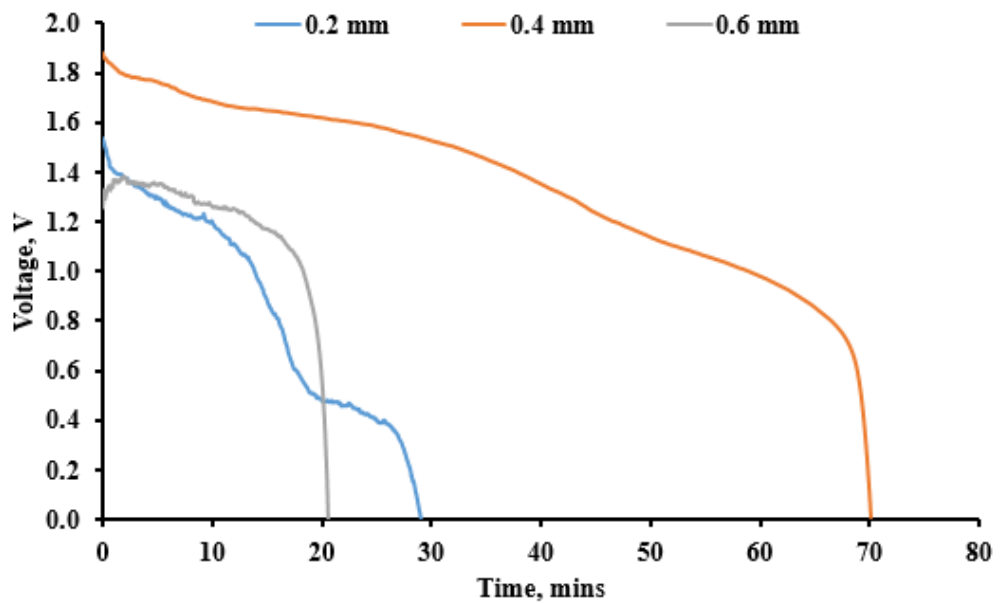


Figure 4.9: Discharge curve of different thickness of separator in the dual electrolyte aluminium-air battery.

4.3.2 Effects of Polypropylene Pad Thickness

In this study, two different thicknesses of polypropylene pads were used, which is known as thin pad with thickness of 1.68 mm and thick pad with thickness of 4 mm. 3M of KOH was used as an anolyte, while the catholyte consists of 3M of H₂SO₄. Polarization test and constant discharge current test were performed to compare the effects of the polypropylene pad thickness on the performance of the battery. The thickness of the polypropylene pad is a crucial factor that affects the amount of electrolyte absorbed. Thick polypropylene pad can absorb more KOH electrolyte than that of the thin polypropylene pad. As a result, more fresh OH⁻ ions are available for the electrochemical reaction and improve the overall performance of the aluminium-air battery.

In the polarization study shown in Figure 4.10 (a), the maximum power density generated is greatly improved by reduce the thickness of the polypropylene pad. Thin polypropylene pad can provide higher power density which is about 240 mW.cm⁻² as compared to about 80 mW.cm⁻² achieved by thick polypropylene pad. The improvement is about three-fold for the thin polypropylene pad used as the medium to absorb the KOH electrolyte. This is because thin polypropylene pad has a better diffusion rate compared to thick polypropylene pad. The movement of ions is more favorable due to the short travel distance between anode and cathode which in turn, improves the power output of the battery as it can enhance the ions movement to facilitate better electrochemical reaction.

There is no distinguishable difference in the voltage reduction at a low discharge current for thin and thick polypropylene pads. At low discharge current, the voltage drop is dominated by the overpotential. Overpotential of the battery is usually affected by the effects of the catalytic surface. Since the cathode used in the experiments are the same, the results of overpotential are not observed when comparing thin and thick polypropylene pads. The voltage tends to drop linearly due to ohmic loss as the discharge current increases. The charge transport of the reactant plays an important role in the ohmic loss. Comparison of thin and thick polypropylene pads, thick polypropylene pad suffers a more severe voltage drop than that of the thin polypropylene pad. This suggested that the movements of electrons in the thin polypropylene pad are freely and contribute to the higher voltage output. The sharp drop in voltage for thick polypropylene pad shows that the resistance in thick polypropylene pad is higher than that of the thin polypropylene pad. Since the resistance in thin polypropylene pad is the lowest, the power generated is also higher. Besides that, reducing the thickness of the polypropylene pad allows high discharge current. At high discharge current, the voltage drop is dominated by mass transport resistance. In thin polypropylene pad, a discharge current of 155 mA is achieved as opposed to 95 mA for thick polypropylene pad. This is due to the reactants traveling in a shorter distance in thin polypropylene pad and enhancing the rate of electrochemical reaction.

The discharge performance of the battery for thin and thick polypropylene pad is illustrated in Figure 4.10 (b). The discharge current used is 30 mA. In general, thin polypropylene pad outperform the thick

polypropylene pad. Thin polypropylene pad can last 75 minutes of discharge while thick polypropylene pad can last only 53 minutes of constant discharge current at 30 mA. The discharge duration is improved by 40% for thin polypropylene pad. Moreover, the discharge voltage of the thin polypropylene pad is also higher than that of thick polypropylene pad. During the discharge cycle, thin polypropylene pad can provide voltage output ranging from 1.8 V to 1.2 V with gradual voltage reduction through the discharge period. On the other hand, thick polypropylene pad can only provide voltage output ranging from 1.5 V to 1.2 V. Since a thin polypropylene pad provides the optimum performance for the aluminium-air battery, the experiment was conducted using thin polypropylene pad for the next study.

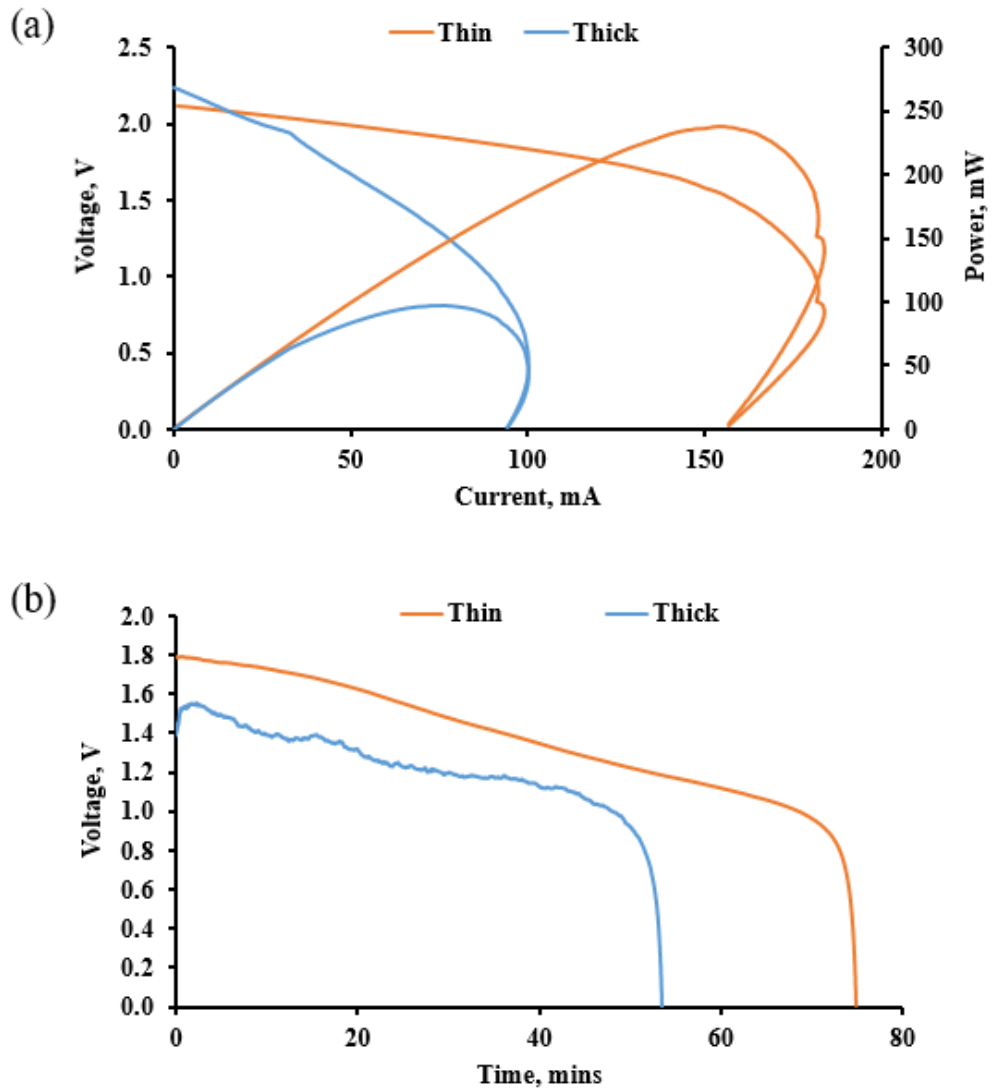


Figure 4.10: (a) Polarization curve and (b) discharge curve of the thin vs thick polypropylene pad in the dual electrolyte aluminium-air battery.

4.3.3 Effects of Anolyte Concentration

The concentration of anolyte is also an important parameter that can affect the performance of the battery. The performance of the aluminium-air battery is investigated by varying the concentration of anolyte while the concentration

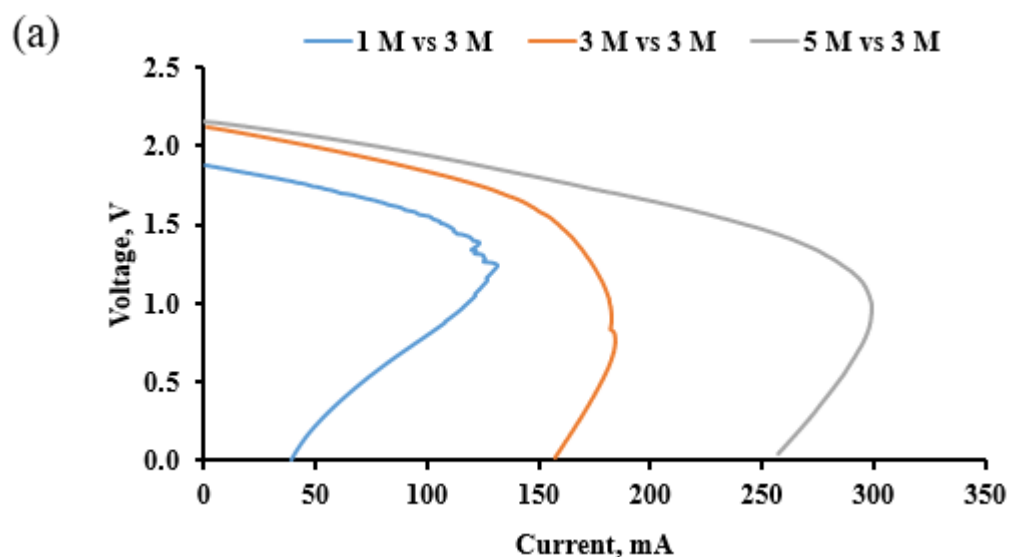
of catholyte is kept constant. The polarization curves of the aluminium-air battery with different concentrations of anolyte and 3M of H₂SO₄ catholyte are shown in Figure 4.11 (a) and (b). In general, the performance of the battery is positively correlated to the concentration of anolyte. The OCV remains almost constant regardless of the concentration of anolyte at about 2.2 V. However, a sharp drop in voltage was observed when 1M of KOH was used. This is due to limited OH⁻ ions available for the electrochemical process in 1M of KOH electrolyte. By using a higher concentration of KOH, more OH⁻ ions are available and help to speed up the electrochemical reaction and more power is generated. At 5M of KOH anolyte, the maximum peak power density is about 350 mW.cm⁻² and higher than that of the 1M of KOH anolyte used in the aluminium-air battery.

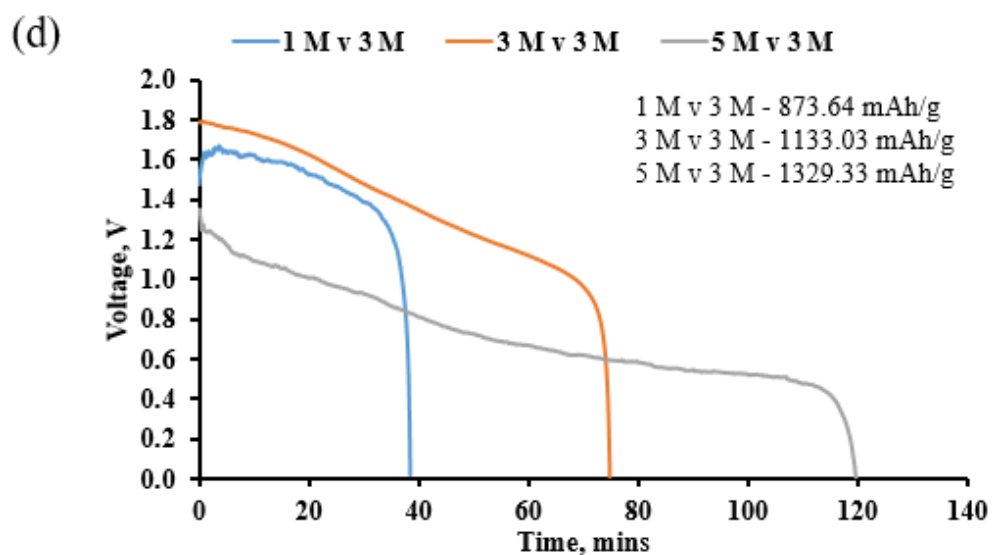
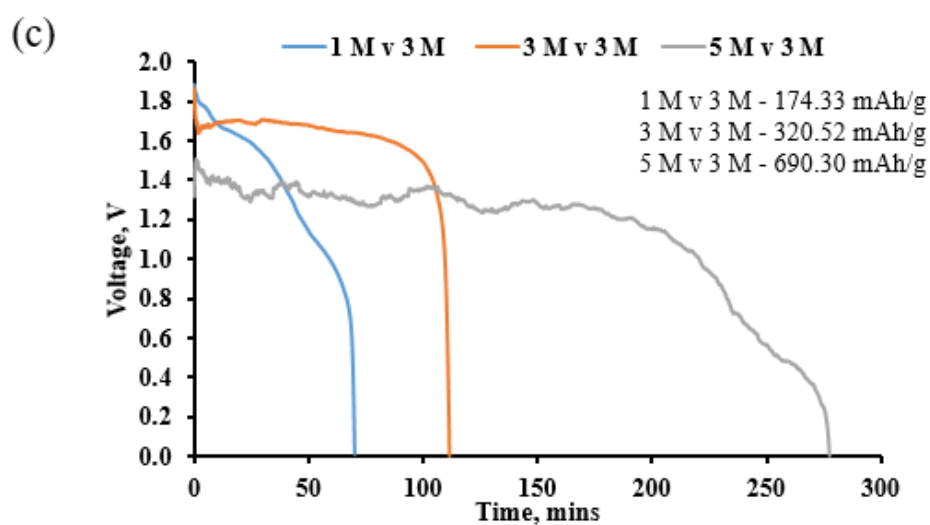
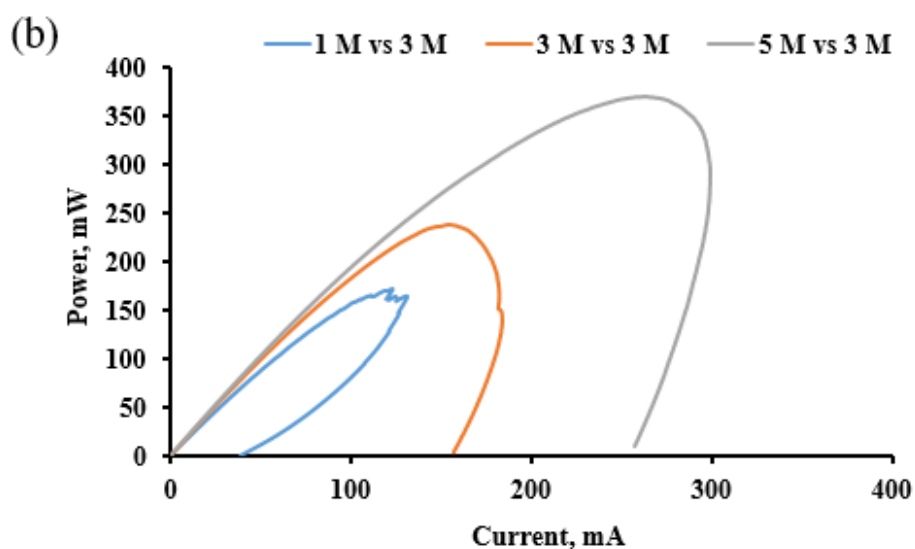
Furthermore, the performance of the aluminium-air battery is investigated with different discharge currents and different concentrations of anolyte while maintaining 3M of catholyte at constant. The discharge curves are plotted in Figure 4.11 (c), (d) and (e). At discharge current of 10 mA, 1M of anolyte shows a quick drop in voltage from 1.9 V to 0 V within 70 minutes. No flat plateau voltage output is observed. Increasing the concentration of anolyte to 3M shows a better performance. It can provide the voltage output in the range of 1.6 V to 1.7 V by maintaining it for about 110 minutes before the energy is depleted. Further increasing the concentration of anolyte to 5M can extend the discharge duration to about 278 mins with the drawbacks of the lower voltage output of about 1.4 V. As the discharge current increases to 30 mA and 50 mA, there is a drop in voltage output and discharge duration. Taking 5M anolyte as

an example, the discharge duration is dropped to about 120 minutes and 50 minutes for discharge current of 30 mA and 50 mA, respectively. Moreover, the output voltage decreased sharply associated with the increase of the discharge current. This is because when discharge current is increased, more energy is drawn from the battery, and the electrochemical reaction rate is also increased. However, due to limited OH^- ions supply, the battery degraded rapidly at high discharge current. The amount of OH^- becomes the limiting factor that reduces the discharge duration. From the literature, the aluminium-air battery should show an improvement in performance with increasing KOH concentration (Pino et al., 2014; Wang et al., 2010). It is predicted that the voltage output and discharge duration should be increased with increasing concentration of KOH electrolyte. However, this is not reflected in the current study with polypropylene pads. On the other hand, the polarization curve is still valid and obeys the general observation in which a high concentration of KOH will result in a higher power and voltage as compared to a low concentration of KOH. This discrepancy observation is because of the design used in this study. A linear relationship between the concentration of KOH with the battery performance only works in a single electrolyte system. In dual-electrolyte aluminium-air battery, the performance is affected not only by the concentration of anolyte but also the concentration of catholyte. The difference in concentration for both the electrolytes will affect the ions cross over to initiate the electrochemical reaction.

The specific discharge capacity of the battery is affected by the concentration of KOH electrolyte, it is shown that higher concentration of KOH electrolytes will produce higher specific discharge capacity. At discharge

current of 10 mA, 1M of KOH achieved a specific discharge capacity of 174.33 mAh.g⁻¹ and it is improved to 690.30 mAh.g⁻¹ for 5M of KOH while maintaining the concentration of catholyte at 5M. The improvement is caused by the increases in OH⁻ ions when higher concentration of KOH is used. This specific discharge capacity is still low and can be improved by increasing the discharge current. When the discharge current is increased to 30 mA, the specific discharge capacity is greatly improved to about five folds for 1M of KOH to 873.64 mAh.g⁻¹ and about two folds for 5M of KOH to 1329.33 mAh.g⁻¹. This is because as the discharge current increases, more OH⁻ ions are utilized in electrochemical reactions and hence, produce better electrical performance and reduce the rate of parasitic reaction.





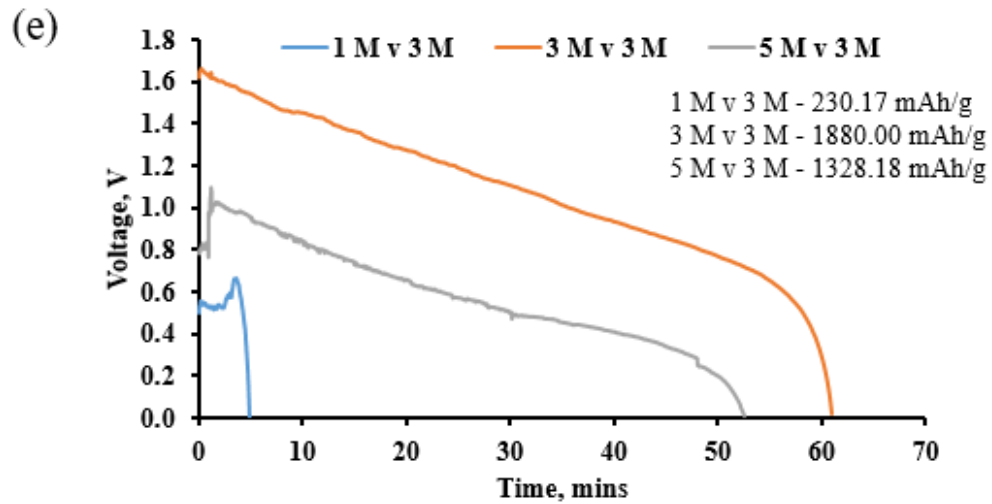
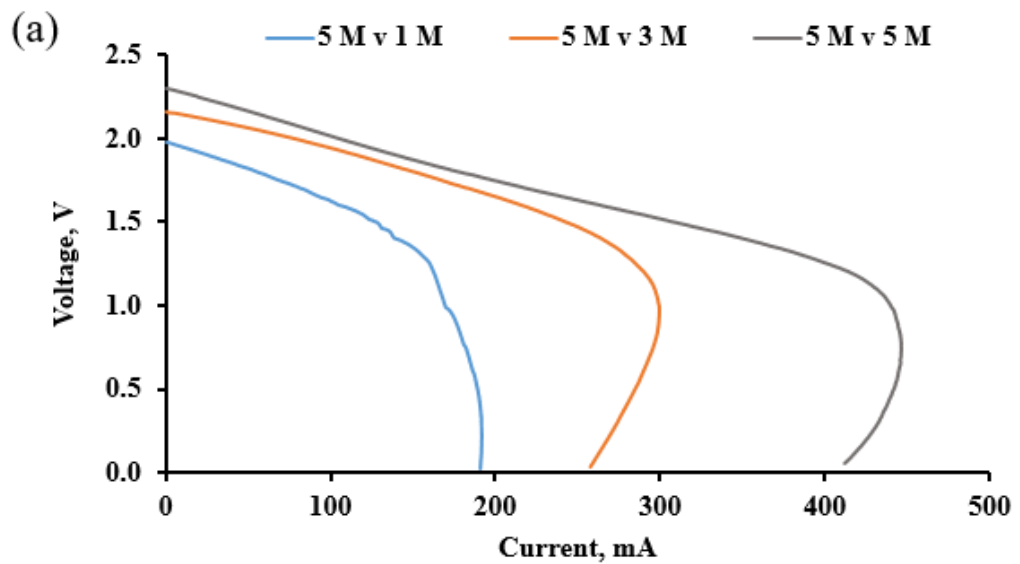


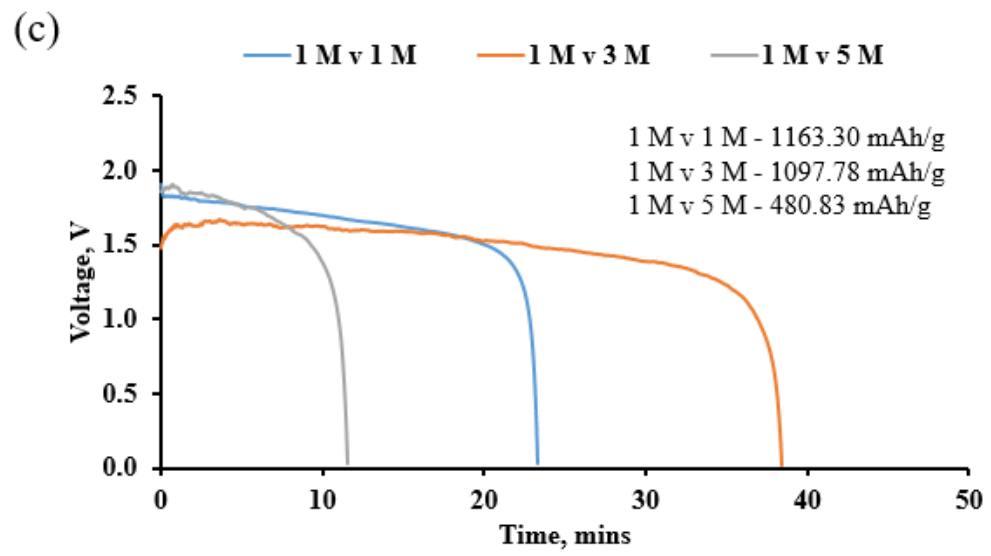
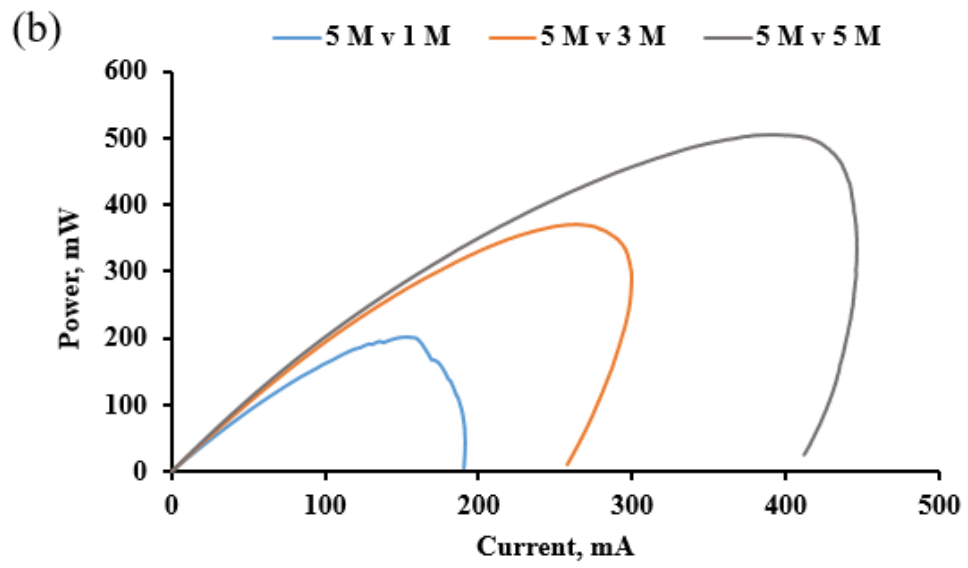
Figure 4.11: Polarization characteristics of the aluminium-air battery (a) Voltage vs current density, and (b) Power density vs current density and the discharge curve for various current densities (c) 10 mA, (d) 30 mA and (e) 50 mA using different concentrations of anolyte.

4.3.4 Effects of Catholyte Concentration

In this section, the effect of different concentrations of H_2SO_4 catholyte is evaluated using 30 mA of discharge current while maintaining same concentration of KOH anolyte. The polarization study of the different concentration of catholyte with 5M of anolyte is illustrated in Figure 4.12 (a) and (b). The test result showed that high concentration of catholyte can boost the performance of the battery. When 1M of catholyte is used, the maximum current and power density achieved are about $190 \text{ mA}\cdot\text{cm}^{-2}$ and $200 \text{ mW}\cdot\text{cm}^{-2}$, respectively. Increasing the concentration of the catholyte to 5M boosts the current and power density to about $450 \text{ mA}\cdot\text{cm}^{-2}$ and $500 \text{ mW}\cdot\text{cm}^{-2}$, respectively. Based on a previous study, a solid-state aluminium-air battery

usually has a low performance due to the impeded ionic diffusion in the electrolyte and usually provides a few or tens of $\text{mW}\cdot\text{cm}^{-2}$ (Wu et al., 2016; Zhang et al., 2014; Wang et al., 2021). In this study, the maximum power density is about $13.88 \text{ mW}\cdot\text{cm}^{-2}$, which is comparable to the solid-state aluminium-air battery. Although the polarization curve shows that increasing the concentration of catholyte improves the power density, the results in the discharge curves do not agree with the observation in the polarization curve. This is because the diffusion of the ions through the polypropylene pad and separator is a complicated process.





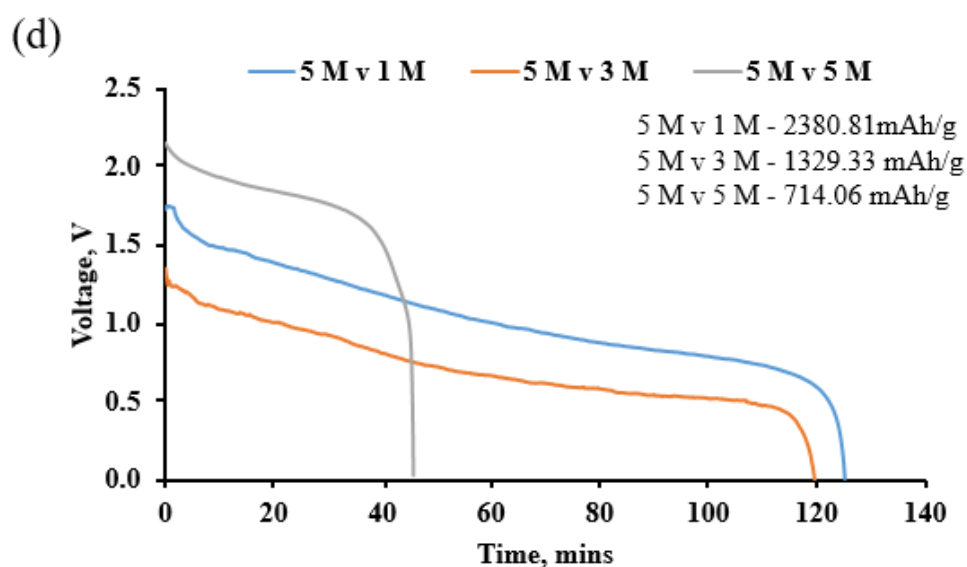


Figure 4.12: Polarization characteristics of the aluminium-air battery (a) Voltage vs current density, and (b) Power density vs current density and the discharge curve at 30 mA for (c) 1M of KOH and (d) 5M of KOH in comparing the effects of catholyte concentration.

When 1M of anolyte is used and the catholyte is varied from 1M to 5M, the initial discharge voltage remains relatively close to each other as shown in Figure 4.12 (c) and (d). This suggested that the discharge voltage is not affected by the concentration of the catholyte when 1M of anolyte is used. The discharge voltage is limited by the anolyte concentration, and this is the limiting factor that affects the performance of the battery. Since the anolyte used is 1M, the performance is relatively low, and the discharge duration is short. The longest discharge duration is achieved by 1M of anolyte with 1M of catholyte is about 23 min only. Hence, the low concentration of catholyte will lower the discharge duration and reduce the capacity of the battery. This is due to an increase of the half-cell reaction at the cathode side, which in turn involves the formation of

water molecules at the cathode. As a result, more water molecules are formed and block the surface area and eventually, causing the battery to discharge rapidly due to the water clogging on the cathode used in the battery. This is also known as flooding of the electrode (Liu et al., 2017). There is no improvement in half-cell reaction on the anode side due to the limited OH^- ions provided by the low concentration of KOH used at the anode. Although the half-cell reaction at the cathode side increases the formation of H^+ ions for the anode to undergo an electrochemical reaction, it does not help in boosting the performance of the battery. The performance is limited due to the low concentration of anolyte used at the aluminium anode and not sufficient fresh OH^- ions supplied to the cathode to complete the electrochemical reaction. Hence, a high concentration of catholyte is unfavourable for low concentration of anolyte as it cannot help to improve the discharge performance while reducing the discharge duration.

There is a significant improvement in the discharge duration when the concentration of the anolyte is increased to 5M. When 5M of KOH and 1M of H_2SO_4 is used, the discharge duration is significantly improved to 125 min. The improvement of discharge duration is due to the higher amount of OH^- ions available in 5M of KOH for the electrochemical reaction. However, the voltage is generally lower as compared to 1M of KOH and 1M of H_2SO_4 . This is because, at a high concentration of anolyte and a low concentration of catholyte, the number of OH^- ions at the anode is much higher than the number of H^+ ions at the cathode side. Therefore, it is more difficult for H^+ ions to flow to the anode side, as OH^- ions occupy the space in the anolyte polypropylene pad. Therefore, the limiting factor now occurs at the cathode in which the half-cell reaction at

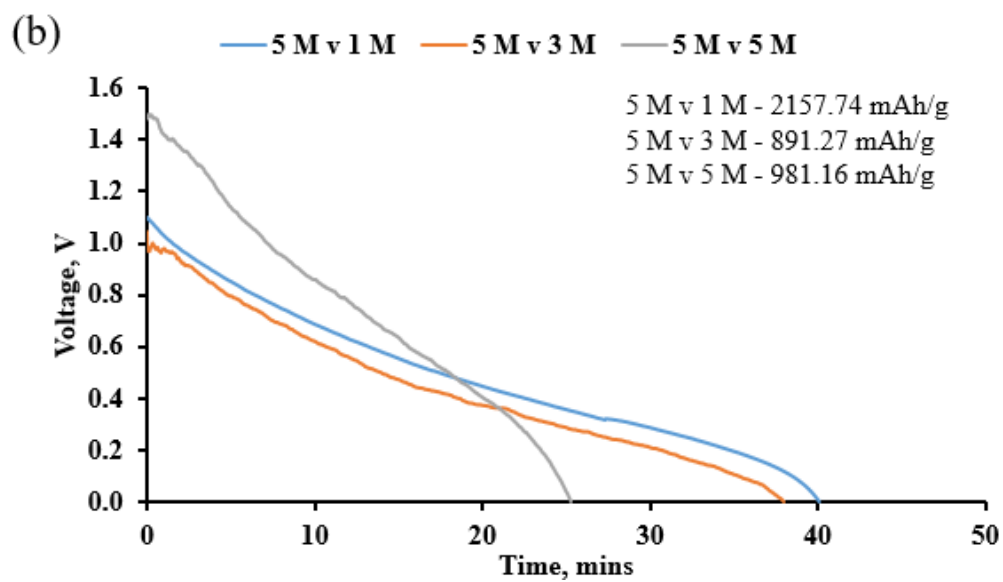
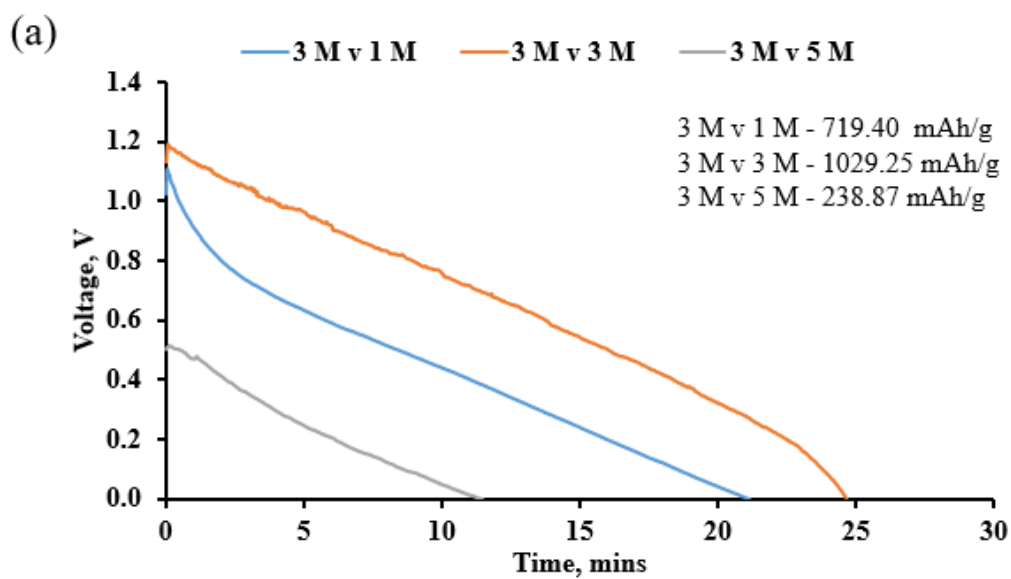
the cathode is not able to match with the anode. As a result, low voltage output is observed. On the other hand, when the concentration of catholyte is increased to 5 M, the voltage output is greatly improved. More than 1.5 V is observed followed by a sharp decrease in voltage suggesting that the discharge duration is short. This is because a high reaction rate induces a large amount of water formation at the cathode which reduces the binding site for electrochemical reaction.

The relationship between the concentration of anolyte and catholyte is significant at high discharge current. Figure 4.13 shows a discharge curve at a discharge current of 100 mA for different concentrations of anolyte and catholyte. The battery equipped with 1M of KOH is not able to discharge using discharge current of 100 mA. Hence, experiments are conducted using 3M, 5M and 8M of KOH with different concentrations of catholyte. At 3M of KOH with different concentrations of catholyte, increasing the concentration of catholyte reduced the discharge duration and the voltage output. However, the combination 3M of KOH and 3M of H₂SO₄ does not obey the phenomenon in which it has the highest discharge duration and voltage output. This behavior is similar to the combination 1 M of KOH and 1 M of H₂SO₄ at discharge current of 30 mA. This suggested that maintaining the same concentration of anolyte and catholyte can provide the highest voltage output and discharge duration for the aluminium-air battery. Maintaining the same concentration is important to ensure a constant flux rate in exchanging H⁺ and OH⁻ ions which in turn maintains a better battery performance. Both the cathode and anode do not overtake each other and hence, ensure more stable performance. However, this

behaviour is not observed for the combination of 5M of KOH and 5M of H₂SO₄. Although it maintains the highest voltage output as shown in Figure 4.12 (d), the discharge duration is not the longest as compared with other concentrations of catholyte. As discussed before, a high concentration of catholyte will reduce the discharge duration due to the formation of water molecules in the half cell reaction. The same observation is recorded when the concentration of anolyte is increased to 8M. Lower voltage output and lower discharge duration is associated with increasing the catholyte concentration.

The specific discharge capacity tends to reduce with increasing catholyte concentration. Under discharge current of 30 mA, the 5M of anolyte with 1M of catholyte achieved the highest specific discharge capacity of 1390.92 mAh.g⁻¹ in this study. It tends to reduce to only 714.06 mAh.g⁻¹ when the concentration of catholyte is increased to 5M. At high catholyte concentration, water flooding of electrolytes tends to limit the reaction at the cathode site. Hence, causing a reduction in ORR and performing poorly in the aluminium-air battery. The same phenomenon is observed for high discharge current as well. Hence, there is a close relationship between the concentration of anolyte and catholyte. At a constant concentration of anolyte, increasing the concentration of catholyte will decrease the discharge duration and voltage output. It is better to keep a low concentration of catholyte to get a better voltage output and longer discharge duration. However, this is not always true as maintaining the same concentration of anolyte and catholyte (for 1M and 3M) can ensure better voltage output and higher discharge duration except for a high concentration of catholyte at 5M. When 5M of KOH and 5M of H₂SO₄ is used, it can increase

the voltage output but not the discharge duration.



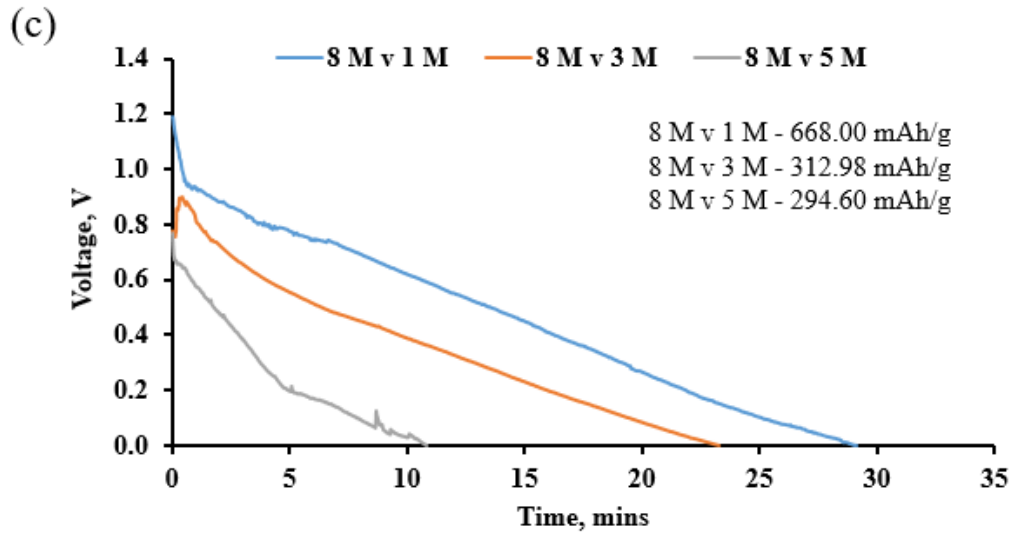


Figure 4.13: Discharge curve for (a) 3M of KOH, (b) 5M of KOH and (c) 8M of KOH in comparing the effects of catholyte concentration using discharge current of 100 mA.

4.3.5 Comparison Between Single and Dual Electrolyte System

Unlike a dual electrolyte system, a single electrolyte system is simple and only needs KOH anolyte for the battery. Besides, filter paper is also not needed and a polypropylene pad act as the separator to isolate the anode and air cathode. Since only KOH is involved in the electrochemical reaction, the electrochemical reaction is different from the dual electrolyte system. The electrochemical reactions for single electrolyte aluminium-air battery are indicated in Eq. 2.3 to Eq 2.5. The theoretical voltage is generally lower for a single electrolyte system. A comparison study between the performance of a single electrolyte system and a dual electrolyte system is conducted using different concentrations of KOH electrolyte. The comparison is based on the

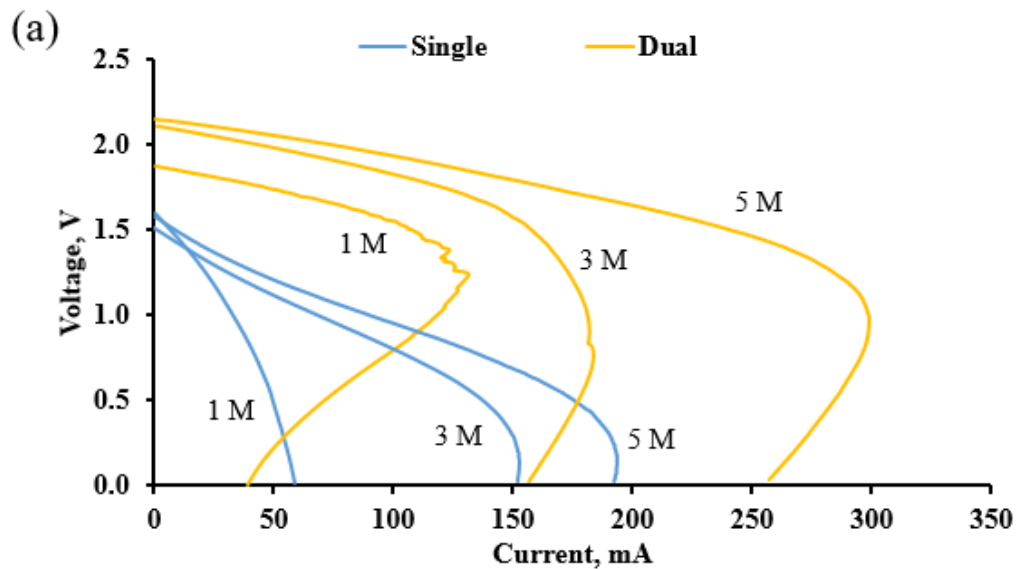
dual electrolyte system with cathode concentration fixed at 3M of H₂SO₄ and 4 ml of KOH electrolyte is added to the polypropylene pad for both electrolyte systems.

As shown in polarization curves in Figure 4.14 (a) and (b), the OCV for the single electrolyte system is lower than that of the dual electrolyte system. Single electrolyte system can achieve OCV of about 1.6 V which is about 30% lower than that of the dual electrolyte system with OCV of about 2.1 V. The improvement of OCV in the dual electrolyte system is due to the higher oxygen reduction reaction in the acidic medium of the cathode as indicated in Eq. 2.6 and Eq. 2.7. There are few benefits associated with the dual electrolyte system. Firstly, the voltage output for a dual electrolyte system is always higher than that of the single electrolyte system. Secondly, the voltage drops due to increasing the discharge current is generally lower for the dual electrolyte systems. Moreover, the dual electrolyte system shows improvement in the maximum capacity of the battery and power generated. For 1M of KOH, the maximum power density produced in the single electrolyte system is about 33 mW.cm⁻² and it is then improved to 170 mW.cm⁻² for the dual electrolyte system. This enhancement is also observed for 3M and 5M of KOH and the power density is increased by 3 folds and 3.5 folds, respectively for the dual electrolyte system. This improvement is obvious, suggesting that dual electrolyte system possess a huge potential for the aluminium-air battery. The improvement in the cathodic reaction is the main factor leading to the high-power density produced in the dual-electrolyte system.

The discharge curve illustrated in Figure 4.14 (c) shows the comparison of the aluminium-air battery for both electrolyte systems. The aluminium-air batteries are tested under discharge current of 30 mA. Two scenarios are observed from the experimental results, the discharge voltage for the dual electrolyte system is always higher than that of the single electrolyte system and the discharge duration for the dual electrolyte system is always lower than the single electrolyte system. In 1M of KOH, a dual electrolyte system can produce voltage higher than 1.5 V and remain for about 39 mins. On the other hand, 1M of KOH single electrolyte system shows a constant voltage of only about 1 V for about 41 mins. The voltage is about 50% lower while maintaining almost similar discharge duration. The difference in discharge duration is more obvious for a higher concentration of KOH electrolyte. In 5M of KOH, the discharge duration for the dual electrolyte and single electrolyte systems are about 84 minutes and 113 minutes respectively. However, the voltage output for a dual electrolyte system range from 2 V to 1.5 V during the discharge cycle while it is only 1.2 V for a single electrolyte system. As discussed previously, the improvement in voltage is due to the improvement of ORR reaction. More OH^- ions will be consumed during the process and leads to higher water generation at the cathode side. Since a limited amount of KOH electrolyte is added in the polypropylene pad, OH^- ions are consumed at a higher rate for electrochemical reaction and the KOH electrolyte for the dual electrolyte system dried out at a rapid rate and the discharge duration is reduced.

Comparison of the specific discharge capacity between single and dual electrolyte systems showed that there is a great improvement especially for 1M

and 3M of KOH electrolytes as indicated in Figure 4.14. The improvement is about three folds and two folds, respectively. However, the improvement is not obvious for 5M of KOH. Although the specific discharge capacity remained same for both systems, the dual electrolyte system still outperforms the single electrolyte system by producing a higher OCV. Hence, the introduction of a dual electrolyte system can enhance the ORR of the cathode which elevates the electric performance of the aluminium-air batteries. Therefore, a dual electrolyte system offers higher voltage and power output with reduced discharge duration as compared to a single electrolyte system. The solution to prolong the discharge duration is to consistently add in fresh KOH to the system to provide fresh OH⁻ ions for the reactions.



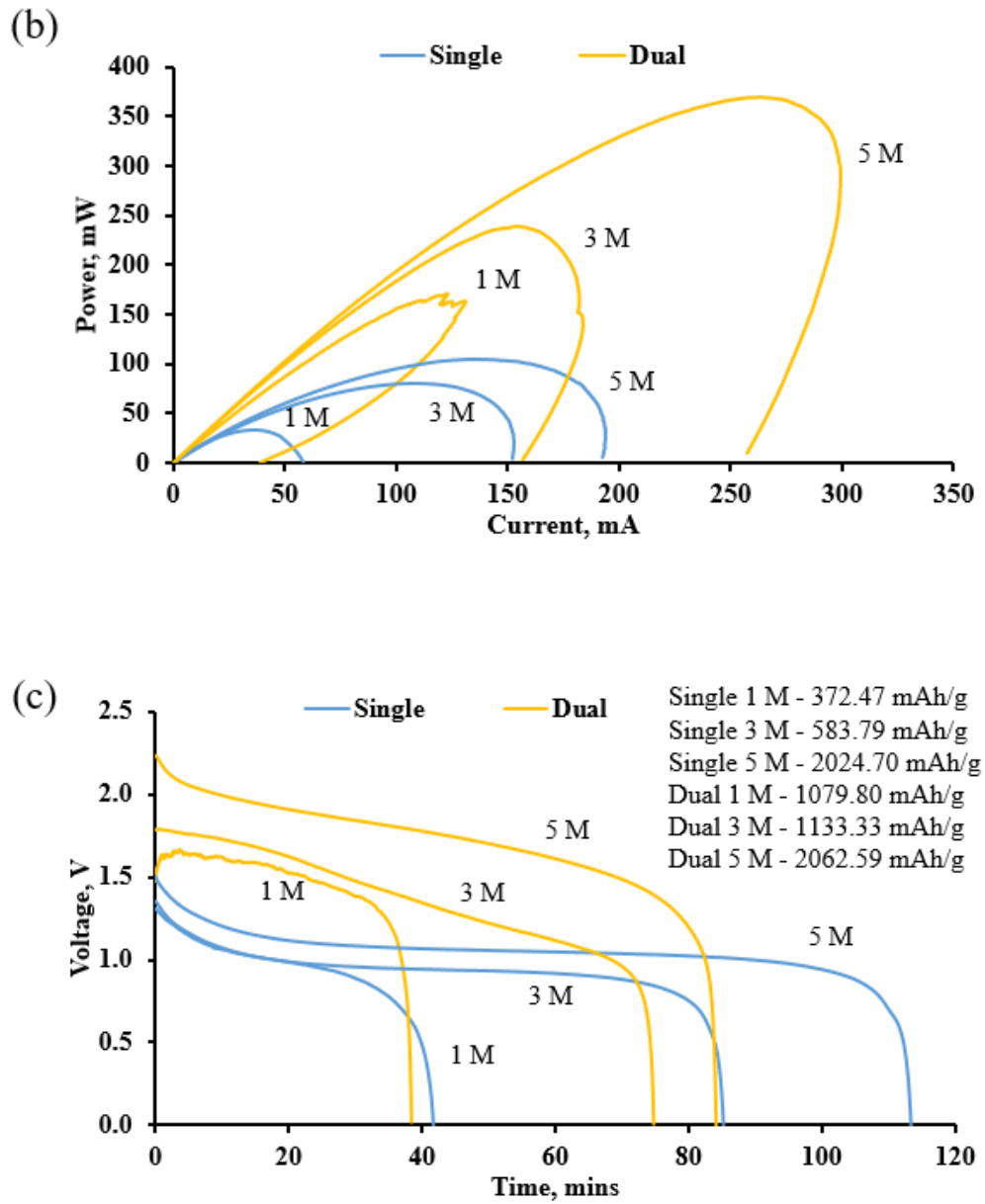


Figure 4.14: Polarization characteristics of the aluminium-air battery (a) Voltage vs current density, (b) Power density vs current density and (c) discharge curve at discharge current of 30 mA for single electrolyte and dual electrolyte system.

4.3.6 EIS Analysis

When comparing the effects of the catholyte, as shown in Figure 4.15 (a), increasing the concentration of catholyte will dramatically reduce the solution resistance, R_s . When 1M catholyte is used, the solution resistance is 12.51 Ω based on curve fittings and reduced to only 1.96 Ω when 5M of catholyte is used. The reduction is due to the great improvement in the oxygen reduction rate at the cathode. The H_2SO_4 plays an essential role in promoting the rate of oxygen reduction by supplying the H^+ ions. The reduction in the value of R_{ct} and W also suggested that the charge transfer resistance and the diffusion of the ions have been improved. High concentration will hinder the movement of ions in the polypropylene, as discussed in a single electrolyte system. However, opposite phenomenon is observed in a dual electrolyte system as the diffusion of the ion is enhanced by high concentration of catholyte. This is due to the introduction of the diffusion flux as the concentration gradient present between the anolyte and catholyte. The movement of ions from catholyte to anolyte is becoming easier. This also explained the output voltage is generally higher when a high concentration of catholyte is used but will also cause a reduction in the discharge time due to the faster movement of ions between anolyte and catholyte, as published in previous work (Tan et al., 2022)

Figure 4.15 (b) shows the effects of anolyte concentration used in the dual electrolyte aluminium-air battery. The Nyquist plot shows a shift in the semicircle from a higher peak to a lower peak when the anolyte concentration is reduced. The radius of the semicircle is reduced as well, suggested that the

R_{ct} tends to drop with a reduction in the anolyte concentration. As discussed previously, due to the larger concentration difference in anolyte and catholyte for 5M of KOH anolyte and 1M of H_2SO_4 used in the battery, the diffusion flux will be improved, which enhances the charge transfer performance. However, the effects of increasing the concentration of anolyte in reducing the R_s value are less significant. This may be due to the low concentration of catholyte used in the aluminium-air battery. The ORR is the limiting factor affecting the aluminium-air battery's performance. Increasing the engagement of anolyte while keeping the same rate of ORR does not show improvement to the battery as the reduction reaction cannot catch up with the oxidation reaction. In comparing the effect of concentration of catholyte, the reduction of R_s value with increasing concentration of catholyte shows that even 1M of KOH electrolyte can meet the improvement on the ORR rate at high concentration of catholyte. Hence, it can be concluded that the effect of ORR is more significant in the design of an aluminium-air battery. Table 4.3 and Table 4.4 summaries the values of the electrical components in the equivalent circuit model.

There is a difference in R_s value when comparing a single and dual electrolyte system with aluminium alloy 6061 as the anode. The main reason is due to the cathode used. In a single electrolyte system, the cathode used is carbon fiber, while a graphite plate with MnO_2 as an electrocatalyst is used as the cathode in the dual electrolyte system. This can greatly enhance the ORR reaction due to the more active area available for electrochemical reactions. The R_s value for a single electrolyte generally ranges between 20 Ω to 36 Ω for different concentration electrolytes. Nevertheless, the dual electrolyte system

recorded a maximum R_s value of about 15 Ω . The graphite cathode has dramatically reduced the resistance of the aluminium-air battery. Furthermore, the R_{ct} and W values are significantly lower for dual electrolyte systems compared to single electrolyte systems. Graphite plate provides a more reactive site for the diffusion of oxygen compared to carbon cloth, reducing the charge transfer resistance. On the other hand, the C_{dl} value is significantly higher than the single electrolyte system in which it is in hundreds of μF as compared to only tenths of μF in a single electrolyte system. Since a dual electrolyte system involved a more complicated movement of ions due to the extra catholyte components at the cathode side, the charge transfer resistance tends to increase. However, it is noted that the impact of charge transfer resistance on the overall electrical discharge performance is less significant than the effects of diffusion and solution resistance. Therefore, the performance of a dual electrolyte system can still perform better than a single electrolyte system as higher discharge voltage is recorded in the study on dual electrolyte systems.

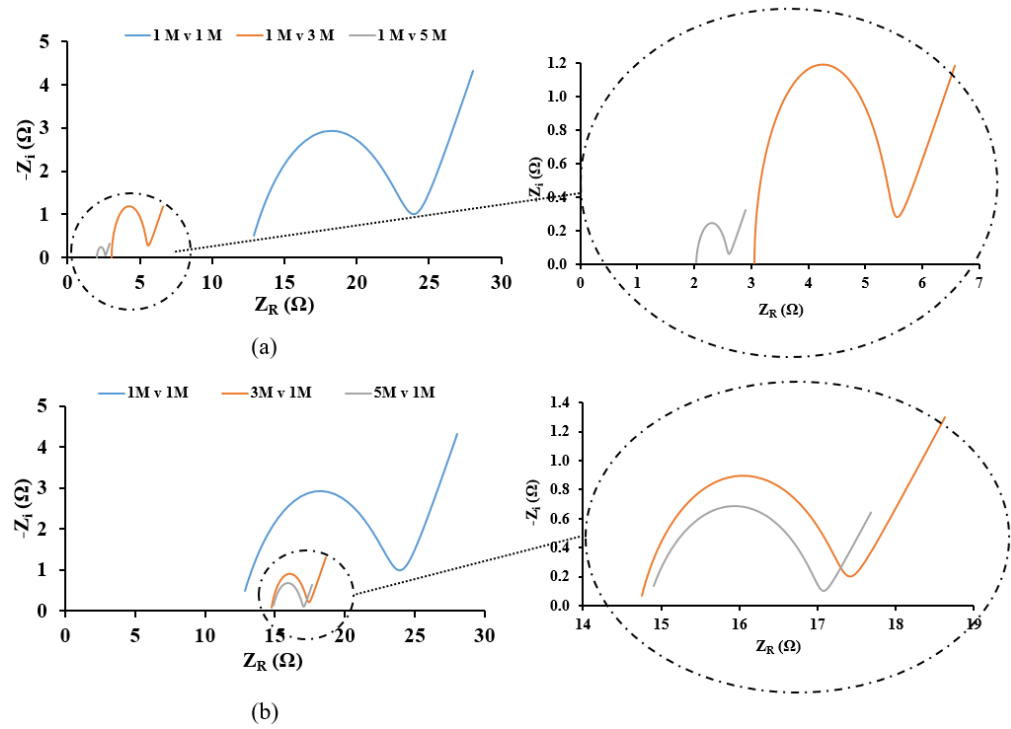


Figure 4.15: Nyquist plot comparing (a) effects of concentration of catholyte and (b) effects of concentration of anolyte.

Table 4.3: Parameter of the electrical components in the equivalent circuit model for different catholyte concentration.

Concentration of catholyte with anolyte 1M	R_s (Ω)	R_{ct} (Ω)	W ($\Omega/s^{1/2}$)	C_{dl} (μF)
1M	12.51	11.14	3.53	505
3M	3.05	2.35	1.48	239
5M	1.96	0.61	0.74	495

Table 4.4: Parameter of the electrical components in the equivalent circuit model for different anolyte concentration.

Concentration of anolyte with catholyte 1M	R_s (Ω)	R_{ct} (Ω)	W ($\Omega/s^{1/2}$)	C_{dl} (μF)
1M	12.51	11.14	3.53	505
3M	14.72	2.62	1.03	500
5M	14.82	2.22	0.51	500

4.4 Tafel Plot

The Tafel plot is a valuable tool to measure the corrosion of the aluminium foil and aluminium alloy 6061 in the KOH electrolyte. The corrosion test is conducted in the presence of 1M, 3M, and 5M of KOH electrolytes, respectively. Figure 4.16 shows the result of the Tafel polarization. The OCV of the battery remains at -1.56 V for all concentrations of KOH electrolyte, with the OCV showing a slight increase (leading to a larger value of voltage in terms of magnitude) with increasing concentration of electrolyte. However, the increase is too little and insignificant. This negative shift in OCV shows that the aluminium anode is more prone to corrosion in the alkaline environment and generate hydrogen.

The value R_p can be calculated by extracting all the required information from the Tafel polarization in Figure 4.16 using Eq 3.4 and Eq. 3.5. Table 4.5 shows a summary of the Tafel polarization parameters. The values of β_a and β_c are approximated by plotting the Tafel slope with a straight line and calculating the gradient of the straight line. The corrosion rate tends to increase with a lower R_p value. From Table 4.5, the R_p value decreases with the increasing of the KOH concentration. Therefore, the aluminium alloy 6061 suffers more significant corrosion at 5M of KOH electrolyte. In 5M of KOH electrolyte, the β_a value is only 0.653 V. dec⁻¹ which shows that the aluminium anode will experience serious corrosion in the 5M of KOH electrolyte. The β_a value determines how large an overpotential is required to drive the reaction (Hosseini et al., 2018). The higher the β_a value, the more overpotential is

needed to activate the corrosion reaction. In other words, the aluminium anode shows less corrosion when immersed in 1M of KOH electrolyte. Although high polarization resistance is good in reducing the corrosion rate in the aluminium-air batteries, it can cause higher overpotential on the aluminium dissolution, especially the fresh aluminium anode is used in the aluminium-air battery due to the passivation layer.

Compared to aluminium alloy 6061, the use aluminium foil as an anode in the aluminum-air battery results in more severe corrosion due to the higher purity of the aluminium foil. From the Table 4.5, it is noted that the R_p value for 1 M and 3 M for aluminium foil is higher than aluminium alloy 6061 respectively. High R_p value suggesting that aluminium foil is suffer from higher rate of corrosion. From the Figure 4.16 (b), it is also noted that the data collected near the tail of the anodic reaction seems to fluctuate a lot especially for the 3 M of KOH electrolyte. This is due to the aluminium foil has been fully consumed during the experiment and no data can be recorded by the potentiostat. No experiment is conducted for 5 M for the aluminium foil due to the reaction of 5 M of KOH with the aluminium foil is too vigorous and causing high level of fluctuation in data collection.

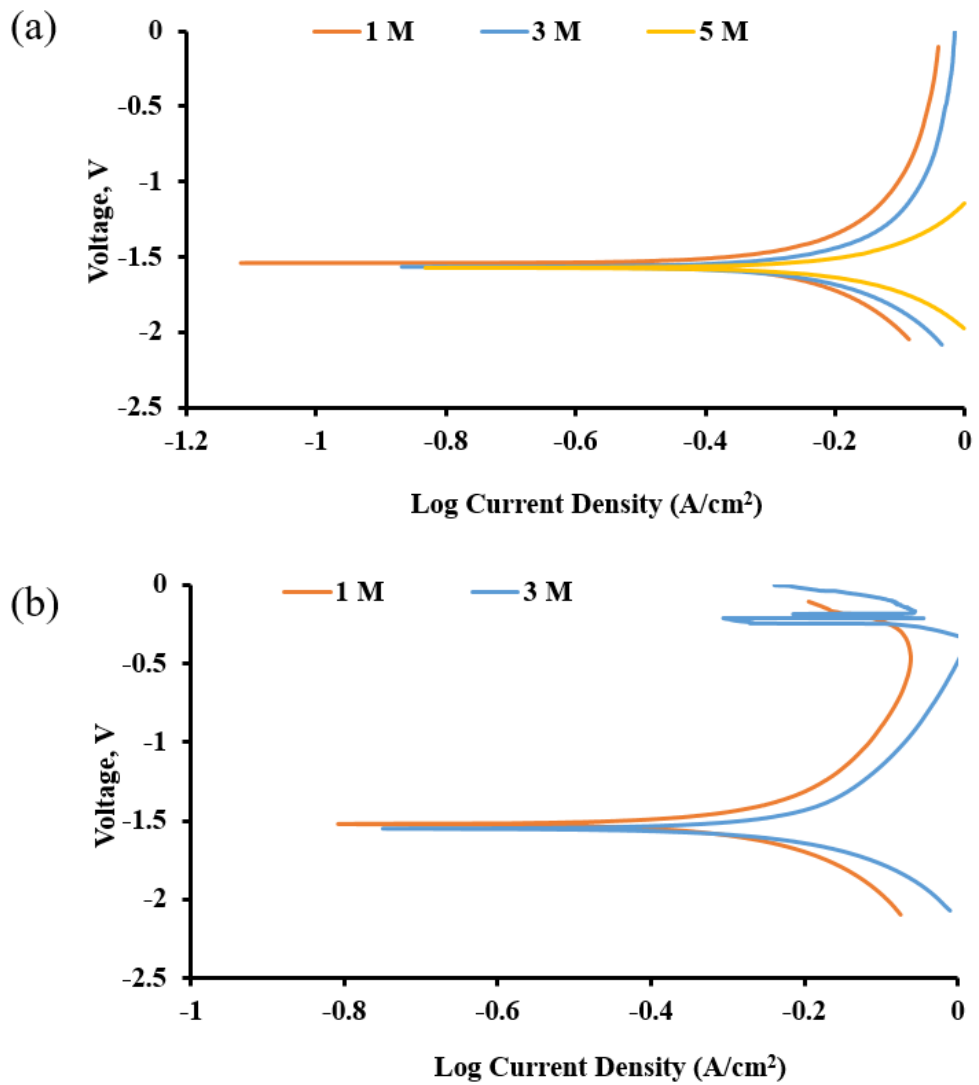


Figure 4.16: Tafel plot comparing the effects of KOH concentration (a) aluminium alloy 6061, (b) aluminium foil.

Table 4.5: Tafel plot data for aluminium alloy 6061 anode and aluminium foil.

Concentration of electrolyte	E_{corr} (V vs. Ag/Cl)	I_{corr} (A.cm ⁻²)	β_a (V.dec ⁻¹)	β_c (V.dec ⁻¹)	R_p (Ω)
Aluminium Alloy 6061					
1M	-1.55	0.0015	4.70	-0.90	211
3M	-1.57	0.0027	2.31	-0.77	94
5M	-1.56	0.0031	0.65	-0.69	46
Aluminium Foil					
1M	-1.52	0.0009	2.10	-0.75	250
3M	-1.55	0.0020	1.60	-0.93	125

4.5 Corrosion rate

Table 4.6 contains information about how the anode in the battery corrodes over time. The weight loss of both aluminium alloy 6061 and aluminium foil anodes are greatly affected by the KOH concentration. The weight loss is larger at high KOH concentration while it tends to reduce when low concentration is used, indicating that the corrosion rate depends on the KOH concentration. At high concentration, more OH^- ions are available to react with the aluminium which speed up the corrosion. However, polypropylene separator works well in reducing corrosion rate, as the change in mass is significantly lower than for aluminium anodes without polypropylene. The most significant reduction in corrosion rate is achieved when using 1M of KOH electrolyte with an aluminium anode alloy 6061, with a reduction of up to 40%. The aluminium-air battery will benefit in terms of discharge time as lower corrosion rate slow down the consumption of the aluminium anode.

Both the aluminium foil and aluminium alloy 6061 are suffer from corrosion when used as the anode and it was found that aluminium foil corrodes more rapidly due to a higher rate of aluminium mass consumption. The aluminium foil used in this study is composed of 100% aluminium elements, making it more susceptible to the reaction OH^- ions, which causes a rapid parasitic reaction. According to a study conducted by Ren et al. (2019), a pure aluminium anode has been proven to have poor corrosion inhibition capabilities. Therefore, using aluminium foil as an anode result in a significant shorter

discharge time as compared to aluminium alloy 6061. The corrosion rate almost shows double than the previous concentration of electrolyte used when the concentration of electrolyte is increasing from 1M to 3M and eventually 5M for both the design, aqueous and polypropylene separator. High concentration of electrolyte will consume the aluminium foil rapidly and hinder from long operating hour. In contrast, aluminium alloy 6061 contains magnesium as an alloying material, which helps to improve its corrosion inhibition capabilities. Magnesium has been shown to perform well as a corrosion inhibitor in previous studies (Ma et al., 2014; Zhang et al., 2021).

This work has shown that the use of aluminium alloy 6061 results in higher anodic utilization efficiency when compared to aluminium foil. The best anodic utilization efficiency of 93.2% is achieved when aluminium alloy 6061 anode is used using 1M of KOH electrolyte in the presence of polypropylene pad. This indicates that a significant portion of the aluminium is consumed to produce electricity, rather than being lost to parasitic reactions that generate hydrogen. However, as the electrolyte concentration is raised, the anodic utilization efficiency decreases, dropping to just 47% with 5M of KOH electrolyte. At this concentration, the parasitic reaction becomes dominant, and the aluminium-air battery generates more hydrogen than electricity. At 3M of KOH electrolyte, the electrochemical and parasitic reactions is almost equal with an anode utilization efficiency of 50.4%. To fully utilize the aluminium anode, it is recommended to keep the electrolyte concentration below 3M, ensuring that most of the aluminium is used to generate electricity. Additionally, the anode utilization efficiency of aqueous systems is always lower than that of

systems using polypropylene as a separator, for both aluminium alloy 6061 and aluminium foil anode. This is because aqueous systems tend to provide excess electrolyte to the aluminium anode even when it is not needed. As a result, the excess electrolyte can corrode the aluminium anode, producing hydrogen and this effect is more severe at high concentrations of electrolyte

Table 4.6: Corrosion rate of the aluminium alloy 6061 anode and aluminium foil anode in 1 hour.

Concentration	Without polypropylene			With Polypropylene			Reduction in corrosion rate (%)
	Change in mass (mg)	Corrosion rate ($\text{mg min}^{-1} \text{cm}^{-2}$)	Anode Utilization efficiency (%)	Change in mass (mg)	Corrosion rate ($\text{mg min}^{-1} \text{cm}^{-2}$)	Anode Utilization efficiency (%)	
Aluminium alloy 6061							
1M	77.6	0.225	38.9	32.4	0.135	93.3	40.0
3M	122.9	0.356	24.6	60.0	0.25	50.4	29.8
5M	126.2	0.368	23.9	63.6	0.265	47.5	28.0
Aluminium foil							
1M	104.9	1.748	28.8	49.5	0.825	61.1	52.8
3M	214.7	3.578	14.1	136.4	2.273	22.2	36.5
5M	414.9	6.915	7.28	221.1	3.685	13.7	28.0

4.6 Surface Characterization

The aluminium anode tends to undergo self-corrosion and remains as a main issue in the aluminium-air batteries that cannot be eliminated. Most studies emphasized on introducing different additives to reduce the corrosion rate. High corrosion rate reduces the aluminium anode utilization efficiency and generates hydrogen gas as a by-product due to the parasitic reaction between OH^- ions and the aluminium anode.

The use of a liquid alkaline electrolyte in the aqueous aluminium-air battery results in more severe corrosion of the aluminium anode. This is attributed to the direct contact between the aluminium anode and the aqueous alkaline electrolyte. Furthermore, the presence of moisture in the electrolyte solution can accelerate the corrosion process by facilitating the formation of an aluminium oxide layer on the surface of the aluminium anode. This oxide layer can act as a barrier, preventing further corrosion, but it can also increase the resistance and reduce the efficiency of the battery.

In order to control the corrosion rate of the aluminium anode, a limited amount of KOH electrolyte was absorbed in polypropylene pad and the polypropylene pad acts as a barrier to prevent excess KOH electrolyte reacts with the aluminium anode. Thus, limiting the rate of parasitic reaction. SEM and XRD analysis were conducted to examine the surface morphology of the aluminium anode after the reaction to gain understanding on the corrosion scenario at the aluminium anode.

Figure 4.17 shows the SEM image of the pristine aluminium anode and the aluminium anode after discharging using 10 mA with different concentrations of KOH electrolyte. It was found that when the concentration of the KOH electrolyte increases from 1M to 5M, the aluminium anode surface becomes rough as compared to the original aluminium anode before the discharging test. As the electrolyte concentration increases to 1M, the surface starts to become uneven, and some powdery structure starts to form on the aluminium anode surface. However, most of the aluminium anode surface is still flat suggesting that the corrosion is not severe. When the concentration of the KOH electrolyte is increased to 3M, a more powdery-like structure is found. The surface becomes very rough, pits and holes are observed. At this point, a very small amount of flat surface is still observable. Lastly, the corrosion is the severest for 5M of KOH. The surface is highly uneven, and a high percentage of the powdery-like structure is observed on the aluminium anode suggesting that many impurities are deposited on the surface. High concentration of alkaline electrolyte promotes the formation of impurities substances on the aluminium anode surface. There is no flat surface as observed from the SEM image. It can be deduced that corrosion is getting severe as the concentration of the KOH electrolyte used is increasing. In the macroscopic view shown in Figure 4.18, it is very obvious that the aluminium anode shows greater corrosion, and the surface of the aluminium anode becomes rougher for high concentration of KOH.

A comparison is conducted to compare the surface morphologies of aluminium alloy 6061 with polypropylene and without polypropylene after the

aluminium anode is in contact with the electrolyte for 1 hour under 5M of KOH electrolyte. The SEM image is as indicated in Figure 4.18, it is found that the corrosion of the aluminium anode with polypropylene is less severe as compared to the case without polypropylene. Most of the aluminium surface remains untouched as a flat surface is still observable when polypropylene is used in the aluminium-air battery. Only a small amount of circular structure is seen along the surface. However, the corrosion is severe for the case without polypropylene. There are mass formation of the circular structure along the surface until no flat aluminium surface is observable. The texture is now very coarse and uneven. At this point, the appearance of aluminium hydroxide has fully covered the surface of the aluminium anode. This suggested that polypropylene is good in reducing the rate of corrosion as it can help to limit the supply of KOH electrolyte to the aluminium anode, which in turn, helps to enhance the life cycle of the aluminium anode.

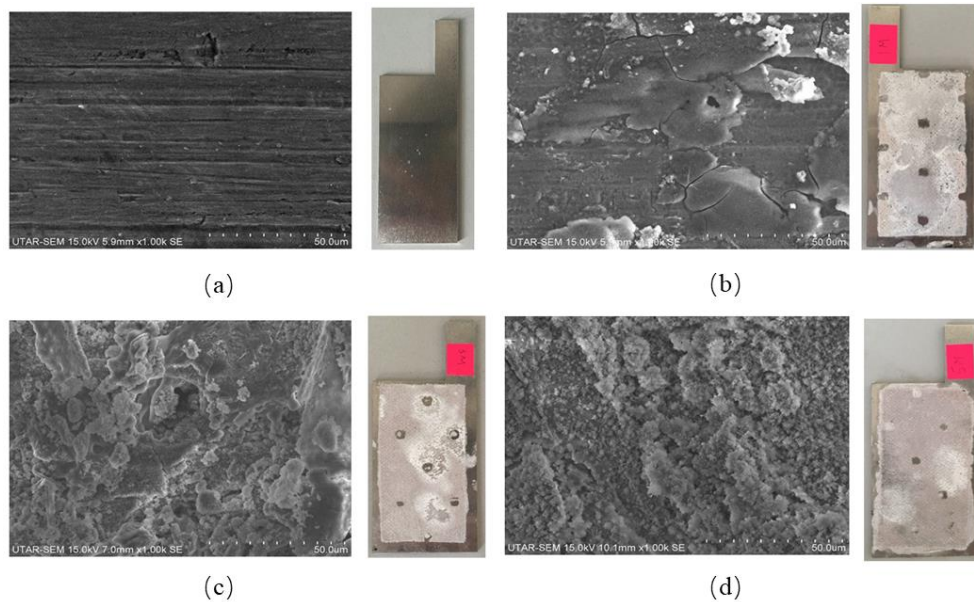


Figure 4.17: SEM images of 1000x magnification and macroscopic view of (a) pristine aluminium anode and after discharging using (b) 1M of KOH, (c) 3M of KOH, (d) 5M of KOH

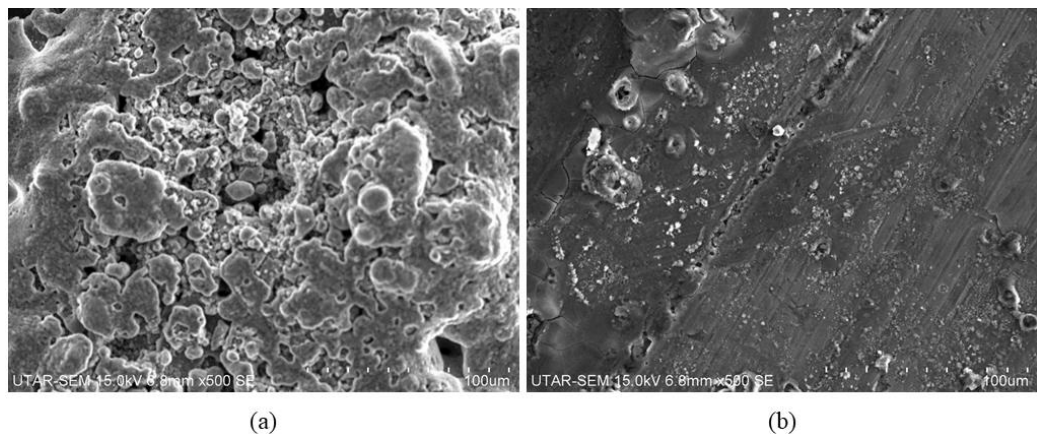
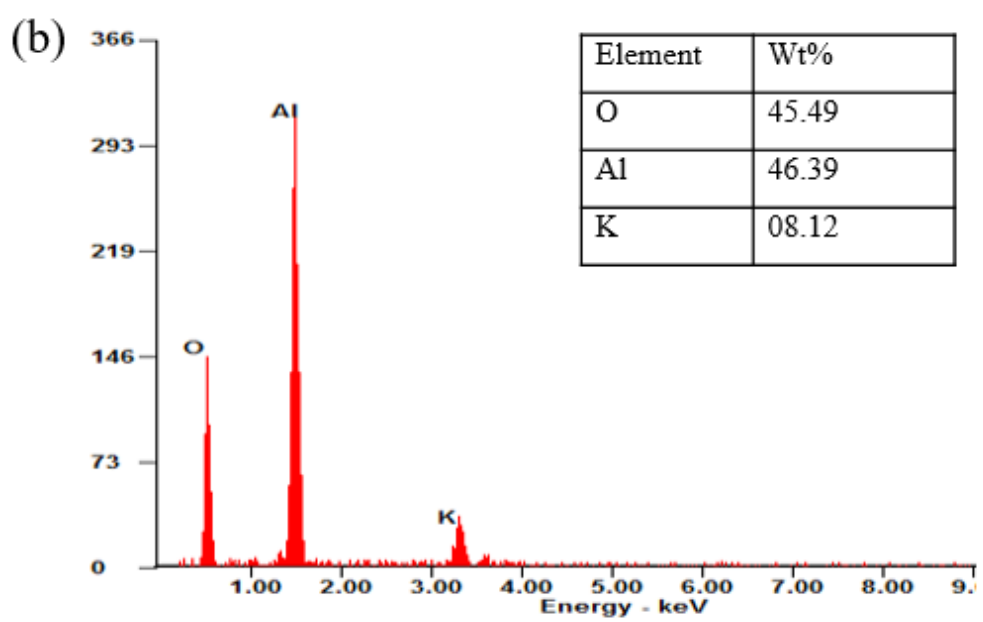
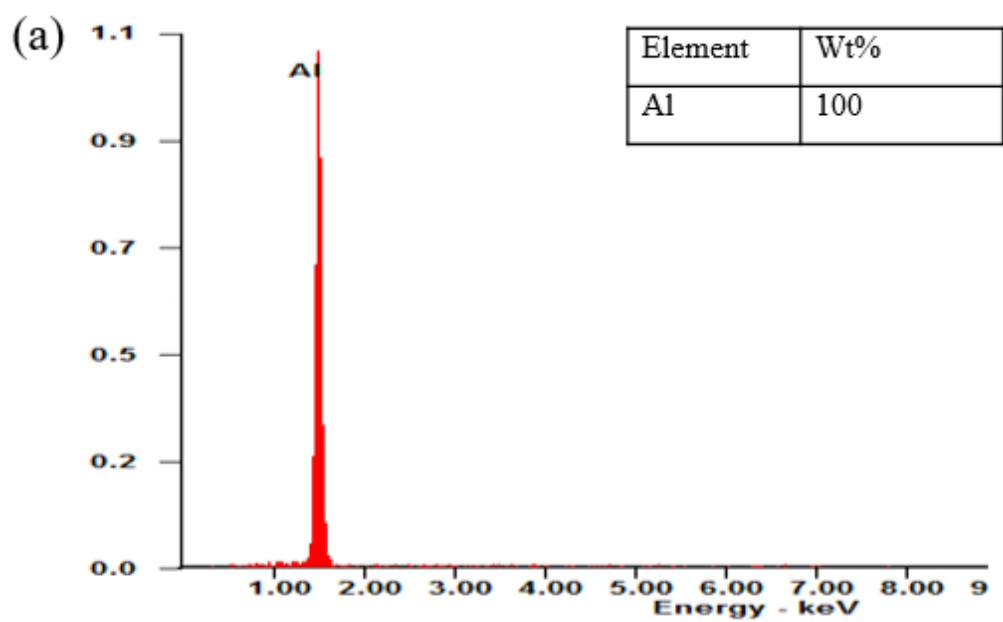


Figure 4.18: SEM image at 500x for Al alloy 6061 discharge for 1 hour for under 5M KOH electrolyte (a) without polypropylene, (b) with polypropylene.

The EDX spectra provide evidence in predicting that the circular structure that formed on the aluminium surface is aluminium hydroxide. In Figure 4.19, the pristine aluminium alloy 6061 only shows aluminium and

magnesium composition while the aluminium foil shows only aluminium peak. However, after the discharge of the aluminium anode for aluminium alloy 6061 and aluminium foil with 3M of KOH electrolyte for 1 hour, the EDX spectra show that oxygen (O) is present together with potassium (K). It is due to the KOH electrolyte is trapped at the aluminium surface and the formation of aluminium hydroxide. Since aluminium hydroxide is formed, the electrochemical reaction occurs as predicted in Eq. 2.3.

XRD test is then performed to investigate the components of the impurities formed on the aluminium anode. After discharge the battery for some time, powdery-like structure is observed along the surface of the aluminium anode. The powdery-like structure can be removed easily by just scratching the surface of the aluminium plate and analyzed using XRD. By comparing the peak of the impurities with the database, it was found out that most of the impurities are aluminium hydroxide and aluminium as shown in Figure 4.20. Aluminium hydroxide is formed as a by-product during the electrochemical reaction in generating electricity after the discharge test, as predicted in the electrochemical reaction in Eq. 2.5. Aluminium hydroxide will shorten the life cycle of the battery. Accumulation of the aluminium hydroxide on the aluminium anode will create a barrier that prevents the active site of the aluminium. Hence, the rate of the reaction will reduce and eventually stop as fresh aluminium is not readily available for the electrochemical reaction. At last, it causes a decrease in battery performance.



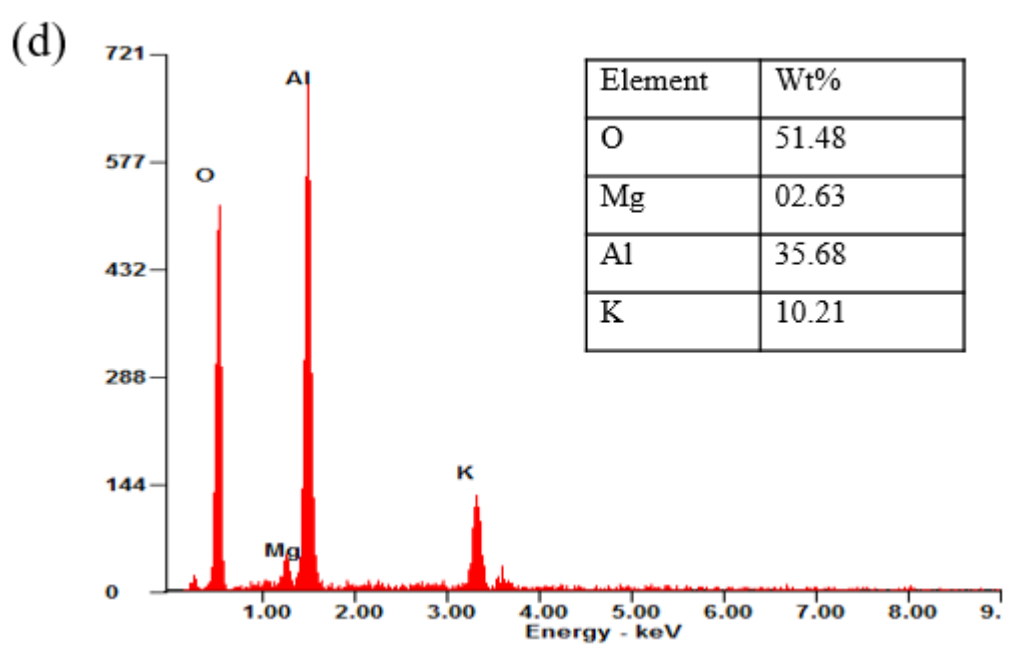
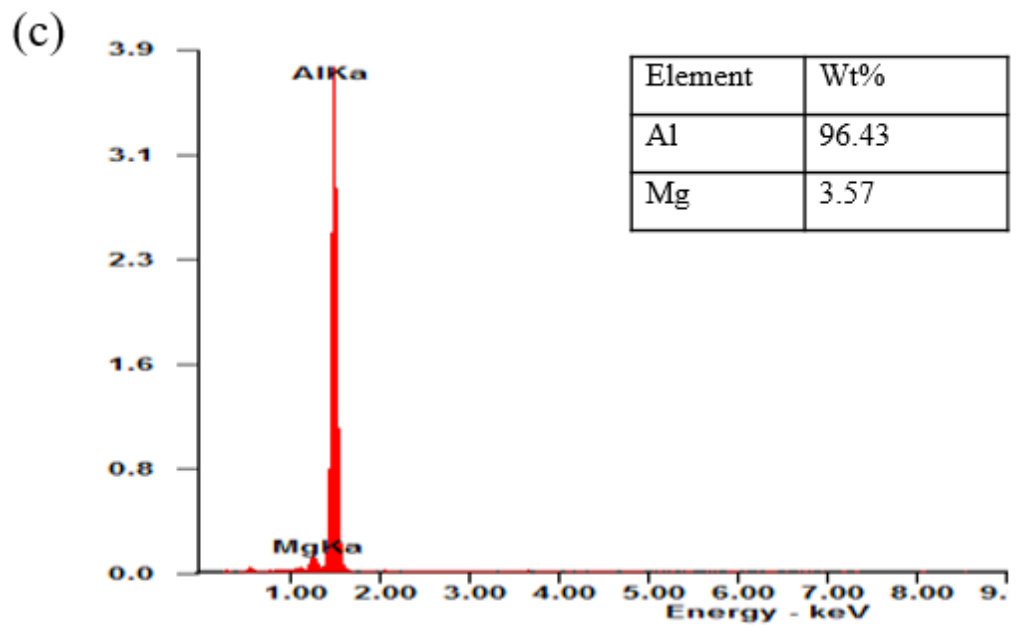


Figure 4.19: Energy-dispersive X-ray spectroscopy (EDX) spectra for (a) Al foil without discharge, (b) Al foil discharge for 1 hour in 3M of KOH without polypropylene, (c) Al alloy 6061 without discharge , (d) Al alloy 6061 discharge for 1 hour in 3M of KOH without polypropylene.

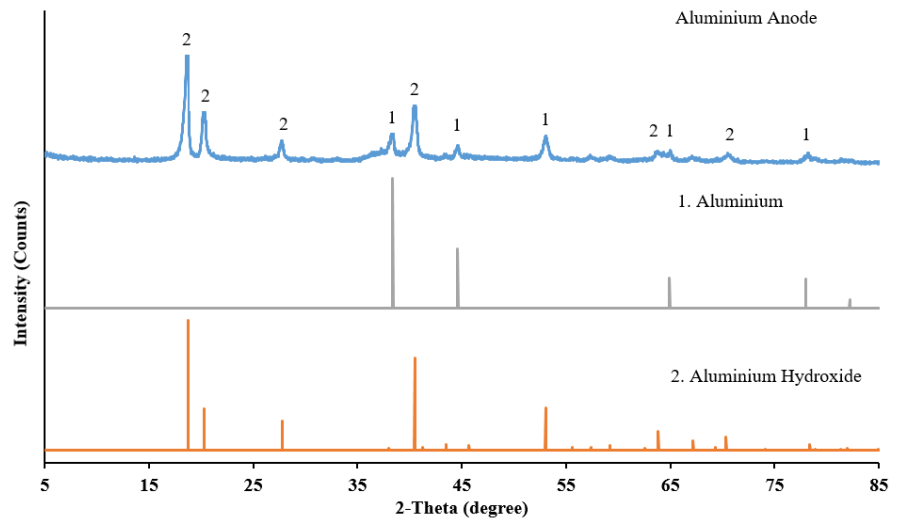


Figure 4.20: XRD results of the aluminium anode after discharge test.

CHAPTER 5

CONCLUSIONS AND FUTURE WORKS

5.1 Conclusions

The performance of the polypropylene-based separator in the aluminium-air battery in a single electrolyte system was benchmarked with different discharge currents and various concentrations of KOH electrolyte. An open circuit test was conducted, and the results demonstrate that an aluminum-air battery, based on a polypropylene separator in a single electrolyte system, exhibits an open circuit voltage of 1.1 V. The concentration of electrolyte used in the separator is important in determining the performance of the battery. A high concentration will cause a higher corrosion rate at the aluminium anode, which deteriorates the battery's performance. The best specific discharge capacity for the battery equipped with a polypropylene separator is about 375 mAh g⁻¹ at a discharge current of 30 mA with 1M of KOH electrolyte. In general, aluminium alloy 6061 performs better than aluminium foil in terms of discharge time, albeit at the expense of lower voltage. Although aluminium alloy 6061 shows higher polarization resistance than aluminium foil, it provides a large amount of aluminium atoms for the electrochemical reaction, which can extend the discharge time.

A novel polypropylene based dual-electrolyte aluminium-air battery with mixed pH electrolyte configurations for the anode and cathode is developed to

improve the performance of the single electrolyte aluminium-air battery, and the performance of the battery is characterized. The thickness of the separator and polypropylene pad, as well as the concentration of anolyte and catholyte, are important parameters affecting the performance of the dual-electrolyte aluminium-air battery. From the study, it was found that a 0.4 mm separator produced optimum battery performance. Moreover, a thin polypropylene pad is more favored than a thick polypropylene pad for the dual-electrolyte aluminium-air battery. It is noted that the effects of the anolyte and catholyte concentration on the electrical performance of the aluminium-air battery are not positively correlated, as the concentration of the anolyte and catholyte depends on each other in affecting the electrical performance of the battery. In general, a high concentration of anolyte and catholyte will improve the power and capacity of the battery. On the other hand, the discharge study showed that a high concentration of catholyte will reduce the discharge duration of the battery. A higher corrosion rate is also associated with a high concentration of the anolyte used at the anode. A comparison of single and dual electrolyte aluminium-air batteries was conducted, and it showed that the dual electrolyte system can perform better than single electrolyte system. The open circuit voltage, discharge voltage, and specific discharge capacity are improved for the dual electrolyte system compared to the single electrolyte system. The optimum combination of the parameters is 5M of anolyte and 1M of catholyte, which can generate a specific discharge capacity of $1390.92 \text{ mAh.g}^{-1}$, almost 3.5 times better than the single electrolyte system. The corrosion rate can be reduced by using a polypropylene separator, achieving an 89.1% reduction in corrosion rate under 3M of KOH electrolyte. Using Randles cell modelling, it is found that a

dual electrolyte system aluminium-air battery shows lower solution resistance and charge transfer resistance compared to a single electrolyte system. This is due to the improvement of ORR at the cathode side.

In conclusion, the aluminium-air battery is a green energy storage system, as the used aluminium anode can be fully recycle. It provides the power system with flexibility and is very useful in increasing the volume of renewable power to overcome several challenges related to large-scale grid renewable energy integration in the future, while also meeting the agenda to promote industry 4.0 in the field of green energy.

5.2 Recommendation and Future Work

The application of the aluminium-air battery is still limited in daily life due to its poor performance. The performance is affected by numerous variable, with one of the primary factors being the poor oxygen reduction rate at the air cathode. The rate of ORR cannot catch up with the rate of oxidation at the aluminium anode, causing a reduction in specific capacity and leading to wastage to the aluminium anode as more aluminium is consumed due to the parasitic reaction. The electrical performance of the aluminum-air battery can be boosted by proposing a new type of air cathode with special characteristics. For example, the air cathode should have a high reaction area and incorporate an electrocatalyst to enhance the binding sites, thereby allowing for more efficient oxygen reduction and improving the rate of the electrochemical

reaction. One proposed air cathode design involves carefully optimizing the ratio of activated carbon, carbon black, and catalyst, which are the main ingredients of the air cathode. The current collector is also an important component for aiding in electricity transmission. The current collector of the air cathode should have low resistance to reduce the overall resistance of the air cathode, thereby improving the electrical performance. Additionally, the air cathode should be made thin to reduce internal resistance and exhibit hydrophobic characteristics to prevent water flooding along the cathode's surface.

Next, the separator used in the dual-electrolyte system in the aluminum-air battery is important. The separator acts as a physical barrier to facilitate the movement of ions between the anolyte and catholyte. The separator should only allow the movement of OH^- while preventing the mixture between the anolyte and catholyte. It should be able to withstand harsh environments and have high chemical resistance, while providing a porous structure for the movement of ions. One of the proposed separators is to use a cellulose-based separator. A cellulose-based separator offers unique characteristics such as being environmentally friendly, having high porosity, and good stability (Li et al., 2021). Cellulose can be extracted from plants and processed into a film that can be used as a separator in the aluminum-air battery. Future work can be conducted to analyze the effects of the separator's properties on power generation by the aluminum-air battery.

As for the discharge time for the aluminium-air battery, it is still considered relatively short in this research project. Future work should focus on improving the discharge time for the aluminium-air battery. One proposed method is to design a system in such a way that the entire battery is enclosed to prevent the electrolyte drying out over time, thereby prolonging the lifetime of the aluminium-air battery. In this new design, mechanisms for releasing the hydrogen generated along the aluminium anode should be considered. This is necessary because the accumulation of hydrogen can lead to increased pressure, potentially damaging the battery in the long run.

Thermal management of the aluminium-air battery has been rarely studied. Although some literature reports that the aluminium-air battery benefits from high temperatures due to increased electrochemical reactions and, consequently, higher power output, the drawbacks are not well-understood. It is estimated that high temperatures can accelerate the drying of the electrolyte and cause degradation of the air cathode due to the interaction between the carbon-based air cathode and the electrolyte. As a result, the operational lifespan of the aluminium-air battery will be reduced. Hence, a comprehensive thermal analysis should be included. The output power, voltage, and current of the aluminium-air battery should show a compromise with the operating temperature. Furthermore, the application in cold climates should also be considered. Sensitivity to the performance of the aluminium-air battery in varying operating temperatures should be measured.

Although the polypropylene-based aluminium-air battery helps reduce the dependency on a circulation system, it still relies on KOH, which is known for its high corrosion potential with aluminium. Therefore, an electrolyte with high conductivity should be introduced. Some findings include the use of gel electrolyte and solid electrolyte in the aluminium-air battery. These solutions resolve the leakage problem and eliminate the need for a circulation system. However, their application is limited due to the poor conductivity performance of gel and solid electrolytes. Hence, future work should focus on the development of such electrolytes to improve the performance of the aluminium-air battery.

REFERENCE

Abdel-Gawad, S.A., Osman, W.M. and Fekry, A.M., 2019. Characterization and corrosion behavior of anodized aluminum alloys for military industries applications in artificial seawater. *Surfaces and Interfaces*, 14, pp.314-323.

Abdin, Z. and Khalilpour, K.R., 2019. Single and polystorage technologies for renewable-based hybrid energy systems. In *Polygeneration with polystorage for chemical and energy hubs*, Academic Press, pp.77-131.

Avoundjian, A., Galvan, V. and Gomez, F.A., 2017. An inexpensive paper-based aluminum-air battery. *Micromachines*, 8(7), p.222.

Bidault, F., Brett, D.J.L., Middleton, P.H. and Brandon, N.P., 2009. Review of gas diffusion cathodes for alkaline fuel cells. *Journal of Power Sources*, 187(1), pp.39-48.

Chen, B., Leung, D.Y., Xuan, J. and Wang, H., 2015. A high performance dual electrolyte aluminium-air cell. *Energy Procedia*, 75, pp.1983-1989.

Chen, B., Leung, D.Y., Xuan, J. and Wang, H., 2016. A high specific capacity membraneless aluminum-air cell operated with an inorganic/organic hybrid electrolyte. *Journal of Power Sources*, 336, pp.19-26.

Chen, B., Leung, D.Y., Xuan, J. and Wang, H., 2017. A mixed-pH dual-electrolyte microfluidic aluminum-air cell with high performance. *Applied Energy*, 185, pp.1303-1308.

Chen, B., Xuan, J., Wang, H. and Leung, D.Y., 2017. Microfluidic Aluminum-air Cell with Methanol-based Anolyte. *Energy Procedia*, 105, pp.4691-4697.

Chen, W., Liang, J., Yang, Z. and Li, G., 2019. A review of lithium-ion battery for electric vehicle applications and beyond. *Energy Procedia*, 158, pp.4363-4368.

Cheng, F. and Chen, J., 2012. Metal–air batteries: from oxygen reduction electrochemistry to cathode catalysts. *Chemical Society Reviews*, 41(6), pp.2172-2192.

Cho, Y.J., Park, I.J., Lee, H.J. and Kim, J.G., 2015. Aluminum anode for aluminum–air battery–Part I: Influence of aluminum purity. *Journal of Power Sources*, 277, pp.370-378.

Choi, J.R., Lee, J.W., Yang, G., Heo, Y.J. and Park, S.J., 2020. Activated carbon/MnO₂ composites as electrode for high performance supercapacitors. *Catalysts*, 10(2), pp.256.

Clark, S., Latz, A. and Horstmann, B., 2018. A review of model-based design tools for metal-air batteries. *Batteries*, 4(1), pp.5.

Di Palma, T.M., Migliardini, F., Gaele, M.F. and Corbo, P., 2021. Aluminum-air Batteries with solid hydrogel electrolytes: Effect of pH upon cell performance. *Analytical Letters*, 54(1-2), pp.28-39.

Doche, M.L., Rameau, J.J., Durand, R. and Novel-Cattin, F., 1999. Electrochemical behaviour of aluminium in concentrated NaOH solutions. *Corrosion science*, 41(4), pp.805-826.

Doshi, B., Sillanpää, M. and Kalliola, S., 2018. A review of bio-based materials for oil spill treatment. *Water research*, 135, pp.262-277.

EIS Spectrum Analyser, 2008. EIS Spectrum Analyser Help. [online] Available at: <
[http://www.abc.chemistry.bsu.by/vi/analyser/parameters.html#:~:text=Warburg%20Short%20\(Ws\).&text=This%20element%20has%20two%20parameters,d%20%2D%20Nernst%20diffusion%20layer%20thickness.](http://www.abc.chemistry.bsu.by/vi/analyser/parameters.html#:~:text=Warburg%20Short%20(Ws).&text=This%20element%20has%20two%20parameters,d%20%2D%20Nernst%20diffusion%20layer%20thickness.)> [Accessed 23 March 2023]

Elia, G.A., Hasa, I., Greco, G., Diemant, T., Marquardt, K., Hoepfner, K., Behm, R.J., Hoell, A., Passerini, S. and Hahn, R., 2017. Insights into the reversibility of aluminum graphite batteries. *Journal of Materials Chemistry A*, 5(20), pp.9682-9690.

Fan, L., Lu, H. and Leng, J., 2015. Performance of fine structured aluminum anodes in neutral and alkaline electrolytes for Al-air batteries. *Electrochimica Acta*, 165, pp.22-28.

Fan, L., Lu, H., Leng, J., Sun, Z. and Chen, C., 2015. The study of industrial aluminum alloy as anodes for aluminum-air batteries in alkaline electrolytes. *Journal of The Electrochemical Society*, 163(2), p.A8.

Hosseini, S., Lao-Atiman, W., Han, S.J., Arpornwichanop, A., Yonezawa, T. and Kheawhom, S., 2018. Discharge performance of zinc-air flow batteries under the effects of sodium dodecyl sulfate and pluronic F-127. *Scientific reports*, 8(1), pp.1-13.

Hu, L. and Cui, Y., 2012. Energy and environmental nanotechnology in conductive paper and textiles. *Energy & Environmental Science*, 5(4), pp.6423-6435.

Hu, L., Choi, J.W., Yang, Y., Jeong, S., La Mantia, F., Cui, L.F. and Cui, Y., 2009. Highly conductive paper for energy-storage devices. *Proceedings of the National Academy of Sciences*, 106(51), pp.21490-21494.

Hu, T., Li, K., Fang, Y., Su, L., Song, Z., Shen, H. and Sheng, L., 2019. Experimental research on temperature rise and electric characteristics of aluminum air battery under open-circuit condition for new energy vehicle. *International Journal of Energy Research*, 43(3), pp.1099-1110.

Huo, G., Wang, X.W., Zhang, Z.B., Song, Z., Kang, X.M., Chen, M.X., Wang, Q., Fu, X.Z. and Luo, J.L., 2020. γ -MnO₂ nanorod-assembled hierarchical micro-spheres with oxygen vacancies to enhance electrocatalytic performance toward the oxygen reduction reaction for aluminum-air batteries. *Journal of Energy Chemistry*, 51, pp.81-89.

Ilyukhina, A.V., Klymenov, B.V. and Zhuk, A.Z., 2017. Development and study of aluminum-air electrochemical generator and its main components. *Journal of Power Sources*, 342, pp.741-749.

Instruments, G., 2007. Basics of electrochemical impedance spectroscopy. *G. Instruments, Complex impedance in Corrosion*, pp.1-30.

Jiang, C., Fang, Y., Zhang, W., Song, X., Lang, J., Shi, L. and Tang, Y., 2018. A multi-ion strategy towards rechargeable sodium-ion full batteries with high working voltage and rate capability. *Angewandte Chemie*, 130(50), pp.16608-16612.

Jiang, M., Fu, C., Cheng, R., Liu, T., Guo, M., Meng, P., Zhang, J. and Sun, B., 2021. Interface engineering of Co₃Fe₇-Fe₃C heterostructure as an efficient oxygen reduction reaction electrocatalyst for aluminum-air batteries. *Chemical Engineering Journal*, 404, p.127124.

Kahan A., 2019. EIA projects nearly 50% increase in world energy usage by 2050, led by growth in Asia. Available at: <https://www.eia.gov/todayinenergy/detail.php?id=41433#:~:text=EIA%20projects%20nearly%2050%25%20increase,led%20by%20growth%20in%20Asia&text=In%20its%20newly%20released%20International,50%25%20between%202018%20and%202050.> [Accessed: 10 May 2023]

Katsoufis, P., Katsaiti, M., Mourelas, C., Andrade, T.S., Dracopoulos, V., Politis, C., Avgouropoulos, G. and Lianos, P., 2020. Study of a thin film aluminum-air battery. *Energies*, 13(6), p.1447.

Koroleva, E.V., Thompson, G.E., Hollrigl, G. and Bloeck, M., 1999. Surface morphological changes of aluminium alloys in alkaline solution: effect of second phase material. *Corrosion Science*, 41(8), pp.1475-1495.

Lai, Y., Wang, Q., Wang, M., Li, J., Fang, J. and Zhang, Z., 2017. Facile synthesis of mesoporous Fe-NC electrocatalyst for high performance alkaline aluminum-air battery. *Journal of Electroanalytical Chemistry*, 801, pp.72-76.

Li, L. and Manthiram, A., 2016. Long-Life, High-Voltage Acidic Zn–Air Batteries. *Advanced Energy Materials*, 6(5), pp.1502054.

Li, S., Zhu, W., Tang, Q., Huang, Z., Yu, P., Gui, X., Lin, S., Hu, J. and Tu, Y., 2021. Mini review on cellulose-based composite separators for lithium-ion batteries: recent progress and perspectives. *Energy & Fuels*, 35(16), pp.12938-12947.

Li, Y. and Lu, J., 2017. Metal–air batteries: will they be the future electrochemical energy storage device of choice?. *ACS Energy Letters*, 2(6), pp.1370-1377.

Liu, P., Liu, X., Dong, F., Lin, Q., Tong, Y., Li, Y. and Zhang, P., 2018. Electricity generation from banana peels in an alkaline fuel cell with a Cu₂O-Cu modified activated carbon cathode. *Science of the Total Environment*, 631, pp.849-856.

Liu, Q., Pan, Z., Wang, E., An, L., and Sun, G., 2020. Aqueous metal-air batteries: Fundamentals and applications. *Energy Storage Materials*, 27, pp. 478-505.

Liu, Y., Sun, Q., Li, W., Adair, K.R., Li, J. and Sun, X., 2017. A comprehensive review on recent progress in aluminum–air batteries. *Green Energy & Environment*, 2(3), pp.246-277.

Liu, Z., Zhao, J., Cai, Y. and Xu, B., 2017, January. Design and research on discharge performance for aluminum-air battery. In *AIP Conference Proceedings*, 1794(1), pp.040006

Ma, J., Wen, J., Gao, J. and Li, Q., 2014. Performance of Al–0.5 Mg–0.02 Ga–0.1 Sn–0.5 Mn as anode for Al–air battery in NaCl solutions. *Journal of Power Sources*, 253, pp.419-423.

Ma, J., Wen, J., Li, Q. and Zhang, Q., 2013. Effects of acidity and alkalinity on corrosion behaviour of Al–Zn–Mg based anode alloy. *Journal of Power Sources*, 226, pp.156-161.

Ma, J., Wen, J., Li, Q. and Zhang, Q., 2013. Electrochemical polarization and corrosion behavior of Al–Zn–In based alloy in acidity and alkalinity solutions. *International journal of hydrogen energy*, 38(34), pp.14896-14902.

Macdonald, D.D., Lee, K.H., Moccari, A. and Harrington, D., 1988. Evaluation of alloy anodes for aluminum-air batteries: corrosion studies. *Corrosion*, 44(9), pp.652-657.

Mohamad, A.A., 2008. Electrochemical properties of aluminum anodes in gel electrolyte-based aluminum-air batteries. *Corrosion Science*, 50(12), pp.3475-3479.

Moon, J., Jeong, J.Y., Kim, J.I., Kim, S. and Park, J.H., 2019. An ultrathin inorganic-organic hybrid layer on commercial polymer separators for advanced lithium-ion batteries. *Journal of Power Sources*, 416, pp.89-94.

Nestoridi, M., Pletcher, D., Wood, R.J., Wang, S., Jones, R.L., Stokes, K.R. and Wilcock, I., 2008. The study of aluminium anodes for high power density Al/air batteries with brine electrolytes. *Journal of Power Sources*, 178(1), pp.445-455.

PalmSens, 2023. Bode and Nyquist Plot. [online] Available at:<
<https://www.palmsens.com/knowledgebase-article/bode-and-nyquist-plot/>> [Accessed 23 March 2023]

Pan, R., Sun, R., Wang, Z., Lindh, J., Edström, K., Strømme, M. and Nyholm, L., 2019. Sandwich-structured nano/micro fiber-based separators for lithium metal batteries. *Nano Energy*, 55, pp.316-326.

Pan, R., Sun, R., Wang, Z., Lindh, J., Edström, K., Strømme, M. and Nyholm, L., 2019. Double-sided conductive separators for lithium-metal batteries. *Energy Storage Materials*, 21, pp.464-473.

Pan, R., Xu, X., Sun, R., Wang, Z., Lindh, J., Edström, K., Strømme, M. and Nyholm, L., 2018. Nanocellulose modified polyethylene separators for lithium metal batteries. *Small*, 14(21), p.1704371.

Phusittananan, T., Kao-Ian, W., Nguyen, M.T., Yonezawa, T., Pornprasertsuk, R., Mohamad, A.A. and Kheawhom, S., 2020. Ethylene glycol/ethanol anolyte for high capacity alkaline aluminum-air battery with dual-electrolyte configuration. *Frontiers in Energy Research*, 8, p.189.

Pino, M., Chacón, J., Fatás, E. and Ocón, P., 2015. Performance of commercial aluminium alloys as anodes in gelled electrolyte aluminium-air batteries. *Journal of Power Sources*, 299, pp.195-201.

Pino, M., Cuadrado, C., Chacón, J., Rodríguez, P., Fatás, E. and Ocón, P., 2014. The electrochemical characteristics of commercial aluminium alloy electrodes for Al/air batteries. *Journal of Applied Electrochemistry*, 44, pp.1371-1380.

Ren, C., Li, K., Lv, C., Zhao, Y., Wang, J. and Guo, S., 2019. Nanorod CoFe₂O₄ modified activated carbon as an efficient electrocatalyst to improve the performance of air cathode microbial fuel cell. *Journal of Electroanalytical Chemistry*, 840, pp.134-143.

Ren, J., Ma, J., Zhang, J., Fu, C. and Sun, B., 2019. Electrochemical performance of pure Al, Al–Sn, Al–Mg and Al–Mg–Sn anodes for Al-air batteries. *Journal of Alloys and Compounds*, 808, pp.151708.

Schwarz, H.G, 2014. Aluminum Production and Energy. *Encyclopedia of Energy*.

Shen, L.L., Zhang, G.R., Biesalski, M. and Etzold, B.J., 2019. based microfluidic aluminum–air batteries: toward next-generation miniaturized power supply. *Lab on a Chip*, 19(20), pp.3438-3447.

Shinagawa, T., Garcia-Esparza, A.T. and Takanabe, K., 2015. Insight on Tafel slopes from a microkinetic analysis of aqueous electrocatalysis for energy conversion. *Scientific reports*, 5(1), pp.1-21.

Song, Q., Li, A., Shi, L., Qian, C., Feric, T.G., Fu, Y., Zhang, H., Li, Z., Wang, P., Li, Z. and Zhai, H., 2019. Thermally stable, nano-porous and eco-friendly sodium alginate/attapulgit separator for lithium-ion batteries. *Energy Storage Materials*, 22, pp.48-56.

Sun, S., Miao, H., Xue, Y., Wang, Q., Zhang, Q., Dong, Z., Li, S., Huang, H. and Liu, Z., 2017. High electrocatalytic activity of silver-doped manganese dioxide toward oxygen reduction reaction in aluminum-air battery. *Journal of The Electrochemical Society*, 164(7), p.F768.

Sun, Z. and Lu, H., 2015. Performance of Al-0.5 In as anode for Al–air battery in inhibited alkaline solutions. *Journal of the Electrochemical Society*, 162(8), p.A1617.

Sun, Z., Lu, H., Fan, L., Hong, Q., Leng, J. and Chen, C., 2015. Performance of Al-air batteries based on Al–Ga, Al–In and Al–Sn alloy electrodes. *Journal of the Electrochemical Society*, 162(10), pp. A2116-A2122.

Tan, W.C., Saw, L.H., Yew, M.C., Sun, D. and Chen, W.H., 2022. High performance aluminum-air battery for sustainable power generation. *International Journal of Hydrogen Energy*, 48(28), pp. 10438-10451

Tan, W.C., Saw, L.H., Yew, M.C., Sun, D., Cai, Z., Chong, W.T. and Kuo, P.Y., 2021. Analysis of the polypropylene-based aluminium-air battery. *Frontiers in Energy Research*, 9, p.599846.

Tan, Y.K., Mao, J.C. and Tseng, K.J., 2011. Modelling of battery temperature effect on electrical characteristics of Li-ion battery in hybrid electric vehicle. In *2011 IEEE Ninth International Conference on Power Electronics and Drive Systems*, pp. 637-642

Teabnamang, P., Kao-ian, W., Nguyen, M.T., Yonezawa, T., Cheacharoen, R. and Kheawhom, S., 2020. High-capacity dual-electrolyte aluminum–air battery with circulating methanol anolyte. *Energies*, 13(9), p.2275.

Tuck, C.D.S., Hunter, J.A. and Scamans, G.M., 1987. The electrochemical behavior of Al-Ga alloys in alkaline and neutral electrolytes. *Journal of the Electrochemical Society*, 134(12), p.2970.

Van, N.R., 2014. The rechargeable revolution: A better battery. *Nature*, 507(7490), pp.26-28.

Wang, C.M., Hsueh, K.L. and Hsieh, C.L., 2013. The Kinetic Reaction of Aluminum-Air Battery in Different Aqueous Solution. *ECS Transactions*, 50(25), pp.29.

Wang, C.Y., Liu, T., Yang, X.G., Ge, S., Stanley, N.V., Rountree, E.S., Leng, Y., McCarthy, B.D., 2022 Fast charging of energy-dense lithium-ion batteries. *Nature*, 611(7936), pp.485-490.

Wang, H., Leung, D.Y., Leung, M.K. and Ni, M., 2010. Modeling of parasitic hydrogen evolution effects in an aluminum– air cell. *Energy & fuels*, 24(7), pp.3748-3753.

Wang, L., Cheng, R., Liu, C., Ma, M.C., Wang, W., Yang, G., Leung, M.K.H., Liu, F. and Feng, S.P., 2020. Trielectrolyte aluminum-air cell with high stability and voltage beyond 2.2 V. *Materials Today Physics*, 14, p.100242.

Wang, L., Liu, F., Wang, W., Yang, G., Zheng, D., Wu, Z. and Leung, M.K., 2014. A high-capacity dual-electrolyte aluminum/air electrochemical cell. *Rsc Advances*, 4(58), pp.30857-30863.

Wang, L., Wang, W., Yang, G., Liu, D., Xuan, J., Wang, H., Leung, M.K. and Liu, F., 2013. A hybrid aluminum/hydrogen/air cell system. *International journal of hydrogen energy*, 38(34), pp.14801-14809.

Wang, Q., Zhang, Z., Wang, M., Liu, F., Jiang, L., Hong, B., Li, J. and Lai, Y., 2018. Bioinspired fiber-like porous Cu/N/C electrocatalyst facilitating electron transportation toward oxygen reaction for metal–air batteries. *Nanoscale*, 10(33), pp.15819-15825.

Wang, S., Yu, Z., Tu, J., Wang, J., Tian, D., Liu, Y. and Jiao, S., 2016. A novel aluminum-ion battery: Al/AlCl₃-[EMIm] Cl/Ni₃S₂@graphene. *Advanced Energy Materials*, 6(13), pp.1600137.

Wang, Y., Kwok, H.Y., Pan, W., Zhang, H., Lu, X. and Leung, D.Y., 2019. Parametric study and optimization of a low-cost paper-based Al-air battery with corrosion inhibition ability. *Applied energy*, 251, pp.113342.

Wang, Y., Pan, W., Kwok, H., Lu, X. and Leung, D.Y., 2019. Low-cost Al-air batteries with paper-based solid electrolyte. *Energy Procedia*, 158, pp.522-527.

Wang, Y., Pan, W., Leong, K.W., Luo, S., Zhao, X. and Leung, D.Y., 2021. Solid-state Al-air battery with an ethanol gel electrolyte. *Green Energy & Environment*, 8(4), pp.1117-1127

Wang, Y., Pan, W., Luo, S., Zhao, X., Kwok, H.Y., Xu, X. and Leung, D.Y., 2022. High-performance solid-state metal-air batteries with an innovative dual-gel electrolyte. *International Journal of Hydrogen Energy*, 47(33), pp.15024-15034.

Wen, H., Liu, Z., Qiao, J., Chen, R., Qiao, G. and Yang, J., 2020. Ultrahigh voltage and energy density aluminum-air battery based on aqueous alkaline-acid hybrid electrolyte. *International Journal of Energy Research*, 44(13), pp.10652-10661.

Wu, G.M., Lin, S.J. and Yang, C.C., 2006. Alkaline Zn-air and Al-air cells based on novel solid PVA/PAA polymer electrolyte membranes. *Journal of Membrane Science*, 280(1-2), pp.802-808.

Wu, N.L., Liu, W.R. and Su, S.J., 2003. Effect of oxygenation on electrocatalysis of La_{0.6}Ca_{0.4}CoO_{3-x} in bifunctional air electrode. *Electrochimica Acta*, 48(11), pp.1567-1571.

Wu, S., Hu, S., Zhang, Q., Sun, D., Wu, P., Tang, Y. and Wang, H., 2020. Hybrid high-concentration electrolyte significantly strengthens the practicability of alkaline aluminum-air battery. *Energy Storage Materials*, 31, pp.310-317.

Xiang, L., Ou, X., Wang, X., Zhou, Z., Li, X. and Tang, Y., 2020. Highly concentrated electrolyte towards enhanced energy density and cycling life of dual-ion battery. *Angewandte Chemie International Edition*, 59(41), pp.17924-17930.

Xie, W., Liu, W., Dang, Y., Tang, A., Deng, T. and Qiu, W., 2019. Investigation on electrolyte-immersed properties of lithium-ion battery cellulose separator through multi-scale method. *Journal of Power Sources*, 417, pp.150-158.

Xu, T., Hu, Z., Yao, C., 2019. The effects of Ca addition on corrosion and discharge performance of commercial pure aluminum alloy 1070 as anode for Aluminum-air battery. *International Journal of Electrochemical Science*, 14, pp. 2606-2620.

Yang, S. and Knickle, H., 2002. Design and analysis of aluminum/air battery system for electric vehicles. *Journal of power sources*, 112(1), pp.162-173.

Yu, Y., Chen, M., Wang, S., Hill, C., Joshi, P., Kuruganti, T. and Hu, A., 2018. Laser sintering of printed anodes for al-air batteries. *Journal of The Electrochemical Society*, 165(3), p.A584.

Zhang, S., Su, W., Li, K., Liu, D., Wang, J. and Tian, P., 2018. Metal organic framework-derived Co₃O₄/NiCo₂O₄ double-shelled nanocage modified activated carbon air-cathode for improving power generation in microbial fuel cell. *Journal of Power Sources*, 396, pp.355-362.

Zhang, Z., Zuo, C., Liu, Z., Yu, Y., Zuo, Y. and Song, Y., 2014. All-solid-state Al–air batteries with polymer alkaline gel electrolyte. *Journal of Power Sources*, 251, pp.470-475.

Zhao, R., Xie, J., Wen, H., Wang, F., Yang, J. and Zhang, D., 2020. Performance modeling and parameter sensitivity analyses of an aluminum-air battery with dual electrolyte structure. *Journal of Energy Storage*, 32, p.101696.

Zhou, C., Bhonge, K. and Cho, K.T., 2020. Analysis of the effect of hydrogen-evolving side reaction in the aqueous aluminum-air battery. *Electrochimica Acta*, 330, p.135290.

Zuo, Y., Yu, Y., Zuo, C., Ning, C., Liu, H., Gu, Z., Cao, Q. and Shen, C., 2019. Low-temperature performance of Al-air batteries. *Energies*, 12(4), p.612.

LIST OF PUBLICATIONS

Tan, W.C., Saw, L.H., Yew, M.C., Sun, D., Cai, Z., Chong, W.T. and Kuo, P.Y., 2021. Analysis of the polypropylene-based aluminium-air battery. *Frontiers in Energy Research*, 9, p.599846.

Tan, W.C., Saw, L.H., Yew, M.C., Sun, D. and Chen, W.H., 2022. High performance aluminium-air battery for sustainable power generation. *International Journal of Hydrogen Energy*.

Tan, W.C., Saw, L.H., Yew, M.C., Pei-Yu, K., Khor, Z.Y. and Sun, D., 2022. Development of hybrid aluminum-air battery fuel-cell system. In *IOP Conference Series: Earth and Environmental Science*, 1074(1), pp. 012034.

Tan, W.C., Saw, L.H., Asrin, S., Yew, M.C., Sun, D., Koh, Y.Y., Chong, W.T., Chen, W., 2023, Modelling of polypropylene-based aluminum-air battery. *Materials Today: Proceedings*.

Tan, W.C., Saw, L.H., Yew, M.C., Yew, M.K. Recycling of Wastes Generated in Automobile Metal–Air Batteries. In *Energy from Waste* (pp. 329-345). CRC Press.

Tan, W.C., Saw, L.H., Yew, M.C., Yew, M.K. *Materials and Technologies of Al-Air Batteries*. CRC Press.

Tan, W.C., Saw, L.H., Yew, M.C., Kuo, P.Y. Recent trends, opportunities, and future prospects of Aluminum-air battery: An Overview (under review)

Tan, W.C., Saw, L.H., Yew, M.C. Characterization of the Aluminium-air Battery Model Based on Electrochemical Impedance Spectroscopy. (under review)